

Nanocalorimetry of vapor-deposited organic glasses: tris-naphthylbenzene, decalin and  
*ortho*-terphenyl

By

Katherine R. Whitaker

A dissertation submitted in partial fulfillment of  
the requirements for the degree of

Doctor of Philosophy  
(Chemistry)

at the

UNIVERSITY OF WISCONSIN-MADISON

2013

Date of final oral examination: 07/30/13

The dissertation is approved by the following members of the Final Oral Committee:

Mark D. Ediger, Professor, Chemistry

Lian Yu, Professor, Pharmacy

Gilbert Nathanson, Professor, Chemistry

James Skinner, Professor, Chemistry

John H. Perepezko, Professor, Materials Science and Engineering

## **DEDICATION**

In memory of Walter W. Whitaker III  
(May 22, 1948 – September 10, 2002)

## ACKNOWLEDGEMENTS

First and foremost, I have to thank my advisor Prof. Mark Ediger. Your encouragement and positive attitude through the ups and downs of research helped me to stick it out and I will always be grateful. You taught me not only about amorphous materials, but also more importantly how to be a good scientist. If I had to do this all over again, joining your group is one thing about my graduate school career that I would absolutely not change.

I would also like to thank all of my collaborators at the University of Rostock: Prof. Christoph Schick, Dr. Mathias Ahrenberg, Dr. Heiko Huth, Yeong Zen Chua and Evgeni Shoifet. It has been a pleasure working with all of you and I've benefitted immensely from your nanocalorimetry expertise. I would particularly like to thank Mathias for helping me get my *in situ* system up and running. Your experience and patience were invaluable.

Thank you to all of the members of the Ediger group that I've had the pleasure of working with. I would especially like to thank Dr. Ken Kearns and Dr. Kevin Dawson. Ken, I couldn't have asked for a better mentor during my first year; you were patient, kind and encouraging in getting me set up to tackle the project on my own. Kevin, you probably had no idea of the Pandora's box you were opening when you started answering my questions around the office. I am grateful for your friendship and that you continue to respond to the never-ending questions I now email you instead. I treasure your advice on science, graduate school and life. To Dr. Zahra Fakhraai, Dr. Alfonso Sepulveda, Shakeel Dalal, Jaritza Gomez-Zayas, Mike Tylinski, Ankit Gujral, and Diane Walters, I am glad to have

worked with you on the vapor deposition project. To Ben Bending, Kelly Christison and Josh Ricci, it's been enjoyable to work with you. To Dan Scifo, it was a pleasure working with you and I appreciate all the evenings and weekends you sacrificed for experiments.

Thank you to my family for your unwavering support throughout my life and especially throughout graduate school. Dad, you got me started with 'trailer school' and I regret that you are not still with us to see me finish with graduate school. Mom, you will always be my role model. Thank you for always listening; even when you didn't quite understand what I was complaining about, I appreciated your advice and support. Anne, you've been a tough act to follow. I've had to work hard to follow in your footsteps and I appreciate how high you set the bar. Thank you for motivating and encouraging me.

I would like to thank all of my friends who were always there to celebrate or commiserate along the way. Beau Monnot, you've bore the brunt of being my support system and I will always be appreciative. Thank you for being willing to listen and brainstorm about my data and for those times when you had to be the one of us that wanted me to finish. Mark Lukowski, together we've logged hundreds of happy hours over the years (and probably one thousand beers therein); I've appreciated every one. Caleb Brian, you were instrumental in my joining the Ediger group and I will always be grateful to you. Michelle Benson, while our friendship and siestas may not have made us the most productive graduate students at times, we could always turn around the worst times together. Melissa Galloway, thank you for leading the way out of graduate school and encouraging me to keep an open mind about the next step.

## Table of Contents

<b>Abstract</b> .....	viii
<b>Chapter 1: Introduction</b> .....	1
1.1 Supercooled liquids and glasses .....	2
1.2 Glass preparation methods .....	5
1.3 Calorimetric techniques for studying glasses .....	10
1.4 Vapor-deposited glasses and stability .....	19
1.4.1 Low stability glasses deposited on low temperature substrates .....	20
1.4.2 Stability as a function of substrate temperature .....	27
1.4.3 High stability glasses deposited near $0.85 T_g$ .....	34
1.5 Original contributions of this thesis to the body of knowledge .....	41
<b>Chapter 2: Vapor-deposited <math>\alpha,\alpha,\beta</math>-tris-naphthylbenzene glasses with low heat capacity and high kinetic stability</b> .....	46
2.1 Abstract .....	47
2.2 Introduction .....	47
2.3 Experimental .....	51
2.3.1 Materials .....	51
2.3.2 Vapor deposition .....	51
2.3.3 AC nanocalorimetry .....	51
2.4 Results .....	53
2.4.1 Heat capacity of vapor-deposited glasses .....	53
2.4.2 Transformation kinetics of stable glasses .....	57

2.5 Discussion .....	64
2.5.1 Heat capacity of vapor-deposited glasses .....	64
2.5.2 Stable glass transformation mechanism and kinetics.....	66
2.6 Summary .....	69
2.7 Acknowledgements .....	70
<b>Chapter 3: Highly stable glasses of <i>cis</i>-decalin and <i>cis/trans</i>-decalin mixtures .....</b>	<b>71</b>
3.1 Abstract .....	72
3.2 Introduction .....	72
3.3 Experimental methods .....	76
3.3.1 Materials .....	76
3.3.2 Sample preparation .....	76
3.3.3 <i>In situ</i> AC nanocalorimetry .....	80
3.3.4 Temperature calibration .....	82
3.4 Results .....	83
3.4.1 Reversing $C_p$ during temperature ramping .....	83
3.4.2 Dependence of glassy $C_p$ and kinetic stability upon substrate temperature.....	88
3.4.3 Isothermal annealing experiments .....	91
3.5 Discussion .....	93
3.5.1 Substrate temperature dependence of vapor-deposited glasses .....	93
3.5.2 Stable glasses and fragility .....	96
3.5.3 Stable glasses of mixtures .....	98
3.5.4 Stability of <i>cis</i> -decalin vs. decalin mixture glasses .....	100
3.5.5 The generality of stable glass formation .....	101
3.6 Conclusions .....	102

3.7 Acknowledgements .....	104
<b>Chapter 4: Reversing heat capacity of vapor-deposited glasses of <i>o</i>-terphenyl .....</b>	<b>105</b>
4.1 Abstract .....	106
4.2 Introduction .....	106
4.3 Experimental .....	109
4.3.1 Materials .....	109
4.3.2 Sample preparation .....	110
4.3.3 <i>In situ</i> AC nanocalorimetry .....	111
4.4 Results .....	113
4.4.1 Reversing heat capacity of as-deposited glasses .....	113
4.4.2 Effect of substrate temperature on the reversing heat capacity .....	115
4.4.3 Effect of substrate temperature on the kinetic stability .....	117
4.4.4 Isothermal transformation kinetics .....	117
4.5 Discussion .....	119
4.5.1 Heat capacity of <i>o</i> -terphenyl .....	119
4.5.2 Kinetic stability of <i>o</i> -terphenyl glasses .....	125
4.6 Summary .....	126
4.7 Acknowledgements .....	127
<b>Chapter 5: High heat capacity of low temperature vapor-deposited glasses of <i>o</i>-terphenyl .....</b>	<b>128</b>
5.1 Abstract .....	129
5.2 Introduction, Results and Discussion .....	129
5.3 Experimental .....	141

<b>Chapter 6: Concluding Remarks</b> .....	143
6.1 Introduction .....	143
6.2 Influence of substrate temperature on kinetic stability .....	143
6.3 Isothermal transformation behavior of vapor-deposited glasses .....	146
6.4 Heat capacity of vapor-deposited glasses .....	148
6.5 Extremely high heat capacity at low temperature .....	151
<b>Chapter 7: Future Directions</b> .....	152
7.1 Introduction .....	152
7.2 Glass vs. crystal heat capacity .....	153
7.3 High throughput nanocalorimetry measurements .....	155
7.3.1 Stable glass deposition rate dependence .....	155
7.3.2 Stable glasses of mixtures .....	159
<b>References</b> .....	163



## Abstract

The reversing heat capacity of vapor-deposited glasses of the organic glassformers  $\alpha\alpha\beta$ -tris-naphthylbenzene ( $\alpha\alpha\beta$ -TNB), decahydronaphthalene (decalin), and *o*-terphenyl was studied using AC nanocalorimetry. For each system, glasses with low heat capacity and high kinetic stability, as compared to the corresponding liquid-cooled glass, were prepared. These results were in agreement with the recent body of literature that has shown vapor-deposited glasses can have extraordinary stability when the optimum deposition conditions are utilized. Prior to this work, most of what was known about the heat capacity of 'stable glasses' was learned from bulk samples using conventional calorimetric techniques.

Thin films of  $\alpha\alpha\beta$ -TNB showed thickness dependent transformation times for films up to one micron in thickness, and low heat capacity with respect to the ordinary glass cooled from the liquid. Quasi-isothermal AC nanocalorimetry experiments on  $\alpha\alpha\beta$ -TNB glasses vapor-deposited at a temperature of  $0.85 T_g$  showed a crossover at a thickness of one micron from thickness-dependent to thickness-independent transformation behavior. It is generally observed that stable glass thin films transform via a surface-initiated growth front mechanism and this is thought to be responsible for the thickness-dependent behavior observed with nanocalorimetry for thin films. All of the vapor-deposited stable glasses of  $\alpha\alpha\beta$ -TNB showed  $\sim 4\%$  lower heat capacity than that of the liquid-cooled glass, regardless of thickness. The low heat capacity of stable vapor-deposited glasses can be understood in terms of the vibrational density of states. In the well-packed vapor-

deposited glasses, low frequency vibrations are shifted to higher frequency, increasing the heat capacity.

Vapor-deposited glasses of a molecular mixture and of a high fragility glassformer show lower heat capacity and higher kinetic stability than the liquid-cooled glass. Glasses of 50/50 *cis/trans*-decalin and pure *cis*-decalin were deposited across a range of substrate temperatures; the vapor-deposited glasses had up to 2.5% and 4.5% lower heat capacity, respectively, relative to the corresponding ordinary glass. The most stable glass of 50/50 *cis/trans*-decalin exhibited kinetic stability similar to that achieved in stable glasses of other materials. This result demonstrated that high fragility glassformers are also capable of stable glass formation, implying that the surface mobility that governs stable glass formation during deposition is also present for high fragility systems. Other compositions of *cis/trans*-decalin mixtures were investigated and each showed enhanced kinetic stability and lower heat capacity as compared to the liquid-cooled glass. The ability to tune the composition and still achieve stable glasses through vapor-deposition argues against the idea of nanocrystals being responsible for the extraordinary features of stable glasses.

The deposition temperature can also be continuously tuned to produce glasses of varying stability. Deposition temperatures ranging from  $0.4 T_g$  to  $T_g$  were utilized to vapor-deposit glasses of *o*-terphenyl. Nearly 150 degrees below  $T_g$ , the glasses deposited at  $0.4 T_g$  had up to 50% higher heat capacity than the ordinary glass. The extraordinarily high heat capacity difference was irreversibly erased on heating, which is consistent with large structural relaxations occurring in the glass. Glasses deposited at temperatures closer to  $T_g$  displayed the kinetic stability and low heat capacity expected of vapor-deposited glasses

produced at similar substrate temperatures. *o*-Terphenyl was the first system to demonstrate vapor-deposited glasses with low, high and ordinary heat capacity compared to the liquid-cooled glass.

## Chapter 1

### Introduction

Glasses are all around us including inorganic silicate glasses in windows and eyeglasses, polymeric glasses in bodies of airplanes, organic glasses in television screens and even metallic glasses in golf clubs and other sports equipment. As these numerous applications show, glasses can be made from many types of materials and are relevant to a wide range of technologies.<sup>1-4</sup> Without continued work in the field of glasses, it would not be possible to take advantage of the properties of amorphous solids in these applications. Yet despite decades of research, there are still many aspects of glasses that remain poorly understood.<sup>5-7</sup> However, common techniques such as calorimetry and physical vapor deposition can be exploited in new ways to continue to expand our knowledge.

In this thesis I will discuss the properties of glasses that have been prepared by physical vapor deposition (PVD) and measured with AC nanocalorimetry. There are a variety of ways glasses, or amorphous solids, can be made and the preparation method can influence the properties of the glass. While PVD is often used to prepare glasses, the importance of selectively controlling the deposition conditions to prepare glasses with different properties is a relatively new and underutilized idea. By optimizing the substrate temperature and deposition rate, low enthalpy glasses with high density and high kinetic stability can be produced.<sup>8-12</sup> These glasses have been aptly termed 'stable glasses'. The heat capacity of such glasses has been measured with conventional calorimetry,<sup>8, 10</sup> but with that technique the sample size cannot be scaled down to measure the properties of

more technologically relevant thin films. Nanocalorimetry, however, is a calorimetric technique that can be used to investigate samples as thin as a few nanometers.<sup>13-15</sup> This thesis will describe nanocalorimetry measurements on vapor-deposited glasses of four different organic molecules:  $\alpha,\alpha,\beta$ -tris-naphthylbenzene ( $\alpha\alpha\beta$ -TNB), *cis*- and *trans*-decahydronaphthalene (*cis*- and *trans*-decalin) and *ortho*-terphenyl (OTP). Glasses of  $\alpha\alpha\beta$ -TNB were vapor-deposited using the conditions<sup>9-10</sup> that have been shown to maximize the stability of the glass and the characteristics of the vapor-deposited glass were investigated as a function of film thickness. The effect of the deposition temperature on the reversing heat capacity of vapor-deposited glasses was determined for decalin and OTP. Vapor-deposited glasses of pure *cis*-decalin and also various compositions of *cis/trans*-decalin mixtures were studied.

This chapter will provide the context for the original research presented in this thesis. The first section will give a general background on supercooled liquids and glasses. The next section will describe methods of preparing glasses, paying particular attention to physical vapor deposition. After that, calorimetric techniques, including nanocalorimetry, will be discussed as tools for studying supercooled liquids and glasses. Last, an overview of vapor-deposited glasses and the range of properties they can demonstrate will be presented.

## **1.1 Supercooled liquids and glasses**

As a liquid is cooled below the melting point there are two different routes that can be followed. The liquid can solidify into a crystal, or it can remain liquid in what is termed

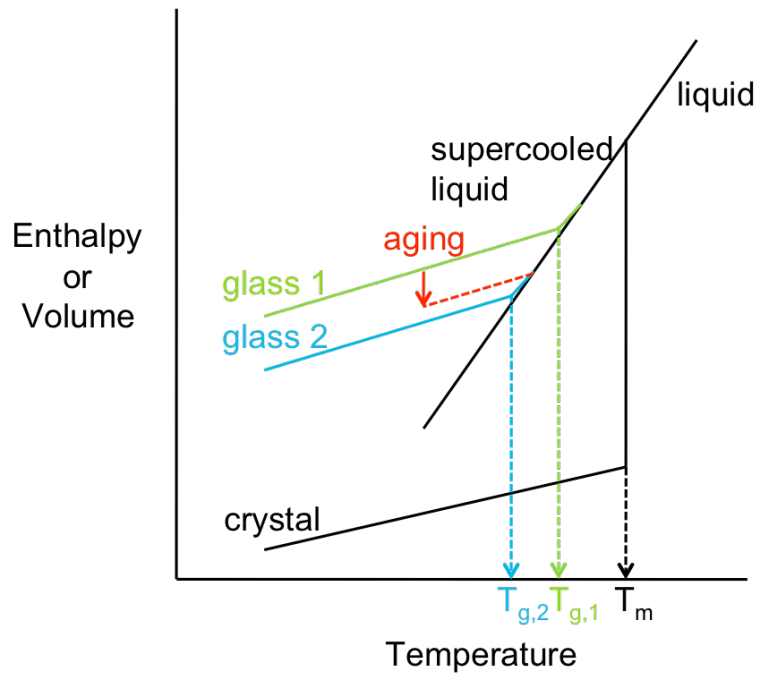


**Figure 1.1.** Schematic of the enthalpy or volume as a function of temperature. Glasses can be prepared by cooling a liquid below the melting point ( $T_m$ ) while avoiding crystallization. Glass 2 was prepared by cooling at a slower rate than was used to prepare glass 1;  $T_{g,2}$  and  $T_{g,1}$  represent, respectively, the glass transition temperatures of glass 2 and glass 1. The red arrow represents the evolution of the glass as it is aged.

the 'supercooled liquid'. Figure 1.1 shows a plot of enthalpy or volume vs. temperature. At high temperature, the liquid is the equilibrium state of the material. At the melting point, denoted by  $T_m$ , the crystal becomes the equilibrium state of the material; crystallization is accompanied by an abrupt change in the volume and enthalpy. However, because crystallization is a nucleation and growth process, it does not occur instantaneously at the melting point. Both nucleation and growth processes are dependent on temperature and there are particular temperatures that maximize the rates of the processes. When these temperature dependences are known, the critical cooling rate, or the cooling rate above which crystallization can be completely avoided, can be determined.<sup>16-17</sup> When crystallization is slow on the timescale of the cooling rate, the molecules continue to follow the supercooled liquid line. However, eventually a temperature is reached where the molecules can no longer rearrange on the timescale of the experiment and the system falls out of equilibrium. The temperature where this occurs is known as the glass transition temperature, below this temperature the system is termed a 'glass'. The green and blue lines in the schematic represent two different glasses. Glasses have the mechanical properties of a solid, but lack the long-range order associated with crystals.

Though the glass transition appears similar to a second order phase transition, it is actually kinetic in nature – the glass transition temperature depends on the rate at which the system is cooled. Figure 1.1 shows glasses prepared by cooling at two different rates. Glass 2 was cooled at a slower rate than glass 1 and thus was able to maintain the supercooled liquid equilibrium to lower temperatures. The glass prepared by slower

cooling has lower enthalpy and volume than the fast-cooled glass.<sup>8, 18</sup> For typical organic glassformers, decreasing the cooling rate by an order of magnitude decreases the glass transition temperature by  $\sim 3$ -4 degrees. Remaining in equilibrium to lower temperatures requires ever increasing amounts of time to be spent cooling the liquid; in order to decrease the standard glass transition temperature, which is measured at a rate of 10 K/min, by 10 degrees, one would have to cool at  $\sim 15$  K/day.

Due to the non-equilibrium nature of glasses, the glass evolves in time towards the equilibrium supercooled liquid state. The properties of the glass such as the enthalpy and volume slowly approach the equilibrium values. This time evolution of the glass is known as aging and is represented by the red downward arrow in Figure 1.1. The equilibrium, or structural, relaxation time defines the time required for the system to reach equilibrium at a given temperature. Conventionally, the structural relaxation time is 100 s at  $T_g$  and increases by roughly an order of magnitude for every 3-4 degrees the temperature is decreased below  $T_g$  for organic glass formers. At this rate, aging a glass to equilibrium at a temperature only ten degrees below  $T_g$  will take on the order of one day. Similar to using slower cooling rates to access the equilibrium supercooled liquid at lower temperatures, the timescale associated with aging a glass to equilibrium quickly becomes too long to be experimentally feasible.

## **1.2 Glass preparation methods**

Quenching from the liquid, as described above, is one way to make glasses, but the amorphous phase can be reached by a number of other routes as well. For some materials,



the critical cooling rate to avoid crystallization is unattainable with normal laboratory quenching methods and thus cooling from the liquid is not a viable means for making a glass of that material. However, amorphous solids can also be quenched from other starting states such as crystalline solids, solutions, and the vapor phase.<sup>19</sup>

Crystalline materials can be converted into amorphous solids through disruption of the crystalline order by such means as irradiation, pressurization and mechanical techniques including ball milling or grinding. When crystalline solids are bombarded with high-energy ions, neutrons and electrons the structural damage to the long-range order can cause amorphization of the material. This glass preparation method is well documented for quartz.<sup>20</sup> Pressurization can be used to make a glass from a crystal because at high pressures and low temperatures, a transition from crystalline to amorphous solid can occur. For example, in one ice polymorph the melting temperature decreases with increasing pressure. If this is carried out below the glass transition temperature, ice will “melt” into an amorphous solid.<sup>21-22</sup>

Three common methods of obtaining amorphous solids from solution are drying from gels, precipitation from solution and electrolytic deposition. In the first method, a solution can be converted to a gel by hydrolysis and then completely drying the gel yields a glass.<sup>23-25</sup> Amorphous precipitates are common products in aqueous solution reactions, therefore this is another route to glass formation. In fact, many sulfide compounds with arsenic, antimony and germanium always precipitate in the amorphous form and are used

in gravimetric analysis.<sup>26-27</sup> While these methods are useful for making some glassy materials, they are not generally applicable; they are limited to particular compounds.

Besides cooling from the liquid, the most universal method of producing glasses begins in the vapor phase.<sup>28</sup> Physical vapor deposition (PVD) is a useful technique because elements, organic and inorganic compounds, alloys, and mixtures can all be vapor-deposited, and amorphous or crystalline films can be formed depending on the deposition conditions. The three main types of PVD are thermal deposition, sputtering and ion plating. While the details of each deposition method can vary, there are three basic steps common to all of the types: 1. creation of the vapor phase species, 2. transport from the source to the substrate, and 3. film growth on the substrate.<sup>29-30</sup> The next few paragraphs will focus on how these steps particularly apply for thermal deposition, as it is the most relevant to this thesis work.

The material to be deposited can either be sublimed or evaporated into the gas phase, depending on its initial state, i.e. solid or liquid. The number of molecules in the gas phase is determined by the vapor pressure. The vapor pressure is the equilibrium pressure of a vapor over the solid or liquid and it is a function of temperature, so changing the temperature of the source material alters the number of molecules that are in the gas phase and thus available for deposition. The Hertz-Knudsen equation gives the evaporation rate of material vaporizing from the source:

$$\frac{dN}{A dt} = C(2\pi mkT)^{-1/2}(p^* - p) \quad (1.1)$$

where  $dN/Adt$  is the rate of evaporating molecules per unit area,  $C$  is related to the sticking coefficient,  $m$  is the mass of the vaporized species,  $k$  is Boltzmann's constant,  $T$  is the temperature,  $p^*$  is the vapor pressure of the material at temperature  $T$ , and  $p$  is the pressure of the vapor above the source. When  $p = 0$  and  $C = 1$ , the evaporation rate is maximized. Typical deposition rates for thermal deposition processes are 1-10 nm/s.

In order to minimize the effect of  $p$  in equation 1.1, physical vapor deposition is carried out in a vacuum environment. Typical base pressures prior to deposition range from  $10^{-5}$  to  $10^{-9}$  torr. At these low pressures, the mean free path is long enough that molecules will experience little to no collisions in the gas phase before reaching the substrate. Depositions that occur in this manner are termed 'line of sight' because only molecules with a direct line from the source to the substrate will contribute to the deposition. In line of sight depositions the sticking coefficient, or the probability of a molecule staying on a surface it impinges on, is equal to one. Surfaces such as the chamber walls are at temperatures where the vapor pressure is negligible and impinging molecules are effectively trapped. When molecules strike the chamber walls, but do not stick it is called a 'random angle' deposition; the angles at which the molecules can approach the substrate are randomized by collisions. Working under high vacuum also reduces the number of contaminants in the chamber; one of the main advantages of PVD is the purity of films that can be deposited.

After the gas molecules travel through the vacuum chamber, they condense on the substrate and grow into a film. In the case of a point source and limited collisions in the gas phase, the flux distribution is described by a cosine distribution:

$$\frac{dm}{dA} = \left( \frac{E}{\pi r^2} \right) \cos^2 \theta \quad (1.2)$$

where  $dm/dA$  is the mass per unit area,  $E$  is the total mass evaporated,  $r$  is the distance from the source to the substrate and  $\theta$  is the angle from the normal to the substrate.<sup>29-30</sup> Directly above the source, the greatest thickness is deposited. For a random angle deposition or when there are many gas phase collisions, the cosine distribution no longer holds. Typical PVD film thicknesses range from a few nanometers to thousands of nanometers.

When vaporized molecules condense on a substrate, their thermal energy is quickly released and this influences the growth of the film. Because the “cooling rate” of condensing molecules is so rapid, vapor deposition is ideal for poor glassformers that easily crystallize on cooling the liquid. When cold substrate temperatures are utilized, arriving molecules are quickly locked into place and rearrangement into the crystal structure is prevented; as a result, amorphous solids are prepared instead. The mobility of depositing molecules in both crystalline and amorphous films can depend on the substrate temperature, substrate morphology and cleanliness, the deposition angle and interfacial reactions at the surface.<sup>30</sup> Often deposited films can have residual stress due to growth stresses or thermal expansion mismatch between the film and substrate.<sup>31-32</sup>

### 1.3 Calorimetric techniques for studying glasses

Calorimetry is the measurement of heat flow and a calorimeter is an object used to measure heat flow. The measurement of heat is useful because thermodynamic quantities such as heat capacity, enthalpy and entropy can subsequently be calculated. Calorimetric measurements date back to the late 1700's and are still useful today. The measurement techniques have continuously evolved and a number of more sophisticated calorimetry methods have been developed commercially over the last 50 years.<sup>33-37</sup> In particular, differential scanning calorimetry (DSC) is commonly used for studying amorphous materials. Hybrids of this method such as temperature modulated DSC and small-scale techniques such as microcalorimetry or nanocalorimetry are also utilized. In this section, the operating principles of these calorimetric methods are related, starting with the basics of DSC. For the work described herein, AC nanocalorimetry was the primary measurement technique.

In DSC, the temperatures of a sample pan and a reference pan are changed in a near identical fashion and the difference in heat applied to the two pans in order to keep them at the same temperature is measured. Generally, the sample pan is an aluminum pan containing the material of interest and the reference pan is an empty aluminum pan. By performing a differential measurement, the contribution of the pan itself is eliminated and the calorimetric signal is due solely to the response of the sample. Throughout the measurement, power is applied to the pan heaters to hold each pan at the temperature defined by a specified profile. When the sample releases or absorbs heat, the power to the

sample pan heater has to be compensated to maintain the two pans at the same temperature. The difference in the power applied to the two pans gives the heat ( $dQ$ ) needed to change the temperature of the sample ( $dT$ ). This is the constant pressure heat capacity ( $C_p$ ):

$$C_p \equiv \frac{dQ}{dT} = \left( \frac{dH}{dT} \right)_p \quad (1.3)$$

where  $H$  is enthalpy.

Constant pressure conditions are common in the laboratory, but the constant volume heat capacity ( $C_v$ ) can also be obtained by:

$$C_v = C_p - TV\alpha^2/\beta \quad (1.4)$$

where  $\alpha$  is the expansivity and  $\beta$  is the compressibility. Often experimental data for expansivity and compressibility are unavailable so it can be difficult to determine  $C_v$ . When the term 'heat capacity' is used through the remainder of the text, it refers to the constant pressure heat capacity. Enthalpy and entropy, however, can be determined exclusively from the heat capacity and temperature. From equation 1.3:

$$dH = C_p(T)dT \quad (1.5)$$

$$\Delta H = \int C_p(T)dT \quad (1.6)$$

Additionally, entropy is related to heat capacity by:

$$dS = \frac{C_p(T)}{T} dT \quad (1.7)$$

$$\Delta S = \int \frac{C_p(T)}{T} dT \quad (1.8)$$

DSC is a heavily utilized technique for studying glasses because the heat capacity and enthalpy provide a great deal of information about the system. As will be described in the next section, these properties and other related quantities can be used to compare different glasses of the same material as well as glasses of different materials. The solid lines in Figure 1.2 show typical heat capacity (red) and enthalpy (blue) curves for glasses, as measured with DSC. At low temperature the material is in the glassy state and increasing the temperature mainly contributes to vibrational motions. In the liquid, thermal energy is required to change the structure of the material as well as the vibrational motion, thus the liquid has a greater heat capacity. At the glass transition, a step in the heat capacity is observed. Typically the glass transition temperature is defined at the midpoint of the heat capacity step; the onset temperature is the temperature where the heat capacity first begins to deviate from the glass heat capacity. Higher onset temperatures indicate the glass is more kinetically stable because higher temperatures are required to dislodge the molecules from the glass. The enthalpy curve is obtained by integrating the area under the heat capacity curve; increases in the heat capacity cause the slope of the enthalpy to become steeper.

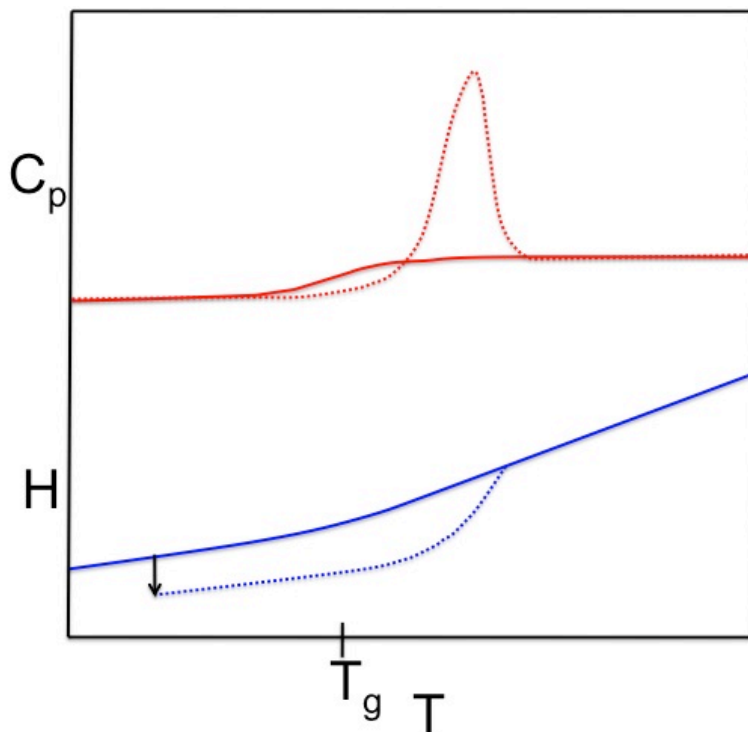


**Figure 1.2.** Schematic of heat capacity and enthalpy curves representative of the results from a DSC measurement. The solid lines represent an unaged glass; the dotted lines represent a glass that has been aged according to the black arrow. The glass transition temperature is denoted by  $T_g$ .



As mentioned in the first section, the enthalpy of a glass slowly evolves toward the equilibrium supercooled liquid value as the system is aged. The downward solid arrow in Figures 1.1 and 1.2 denotes aging. The dotted lines in Figure 1.2 show the heat capacity and enthalpy curves of an aged glass. Because the system has evolved to lower enthalpy, more heat is required to warm the glass into the supercooled liquid. This results in a peak in the heat capacity curve known as the enthalpy overshoot peak. As the aging time is increased, the peak becomes larger and shifts to higher temperature.<sup>8</sup> A value termed the fictive temperature is determined by extrapolating the supercooled liquid enthalpy to intersect the enthalpy of the aged glass. The fictive temperature is the temperature at which the glass exhibits the same enthalpy as that of the equilibrium liquid.<sup>38</sup> Fictive temperatures lower than  $T_g$  indicate a glass that is more energetically stable, while a fictive temperature greater than  $T_g$  indicates a glass that is less stable. This quantification of stability is a useful metric for comparing different glasses of the same material.

Temperature modulated DSC (TMDSC) was introduced twenty years ago as an extension to DSC.<sup>34</sup> In this technique, a sinusoidal temperature oscillation is superimposed onto the DSC temperature profile. Equation 1.9 defines the temperature profile in a TMDSC experiment:

$$T = T_0 + \beta t + A \sin(\omega t) \quad (1.9)$$

where  $T_0$  is the initial temperature,  $\beta$  is the heating rate and  $A$  and  $\omega$  are the amplitude and frequency of the oscillation. Commonly, the heat flow in TMDSC is separated into reversing and non-reversing heat capacity.<sup>34, 39-40</sup> Generally speaking, the reversing heat flow is

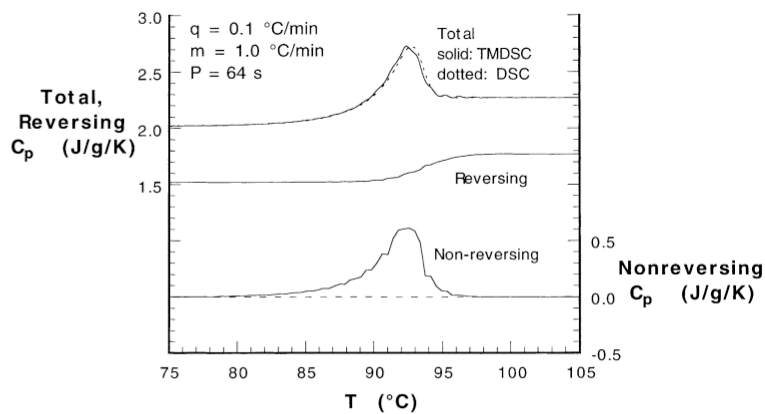


**Figure 1.3.** TMDSC heat capacity curves of aged polystyrene, divided into the reversing and non-reversing components. The total heat capacity from TMDSC and conventional DSC are also shown. Reprinted from reference 39 with permission from Elsevier.

associated with heat capacity changes while the non-reversing heat flow is associated with irreversible kinetic effects such as the enthalpy overshoot peak. Figure 1.3 shows the total heat capacity for a glass as broken down into the reversing and non-reversing components. As discussed above, the cooling rate determines where the supercooled liquid falls out of equilibrium and thus the glass transition temperature.  $T_g$  is also frequency dependent and thus the dynamic glass transition observed with TMDSC depends on the frequency of the applied oscillation.<sup>39</sup>

In addition to temperature ramps, TMDSC can also be used for isothermal measurements. During such measurements, the base temperature is held constant while a temperature oscillation is applied; these measurements are termed quasi-isothermal TMDSC. With this technique, slow transitions such as the crystallization of polymers can be observed as a function of time.<sup>41-42</sup> The heat capacity evolves from that of the liquid to that of the crystal, while the change in heat capacity at any given time is proportional to the fraction of the polymer that has crystallized. As will be seen below, the kinetics of stable glass transformation can also be tracked with quasi-isothermal measurements.

As relevant samples become thinner, measurement techniques likewise have to be able to measure smaller quantities. For DSC and the specialized DSC methods described above, the sensitivity of the measurement is limited by the symmetry of the reference and sample pans. As the sample and thus the signal becomes smaller, the asymmetry becomes a larger contribution to the heat capacity signal. Eventually a point is reached where the sample heat capacity can no longer be distinguished from the noise. One solution to this

problem is to reduce the addenda heat capacity, i.e. the heat capacity of the calorimeter itself.<sup>15, 35</sup> This has been achieved in practice by microfabricating devices that can function as small-scale calorimeters. These devices have thin silicon nitride membranes that serve as the ‘pan’ and a heater and thermopile are integrated into the membrane to change and monitor the temperature. Microcalorimeters and later nanocalorimeters have been fabricated by a number of groups<sup>43-44</sup> and are now also commercially available<sup>35-36</sup> to measure the heat capacity of films as thin as a few nanometers. Similar to the methods described above, nanocalorimetry measurements can be performed as scanning experiments or AC modulated experiments.<sup>14, 45-47</sup> Due to the fact that heating is localized to very small areas and masses, scanning rates over  $10^5$  K/s can be achieved.<sup>48</sup>

Figure 1.4 shows the commercially available chip sensor used for the nanocalorimetry measurements in this thesis. The silicon nitride membrane is approximately one micron thick. In the center of the membrane is the  $60 \times 60 \mu\text{m}$  active measurement area, bracketed by the heaters. The hot junction of the thermopile is located in the active area while the cold junction is on the silicon frame. To maximize the sensitivity, a differential setup is utilized.

All of the reversing heat capacity data reported in the original work presented here was measured using AC temperature modulated nanocalorimetry. Analogous to TMDSC, an AC voltage is applied to the nanocalorimeter heaters to superimpose a small oscillation on the specified temperature profile. The complex amplitude of the differential thermopile signal ( $\Delta U$ ) is proportional to the heat capacity<sup>14</sup>:

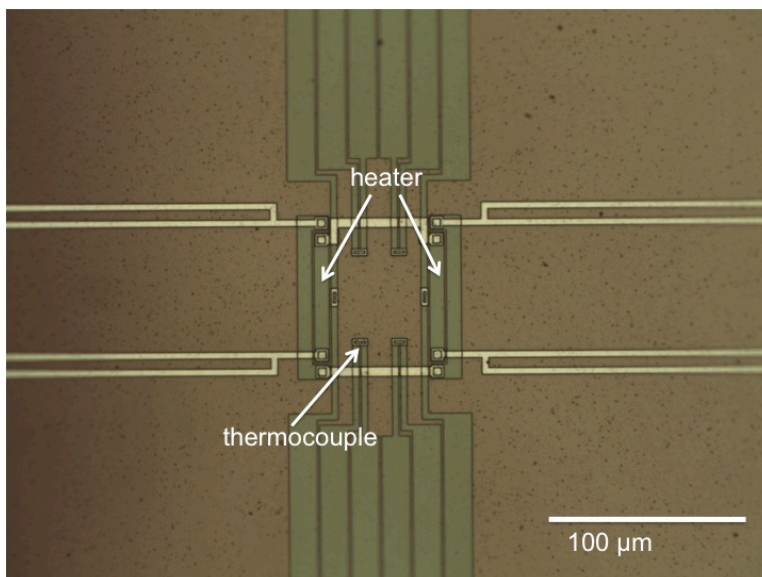


**Figure 1.4.** Image of Sensor Integration XEN-39391 nanocalorimeter membrane. The center active area is bracketed by the heater and measures  $60 \times 60 \mu\text{m}$  for this particular sensor. The hot junctions of the thermopile are located within the active area; one of the six thermocouples is indicated.

$$\Delta U = \frac{P_0}{Si\omega c_R} - \frac{P_0}{Si\omega c_S} \quad (1.10)$$

where  $P_0$  is the power applied to the heaters,  $S$  is the sensitivity,  $\omega$  is the angular frequency and  $c_R$  and  $c_S$  are the heat capacity of the reference and sample sensor, respectively. As with TMDSC, quasi-isothermal experiments can also be performed to measure kinetic events that occur over long timescales.

#### 1.4 Vapor-deposited glasses and stability

Vapor deposition can be used to make glasses with a wide array of properties. Originally this technique was mainly used to prepare glasses of materials that easily crystallized on cooling and thus deposition onto cold substrates was desirable.<sup>49-50</sup> Based on these early measurements, vapor-deposited glasses were considered to have glass transition temperatures comparable to the liquid-cooled glass, but higher enthalpy and lower density, i.e. vapor-deposited glasses were less stable.<sup>51-54</sup> Despite being an important factor in the deposited structure of crystalline materials,<sup>55-56</sup> the substrate temperature was rarely taken into consideration for vapor-deposited glasses. In the last decade, however, numerous reports have been made exemplifying the exceptional stability of glasses deposited at substrate temperatures closer to  $T_g$ .<sup>8-12, 57</sup>

The remainder of this section is divided into three parts. The first subsection will focus on the properties of glasses deposited at low substrate temperatures. Next the stability of vapor-deposited glasses as a function of deposition temperature will be discussed. As will be seen, the optimal substrate temperature for producing stable glasses

of many materials is near  $0.85 T_g$ . Finally the exceptional properties observed for stable glasses will be summarized and the systems for which this behavior has been reported so far will be recounted.

#### **1.4.1 Low stability glasses deposited on low temperature substrates**

The pioneering quantitative work on vapor-deposited glasses was performed by Suga and coworkers using adiabatic calorimetry and differential thermal analysis.<sup>54, 58-59</sup> In their work,<sup>51-54, 58-60</sup> cold substrate temperatures were utilized to ensure that the deposited films of the small organic molecules would indeed be amorphous rather than crystalline. The properties of the vapor-deposited glasses were compared to the properties of a liquid-cooled glass of the same material for two of the systems that were studied: 1-pentene and butyronitrile. A glass of 1-pentene ( $T_g = 70$  K) was vapor-deposited into an adiabatic calorimeter held at temperatures between 38 and 47 K, which is  $0.54-0.67 T_g$ . The liquid-cooled glass was prepared by cooling the supercooled liquid at a rate of 3 K/min. Heat capacity curves were collected for both samples from 12 K to above the glass transition temperature. A similar investigation was done for butyronitrile ( $T_g = 97$  K). Vapor-deposited glasses of two different substrate temperatures, 40 K ( $0.41 T_g$ ) and 67 K ( $0.69 T_g$ ), were measured, as well as a glass prepared by cooling the liquid at a rate of  $\sim 10$  K/min.

The vapor-deposited glasses of each molecule had the same glass transition temperature as the corresponding liquid-cooled glass and the heat capacities of the glasses prepared by the two different methods were essentially identical at all but the lowest temperatures. However, the configurational enthalpy of the vapor-deposited glasses was

much larger than that of the liquid-cooled glass. For 1-pentene, the total enthalpy change for the vapor-deposited glass exceeded 1 kJ/mol.<sup>53</sup> For butyronitrile, the configurational enthalpy of the glass deposited at 40 K was higher than that of the glass deposited at 67 K, with values of 1.33 kJ/mol and 0.80 kJ/mol, respectively.<sup>51</sup> Within a given system, deposition at lower substrate temperature results in higher configurational enthalpy. For comparison, the liquid-cooled butyronitrile and 1-pentene glasses had configurational enthalpy values of  $\sim 0.1$  kJ/mol. The observed difference in configurational enthalpy indicates the structure of the vapor-deposited glass is much more unstable than that of the liquid-cooled glass and is consistent with the idea that the deposited molecules on a whole have weaker interactions than in liquid-cooled glasses.

The configurational enthalpy of the vapor-deposited glasses of 1-pentene and butyronitrile showed large structural relaxation at temperatures far below  $T_g$ . Figure 1.5 shows the enthalpy relaxation curves for the vapor-deposited and liquid-cooled butyronitrile glasses. As described above, both of the vapor-deposited glasses have much higher configurational enthalpy compared to the liquid-cooled glass, but the initial configurational enthalpy is higher for the glass deposited at the lower temperature. On heating, the enthalpies of the vapor-deposited glasses stay approximately constant until the respective deposition temperatures are reached; then the enthalpy relaxation begins. The enthalpy relaxation paths of the two vapor-cooled glasses are quite similar at temperatures above  $\sim 80$  K. The liquid-cooled glass, on the other hand, does not show relaxation behavior



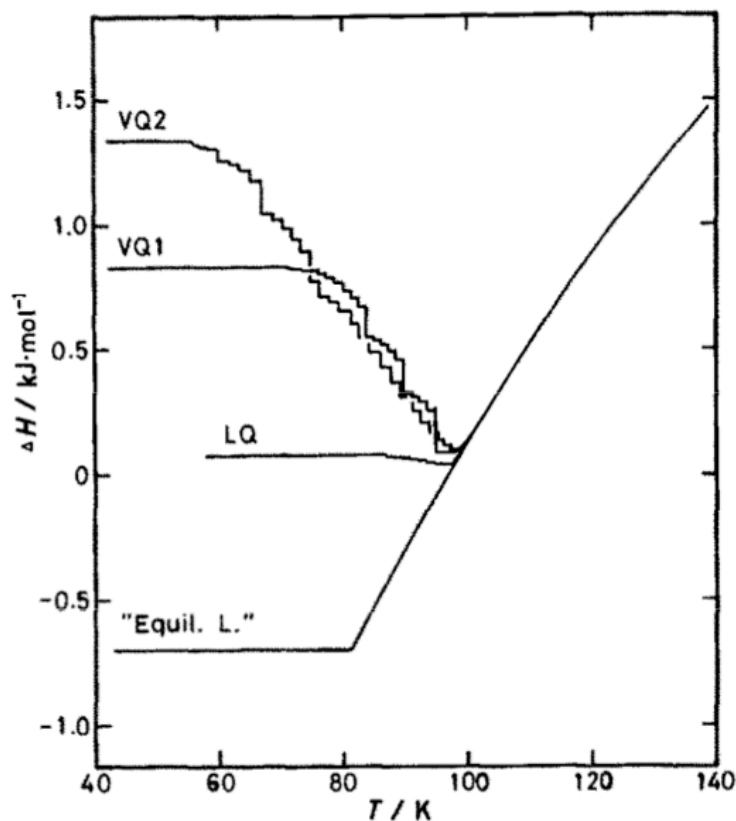


**Figure 1.5.** Configurational enthalpy of butyronitrile glasses. The curves labeled VQ2, VQ1 and LQ correspond to the glasses deposited at 40 K and 67 K and the liquid-quenched glass, respectively. The configurational enthalpy follows the temperature profile of the measurement; vertical lines correspond to temperatures where the samples were annealed for some period of time. "Equil. L." corresponds to the equilibrium liquid line derived from extrapolated equilibrium heat capacity values. Reprinted from reference 51 with permission from Elsevier.

until closer to the glass transition temperature. The authors interpreted the evolution of the vapor-deposited glasses in terms of formation of cluster structures during deposition.<sup>54</sup> Depositing at low temperature limits the size of the clusters, but as the temperature is increased, molecular rearrangement becomes possible and short-range order can be developed. This is manifested as the low temperature enthalpy stabilization (decrease); the small clusters of the vapor-deposited glass grow to be the size of the clusters in the liquid-cooled glass. At that point, the two glasses will have the same behavior and thus the same glass transition temperature, as was observed.

Because the vapor-deposited glasses have high enthalpy, this also translates to the glasses having high fictive temperatures. In fact, the fictive temperatures of the vapor-deposited glasses of 1-pentene and butyronitrile were up to 15 and 35 K higher than  $T_g$ , respectively. This means that the enthalpy of the vapor-deposited glass is equivalent to that of the equilibrium supercooled liquid far above  $T_g$  and the vapor-deposited glasses are less energetically stable than the liquid-cooled glass. The glasses made by vapor-deposition also had large residual entropy by comparison, implying large-scale disorder in the molecular arrangement and conformation of the glass. Based on the properties displayed by 1-pentene and butyronitrile, it was a commonly held notion that all vapor-deposited glasses would be similarly unstable as compared to the liquid-cooled glass. In the next two subsections, results to the contrary will be presented.

In addition to the thermodynamic variables discussed above, the volume and density of glasses deposited at low substrate temperatures have also been reported. In one

set of measurements, glasses of toluene, ethylbenzene and propylbenzene were deposited at 78 K, which corresponds to 0.62-0.68  $T_g$  for these molecules.<sup>61</sup> The intensity of laser light reflected off the samples was related to the interference between the light reflected at the substrate and vacuum interfaces. Based on the changes in intensity during the measurement, the refractive index, density and thickness of the glasses were calculated.

The changes in the refractive index and molar volume associated with heating a vapor-deposited glass of ethylbenzene are shown in Figure 1.6. The dotted line is an extrapolation of the supercooled liquid volume. The as-deposited ethylbenzene glass has 7% larger molar volume than the extrapolated supercooled liquid, as measured at the deposition temperature of 78 K. Vapor-deposited toluene and propylbenzene likewise had 4% and 10%, respectively, higher molar volume than their corresponding extrapolated supercooled liquid at 78 K. These results indicate that longer substituents are associated with larger initial excess volumes. Based on the initial molar volume, Ishii et al. report the fictive temperatures of the vapor-deposited glasses were 124 K ( $T_g + 7$  K), 150 K ( $T_g + 35$  K), and 195 K ( $T_g + 69$  K) for toluene, ethylbenzene and propylbenzene, respectively.<sup>61</sup>

The authors estimated the excess enthalpy of the ethylbenzene vapor-deposited glass based on the molar volume.<sup>61</sup> Two approximations went into the estimation: (1) the energy to generate a void in a liquid is approximately half the energy required to evaporate the number of molecules that would fill the void volume and (2) the enthalpy of vaporization at low temperature is a little larger than that at room temperature. Using this

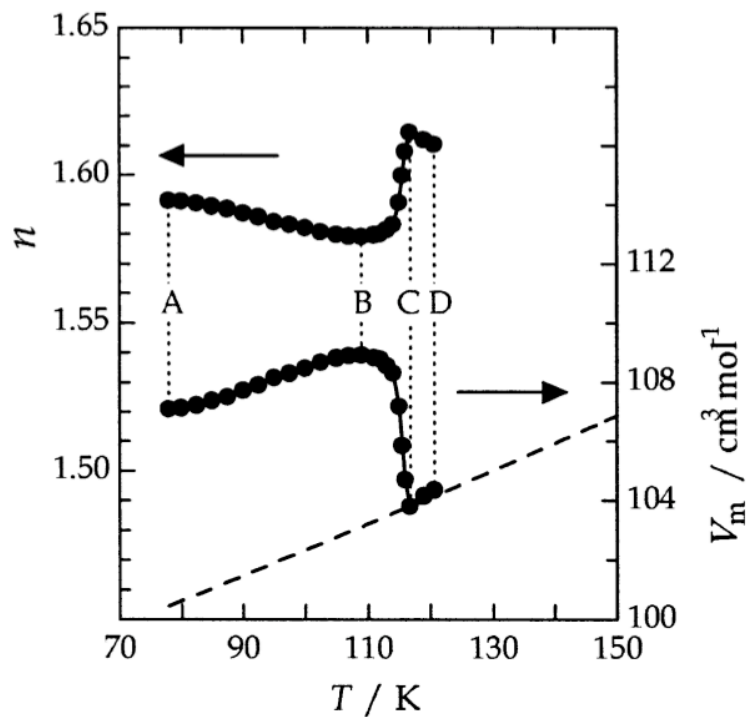


**Figure 1.6.** Index of refraction and molar volume of a vapor-deposited glass of ethylbenzene. The dotted line shows the extrapolated molar volume of the supercooled liquid. Reprinted with permission from reference 61. Copyright 2003 American Chemical Society.

estimation, the 7% difference in molar volume was equated to  $\sim 2$  kJ/mol excess enthalpy, which is on par with the 1-pentene and butyronitrile measurements.<sup>51, 53, 61</sup>

Other reflected light intensity measurements on vapor-deposited organic glasses also showed features consistent with a poorly packed glass. The phenyl halides fluorobenzene, chlorobenzene and bromobenzene were deposited at substrate temperatures down to 15 K.<sup>62-63</sup> The reflected light intensity was monitored during deposition and in all depositions except that of the highest substrate temperature glass, the light intensity decreased after a period of deposition. Furthermore, the lower the substrate temperature, the less time elapsed before the intensity decrease was observed. This effect was interpreted as inhomogeneity in the molecular density.<sup>62</sup> At low deposition temperatures, the arriving molecules are rapidly frozen at positions of local potential minima and continued deposition builds voids into the poorly packed molecular structure, potentially explaining the light scattering. Low substrate temperatures yielding poorly packed vapor-deposited glasses are consistent with the molar volume results presented above.

Another inference of low density in vapor-deposited glasses comes from an inelastic neutron scattering study. A propene glass was vapor-deposited at 20 K (0.36  $T_g$ ) and compared to a propene glass that was annealed at  $T_g$ .<sup>64</sup> A broad low energy excitation peak was observed in both samples, but that of the as-deposited glass had more vibrational modes associated with it. This result was interpreted as the annealed glass being more ordered and dense. The density of states difference between the as-deposited and annealed

glass was greatest in the low energy region. As the authors point out, it is logical that the low energy region is affected by annealing because those modes reflect the density of states of vibrations of loosely packed structures.<sup>64</sup> Thus annealing densifies poorly packed vapor-deposited glasses.

#### 1.4.2 Stability as a function of substrate temperature

Based on the data presented above, it was generally accepted that vapor-deposited glasses had higher enthalpy and were less dense than glasses cooled from the liquid. In 2007 the first papers were published challenging that idea and showing that the deposition temperature was instrumental in controlling the properties of the as-deposited glass.<sup>8-9</sup> The earlier results were not contradicted, but instead extended to higher substrate temperatures relative to  $T_g$  to show that a range of properties can be obtained for vapor-deposited glasses.

Vapor-deposited glasses of indomethacin (IMC) can have *lower* enthalpy than the corresponding liquid-cooled glass. IMC ( $T_g = 315$  K) was vapor-deposited into DSC pans held at substrate temperatures between 0.6-1.0  $T_g$ .<sup>8</sup> DSC scans were measured for the as-deposited glasses, then the liquid was cooled to produce the ordinary liquid-cooled glass and a second DSC scan was collected. The resulting heat capacity curves were used to determine the enthalpy, fictive temperatures and onset temperatures of the vapor-deposited glasses. Figure 1.7 summarizes the fictive temperature of the as-deposited glass as a function of the deposition temperature. The fictive temperature is a measure of the enthalpic stability of the glass. The lower the fictive temperature of the glass, the lower the

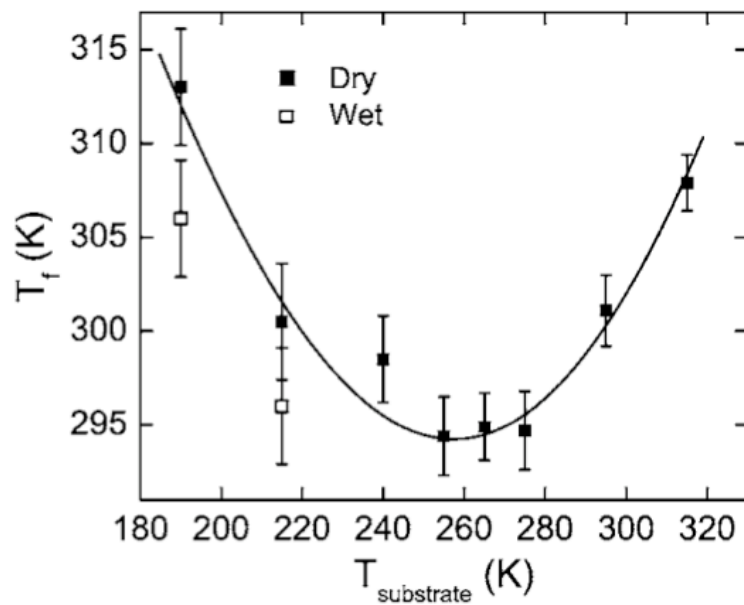


**Figure 1.7.** Fictive temperature of vapor-deposited glasses of indomethacin as a function of substrate temperature. Reprinted with permission from reference 8. Copyright 2007, American Institute of Physics.

enthalpy. As can be seen in Figure 1.7, the fictive temperature and thus energy of IMC vapor-deposited glasses is minimized for deposition temperatures near 265 K ( $\sim 0.85 T_g$ ); the fictive temperature is 20 K lower than the liquid-cooled  $T_g$ . This corresponds to an enthalpy that is 8 J/g lower than that of the glass cooled from the liquid.<sup>8</sup> This is the opposite behavior from what is expected for vapor-deposited glasses based on low substrate temperature depositions.

The kinetic stability of vapor-deposited glasses of IMC was also influenced by the deposition temperature. The onset temperature is a measure of the kinetic stability of a glass; it reflects how high the material can be heated before becoming a liquid. Higher onset temperatures indicate greater kinetic stability. The onset temperatures were determined from the heat capacity curves and are shown in Figure 1.8. Similar to the fictive temperature results, the kinetic stability of vapor-deposited glasses of IMC is also maximized near  $0.85 T_g$ , with the onset temperatures and thus kinetic stability decreasing in either direction with substrate temperature.<sup>8</sup> The low temperature vapor-deposited glasses reported in the previous section exhibited glass transition temperatures similar to the corresponding liquid-cooled glass. In contrast, the onset temperatures of IMC vapor-deposited glasses are shifted to above and then below the onset temperature of the ordinary liquid-cooled glass (315 K) as the substrate temperature is decreased.

The substrate temperature dependence of the stability of vapor-deposited glasses has also been measured in thinner films and with smaller molecules. Fast-scanning nanocalorimetry was used to measure 100 nm thick vapor-deposited glasses of toluene ( $T_g$



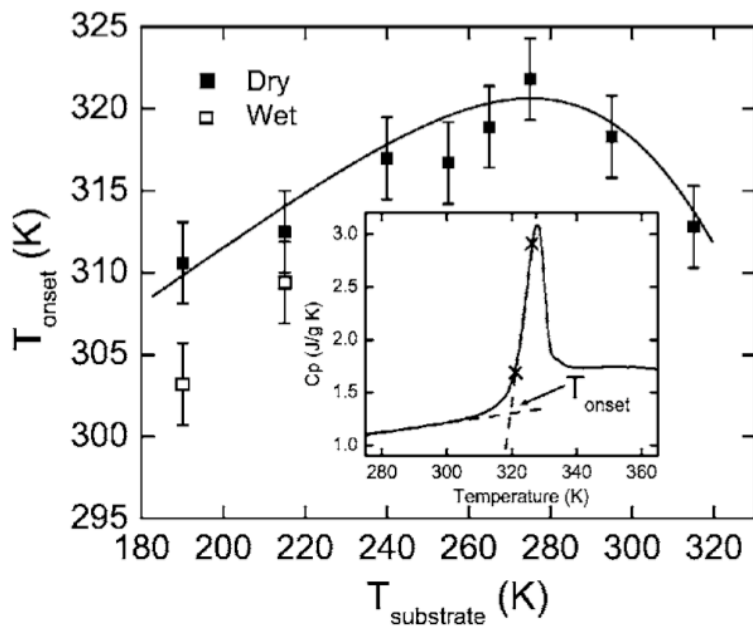


**Figure 1.8.** Onset temperature of vapor-deposited glasses of indomethacin as a function of substrate temperature. The inset shows how the onset temperature is determined. Reprinted with permission from reference 8. Copyright 2007, American Institute of Physics.

= 117 K) and ethylbenzene ( $T_g = 115$  K) deposited at temperatures between  $\sim 0.77 T_g$  and  $T_g$ .<sup>12</sup> The design of the apparatus limited the substrate temperatures to values of 90 K and above. For both materials, the fictive temperature decreased with substrate temperature while the onset temperature increased. Similar to indomethacin, the vapor-deposited glasses had enhanced stability as compared to the liquid-cooled glass.

Low substrate temperature glasses exhibit low density compared to the ordinary liquid-cooled glass, but similarly to how the enthalpy can vary across the substrate temperature range, the density has also been found to vary with deposition temperature. Glasses of  $\alpha,\alpha,\beta$ -tris-naphthylbenzene ( $\alpha\alpha\beta$ -TNB) were vapor-deposited at substrate temperatures ranging from  $\sim 0.7 T_g$  to  $T_g$  (242 to 342 K).<sup>65</sup> The thickness of the as-deposited films was determined with x-ray reflectivity at room temperature. The glasses were then annealed near  $T_g$  for one day before cooling to room temperature and measuring the thickness of the liquid-cooled glass. The ratio of the densities of the vapor-deposited and liquid-cooled glasses is determined from the ratio of the thicknesses. Figure 1.9 shows the density ratio as a function of deposition temperature for two different deposition rates. For every substrate temperature, the density of the vapor-deposited glass is greater than that of the liquid-cooled glass.<sup>65</sup> Within a given deposition rate, glasses deposited near  $0.85 T_g$  exhibited the largest as-deposited density; the maximum density increase over the liquid-cooled glass was  $\sim 1.4\%$ . Slower deposition rates also led to a greater enhancement in the density.

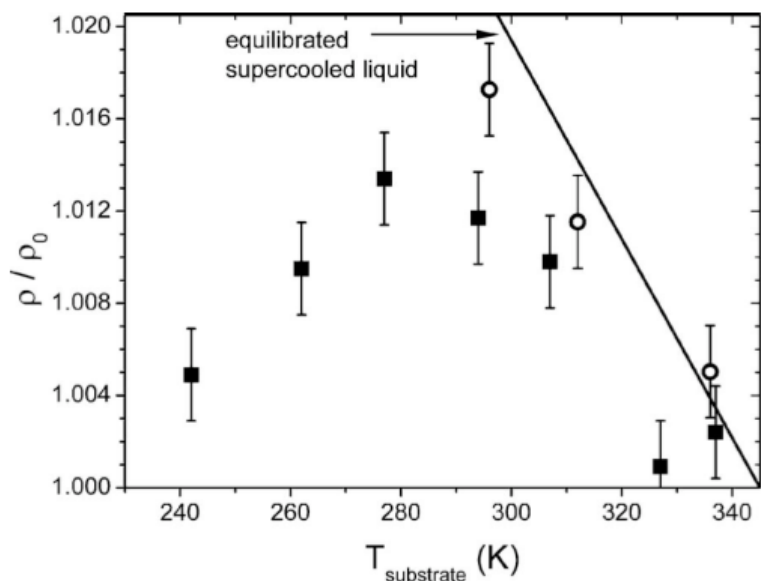


**Figure 1.9.** Density of vapor-deposited glasses of  $\alpha,\alpha,\beta$ -tris-naphthylbenzene. The samples were deposited at the temperatures given by the abscissa at a rate of  $\sim 0.25$  nm/s (solid squares) or  $\sim 0.12$  nm/s (open circles). The density is relative to that of the liquid-cooled glass and the solid line is an extrapolation of the supercooled liquid equilibrium line. Reprinted with permission from reference 65. Copyright 2008, American Institute of Physics.

The effect of substrate temperature on the molar volume of vapor-deposited alkylbenzene glasses has also been reported. Toluene, ethylbenzene, propylbenzene and isopropylbenzene were deposited at substrate temperatures ranging from  $\sim 0.6 T_g$  to  $T_g$ .<sup>11</sup> For each system, substrate temperatures up to  $\sim 0.85 T_g$  yielded glasses with larger initial molar volume than the extrapolated supercooled liquid. Above  $\sim 0.85 T_g$ , the initial molar volume was less than that predicted for the supercooled liquid.

The same logic that was used to understand the properties of glasses deposited at low substrate temperature can be extended to understand the properties of vapor-deposited glasses at all substrate temperatures. At low deposition temperatures the mobility of the depositing molecules is limited. The molecules are unable to find efficient packing and voids are built into the film, yielding glasses that have high enthalpy and low density. As the deposition temperature is increased, arriving molecules can take advantage of the mobile surface layer<sup>8, 66</sup> and explore the energy landscape for stable configurations. During the deposition process, all of the molecules spend some amount of time in the mobile surface layer before getting buried into the bulk. As a result, glasses with low enthalpy and high density can be made from the bottom up. Close to the glass transition temperature, the molecules rapidly equilibrate to the supercooled liquid structure and enhanced stability is not observed.

Mobility on the surface of glasses has been inferred or measured by a number of techniques. Reports of thin films of polystyrene having lower glass transition temperatures than bulk films are numerous.<sup>67-69</sup> The lower  $T_g$  has been credited to a mobile surface layer;

for thinner films the surface layer is a larger percent of the film and thus contributes more to the observed properties. Mobility has been measured directly by Cowin and coworkers<sup>70</sup> for 3-methylpentane. In that study, molecular beam epitaxy was used to prepare films of 3-methylpentane. It was found that the three nanometer region closest to the vacuum-liquid interface was much less viscous. Eight degrees above the glass transition temperature, the glass interface was predicted by extrapolation to be six orders of magnitude less viscous than the bulk. Surface self-diffusion has been measured in ordinary liquid-cooled IMC glasses, through the use of grating decay.<sup>66</sup> Consistent with the results on 3-methylpentane, the surface diffusion was measured to be six orders of magnitude faster than bulk diffusion.

To summarize, surface mobility is a key factor in dictating the properties of vapor-deposited glasses. At high deposition temperatures, each depositing molecule spends some time in the highly mobile surface layer after deposition. Because of this, all molecules have a chance to find low enthalpy, dense configurations and a glass with enhanced stability can be built from the bottom up through vapor deposition. At cold substrate temperatures, surface mobility is ineffective and high enthalpy glasses filled with voids result.

### **1.4.3 High stability glasses deposited near $0.85 T_g$**

Vapor deposition can produce glasses with a wide variety of properties but a common thread running through all the results is that the stability of these glasses is maximized when the glass is deposited at temperatures near  $0.85 T_g$ .<sup>8, 11-12, 65</sup> Including the systems mentioned in the previous subsection, stable vapor-deposited glasses have been reported for over a dozen glassformers.<sup>57, 71</sup> In addition to low enthalpy, high kinetic

stability and high density, these materials can also have high mechanical moduli<sup>72-73</sup>, low water vapor uptake<sup>74</sup>, and anisotropic packing<sup>75</sup>. The combined characteristics of these vapor-deposited glasses have earned them the title 'ultrastable glasses'. As a result of the exceptional stability, glasses deposited at  $0.85 T_g$  exhibit thickness dependent properties that are not observed in liquid-cooled glasses.<sup>76-78</sup> These properties will be discussed at the end of this subsection.

The effect of the deposition rate on the stability of vapor-deposited glasses has also been measured. Glasses of IMC and  $\alpha\alpha\beta$ -TNB were deposited at the previously determined optimum deposition temperature of  $0.85 T_g$  and deposition rates ranging from 15 to 0.2 nm/s.<sup>8-10</sup> The surface mobility argument given above suggests that a slower deposition rate should allow the arriving molecules more time to reconfigure before they are buried into the bulk. By this logic, glasses of even greater stability should be obtained when slower deposition rates are utilized. However, it should be noted that once equilibrium is attained on the timescale of the deposition, further lowering of the deposition rate will no longer have an effect. As predicted, the stability of vapor-deposited glasses was further enhanced by utilizing slower deposition rates. Glasses of IMC and  $\alpha\alpha\beta$ -TNB deposited at  $0.85 T_g$  and the lowest deposition rate used (0.2 nm/s) had fictive temperatures almost 30 K and 40 K, respectively, below that of the liquid-cooled glass and onset temperatures over 25 K greater. It is estimated that one thousand to one million years of aging an ordinary liquid-cooled glass would be necessary to produce a glass of similar stability.

In addition to IMC and  $\alpha\alpha\beta$ -TNB, stable glass behavior has been reported for a number of pharmaceutical molecules and the rest of the family of TNB isomers. A simple sublimation apparatus was used to vapor-deposit glasses of IMC, phenobarbital, felodipine, and nifedipine.<sup>57</sup> The vapor-deposited glasses of each of these materials showed high onset temperatures and large enthalpy overshoot peaks in the heat capacity. The results for the IMC glass prepared in the simple sublimation apparatus and previously in a dedicated vacuum deposition chamber were comparable. A study on the family of TNB isomers ( $\alpha\alpha\alpha$ -TNB,  $\alpha\alpha\beta$ -TNB,  $\alpha\beta\beta$ -TNB, and  $\beta\beta\beta$ -TNB) demonstrated that stable glass formation is not limited to good glassformers.<sup>71</sup>  $\beta\beta\beta$ -TNB is such a poor glassformer that fast-quenching of the liquid with liquid nitrogen is required to avoid crystallization and produce an ordinary liquid-cooled glass sample. Despite the tendency of  $\beta\beta\beta$ -TNB to crystallize, a stable glass was successfully made through vapor deposition onto a substrate held at  $0.85 T_g$ . These examples demonstrate the generality of stable glass formation. In addition to organic molecules, stable glass characteristics have also been recently reported for polymeric glasses<sup>79</sup> and in a variety of simulations<sup>80-83</sup>.

Due to the extraordinary stability of glasses vapor-deposited near  $0.85 T_g$ , size effects that are not present in liquid-cooled glasses are found to play a role in some of the properties of stable glasses. One surprising aspect of highly stable vapor-deposited glasses is that thin films transform via a surface-initiated growth front mechanism. In ordinary glasses, transformation to the liquid state is independent of thickness and occurs homogeneously throughout the sample.<sup>76</sup> In stable glasses, a growth front moves in from

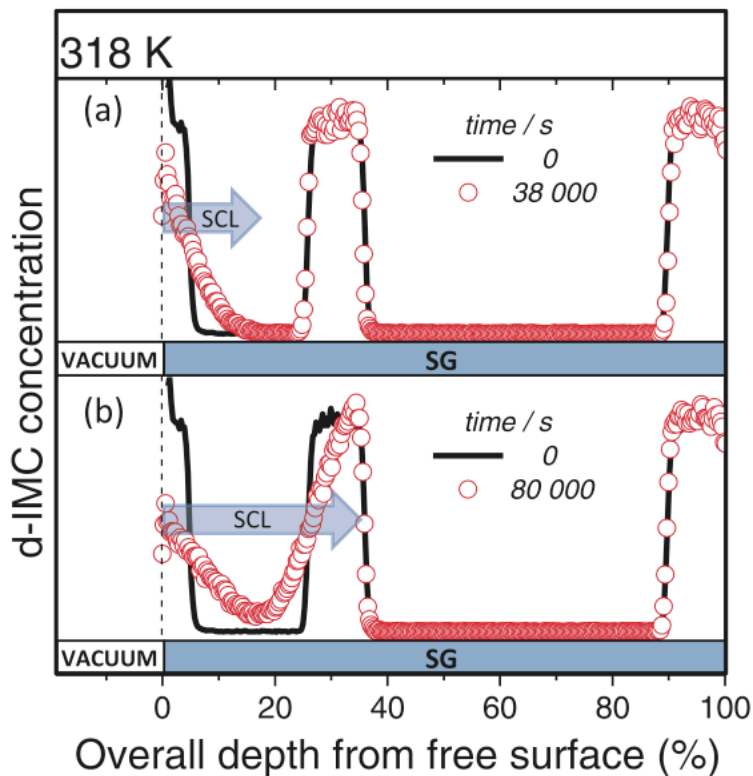


**Figure 1.10.** SIMS measurement of the evolution of the surface-initiated growth front in stable glass thin films of IMC. The black lines give the initial deuterated IMC concentration profile. The progression of the growth front after 38,000 and 80,000 seconds at 318 K is given by the red open circles in panel (a) and (b), respectively. The arrow shows the depth that the growth front and thus the supercooled liquid have penetrated into the sample. Reprinted with permission from reference 84. Copyright 2013, American Institute of Physics.



the surface to travel through the film, leaving supercooled liquid in its wake. The vapor-deposited glasses are so well-packed that mobility has to arrive from the surface before the molecules are able to rearrange into the liquid.

Growth fronts in stable glass thin films have been measured directly with secondary ion mass spectrometry (SIMS) in both IMC and  $\alpha\alpha\beta$ -TNB.<sup>76, 84-85</sup> For the measurement, glasses were deposited at  $0.85 T_g$  with alternating layers of protio and deuterio molecules. SIMS measures the mixing of these layers and thus can give a snapshot of the mobility in the film. For an ordinary liquid-cooled glass, mixing is observed uniformly throughout the sample, but in the vapor-deposited glass no mixing is observed until a growth front has reached that depth of the film.<sup>76, 84-85</sup> Figure 1.10 shows the original deuterated-IMC concentration profile as well as the profile after two different annealing steps. The growth front can be observed moving into the film from the vacuum-sample interface at the left edge of the figure. The concentration profile to the right of the growth front remains unchanged.

An observation consistent with the presence of growth fronts in stable glass thin films is that IMC stable glass films thicker than one micron exhibit bulk transformation behavior but thin films show thickness-dependent transformation times. The stable glass transformation behavior of IMC films with thicknesses from 75 nm to 3000 nm was observed using AC nanocalorimetry.<sup>78</sup> Figure 1.11 shows the stable glass transformation time as a function of thickness for the vapor-deposited IMC glasses. Between 600 nm and 1400 nm there is a crossover from thickness-dependent to thickness-independent

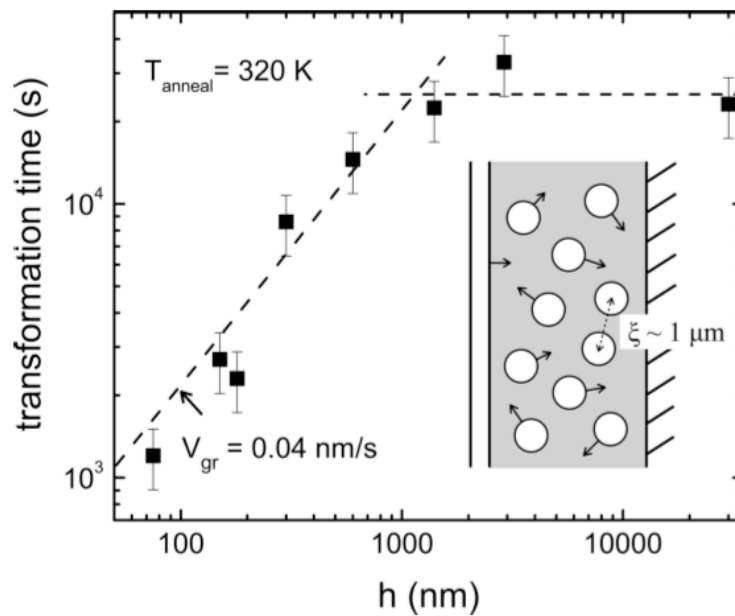


**Figure 1.11.** Effect of thickness on the transformation times of stable glasses of IMC. The inset shows a schematic of the surface initiated growth front and also transformation initiation sites within the bulk. See the text for more information. Reprinted with permission from reference 78. Copyright 2010 American Chemical Society.

transformation times. The transformation behavior of the thin films is consistent with the presence of a surface-initiated growth front, while the thicker films have a bulk transformation mechanism. For bulk transformation, it was proposed that transformation initiation sites exist within the glass. Given enough time to become mobile, these sites can also initiate growth fronts that propagate into the more stable areas of the film. The crossover thickness of  $\sim 1$  micron between transformation mechanisms was interpreted to signify the average distance between such transformation sites.<sup>78</sup> This concept is illustrated in the inset of Figure 1.11. Additional thickness-dependent stable glass measurements using AC nanocalorimetry can be found in Chapters 2 and 4.

Size effects in vapor-deposited glasses have also been measured with fast-scanning nanocalorimetry. Unlike AC nanocalorimetry, which only measures the reversing heat capacity, with fast-scanning calorimetry the enthalpy and fictive temperature can be quantitatively determined. Toluene films with thicknesses between 4 and 100 nm were vapor-deposited at  $0.80 T_g$  and measured with fast-scanning calorimetry.<sup>77</sup> Both the onset temperature (kinetic stability) and fictive temperature were thickness dependent for films thinner than  $\sim 40$  nm. Interestingly, the thinnest films had the lowest fictive temperatures and also the lowest onset temperatures. This example of a low enthalpy, but kinetically unstable vapor-deposited glass was unprecedented. The authors rationalized this through a surface-to-volume ratio argument.<sup>77</sup> In the thinnest films, most of the film is actually part of the mobile surface layer so the molecules can find low energy configurations with respect to their neighbors, thus resulting in glasses with low enthalpy and low fictive

temperature. However, this high mobility film has enhanced dynamics and is thus less kinetically stable than a thicker film where the surface layer is a smaller proportion of the film.

### 1.5 Original contributions of this thesis to the body of knowledge

When I entered the field five years ago, most of the information available about the heat capacity of vapor-deposited glasses was limited to bulk samples.<sup>8, 10, 86</sup> In the intervening years, this has changed as the heat capacity of thin films of a number of vapor-deposited glasses has been characterized through a successful collaboration between the Ediger lab and the Schick lab at the University of Rostock<sup>78, 87-91</sup>, and also with work from the Rodriguez-Viejo group<sup>12, 77, 92-94</sup>. Through my involvement in the international collaboration, I have investigated vapor-deposited glasses of three different small organic molecules with AC nanocalorimetry. The first system,  $\alpha,\alpha,\beta$ -tris-naphthylbenzene ( $\alpha\alpha\beta$ -TNB), was studied using an *ex situ* setup. I completed the construction of a new vacuum chamber equipped for *in situ* nanocalorimetry measurements and decalin and *o*-terphenyl were characterized *in situ*.

A number of important and new results came out of the AC nanocalorimetry experiments on these molecules. In agreement with the work on IMC,  $\alpha\alpha\beta$ -TNB thin films also showed thickness dependent transformation times for films up to one micron in thickness. This result suggests that highly suppressed bulk transformation rates may be a general feature associated with the kinetics of stable glass transformation. One way glassformers can be characterized is by their fragility, or their temperature dependent

behavior near  $T_g$ .<sup>5, 95-96</sup> Decalin, the molecular glassformer with the highest reported fragility, was shown to be capable of stable glass formation. This result implies that surface mobility, which is deemed the controlling mechanism for stable glass formation, is also present in high fragility systems. Experiments on a variety of *cis/trans*-decalin mixture compositions showed that mixtures can also form stable glasses when vapor-deposited. This is a strong argument against nanocrystals being responsible for the observed stable glass features. Finally, *in situ* experiments on *o*-terphenyl were able to span the range of vapor-deposited glass behavior from low temperature unstable glasses to high temperature stable glasses.

Chapter 2 will discuss the difference in reversing heat capacity between stable vapor-deposited glasses and ordinary liquid-cooled glasses of  $\alpha\beta$ -TNB. This work was published in the Journal of Chemical Physics, with myself, Mathias Ahrenberg, Christoph Schick and Mark Ediger as authors. Glasses deposited at  $0.85 T_g$  had 4% lower heat capacity than the liquid-cooled glass. Prior to this work, the heat capacity of  $\alpha\beta$ -TNB had only been measured with DSC, which was not sensitive to this difference. In agreement with the high onset temperatures measured with DSC, enhanced kinetic stability was also exhibited in isothermal annealing experiments. The time required to transform stable glass films into the supercooled liquid approached  $10^5$  times the structural relaxation time of the equilibrium supercooled liquid at the annealing temperature. Films up to one micron in thickness had thickness dependent transformation times, which supported the results on

IMC. This was also consistent with stable glass thin films transforming via a surface-initiated growth front mechanism.

Chapter 3 will discuss the substrate temperature dependence of vapor-deposited glasses of decalin. This work was published in the Journal of Physical Chemistry B with myself, Dan Scifo, Mark Ediger, Mathias Ahrenberg and Christoph Schick as authors. Decalin has the highest known fragility of molecular glassformers. Prior to this work, stable glass behavior had only been reported for glasses with intermediate and medium-range fragility. Glasses of *cis*-decalin and several *cis/trans*-decalin mixtures were shown to have low heat capacity and high kinetic stability, as compared to their corresponding ordinary liquid-cooled glasses. The fractional heat capacity decrease for *cis*-decalin stable glasses was comparable to other systems that have been measured thus far, with a value of 4.5%. The as-deposited heat capacity of the 50/50 *cis/trans*-decalin mixture was only up to ~2.5% lower than the ordinary glass heat capacity. However, the kinetic stability was on par with that of single component systems. This was the first report of stable glass formation for a molecular mixture.

Chapter 4 will discuss the substrate temperature dependence of vapor-deposited glasses of *o*-terphenyl. This chapter is the draft of a manuscript to be submitted to the Journal of Chemical Physics with myself, Mike Tyllinski, Mathias Ahrenberg, Christoph Schick and Mark Edgier as the authors. *o*-Terphenyl is one of the best-characterized organic glassformers but stable glasses of the material had yet to be studied. By depositing at substrate temperatures ranging from less than  $0.4 T_g$  up to  $T_g$ , unstable, stable and ordinary

glasses of *o*-terphenyl were able to be deposited. Glasses deposited near  $0.4 T_g$  had  $\sim 1\%$  higher heat capacity than that of the liquid-cooled glass, while glasses deposited near  $0.85 T_g$  had  $\sim 1\%$  lower heat capacity than that of the liquid-cooled glass. This was the first report of the heat capacity of a vapor-deposited glass being higher than the heat capacity of the ordinary glass at temperatures near  $T_g$ . Isothermal annealing experiments were performed on samples up to  $\sim 1400$  nm in thickness and all films showed thickness dependent transformation times. Vapor-deposited *o*-terphenyl glasses showed kinetic stability comparable to IMC and  $\alpha\alpha\beta$ -TNB.

Chapter 5 will further explore the interesting reversing heat capacity of low substrate temperature *o*-terphenyl vapor-deposited glasses. This chapter is a draft of a letter to be submitted to the Journal of Physical Chemistry Letters with myself, Yeong Zen Chua, Christoph Schick and Mark Ediger as co-authors. *o*-Terphenyl glasses vapor-deposited between  $0.39$  and  $0.49 T_g$  displayed reversing heat capacities up to  $\sim 50\%$  higher than that of the liquid-cooled ordinary glass at  $105$  K. Prior to this work, the only vapor-deposited glassy material reported to show a larger heat capacity than the ordinary glass at low temperature was 1-pentene; for 1-pentene the difference was on the order of  $18\%$ . The extraordinarily high heat capacity of vapor-deposited glasses of *o*-terphenyl was irreversibly erased upon heating.

Chapter 6 will summarize the work presented in the earlier chapters and give concluding remarks on the original work in this thesis.

Chapter 7 will present possible future directions for research based on the original work described herein. New questions that arise from the results of this thesis will be discussed and suggestions for experiments to explore the potential resolutions will be given.



## Chapter 2

### **Vapor-deposited $\alpha,\alpha,\beta$ -tris-naphthylbenzene glasses with low heat capacity and high kinetic stability**

Katherine R. Whitaker and M. D. Ediger

Department of Chemistry, University of Wisconsin–Madison, Madison, Wisconsin 53706

Mathias Ahrenberg and Christoph Schick

Institute of Physics, University of Rostock, Rostock, 18051 Germany

Reprinted with permission from Journal of Chemical Physics, Volume 137, article 154502, 2012. Copyright 2012, American Institute of Physics.

## 2.1 Abstract

The reversing heat capacity of vapor-deposited glasses of  $\alpha,\alpha,\beta$ -tris-naphthylbenzene ( $\alpha\alpha\beta$ -TNB) was measured using alternating current (AC) nanocalorimetry. Glasses deposited at  $0.85 T_g$ , where  $T_g$  is the glass transition temperature, have a  $4 \pm 1\%$  lower heat capacity than the ordinary glass prepared by cooling from the liquid. This is a result of efficient packing and is consistent with the higher density of the vapor-deposited glass. Isothermal experiments show that vapor-deposited  $\alpha\alpha\beta$ -TNB glasses also have enhanced kinetic stability with respect to transformation into the supercooled liquid, as expected from previous work, with transformation times approaching  $10^5$  times the structural relaxation time of the liquid. Films thinner than 1 micron exhibit a thickness dependence to their transformation times that is consistent with transformation to the supercooled liquid via a surface-initiated growth front.

## 2.2 Introduction

Amorphous materials can be produced through a number of methods, including cooling from the liquid, precipitation from aqueous solution and deposition from the vapor.<sup>27, 97</sup> The glasses created by these methods are not equivalent. For example, until recently it appeared that glasses made by physical vapor deposition had lower densities and higher enthalpies than glasses prepared by cooling the supercooled liquid at typical laboratory rates.<sup>51-54, 98</sup> While this is the case for films deposited at low substrate temperatures, the opposite is true for glasses vapor-deposited at substrate temperatures closer to the glass transition temperature  $T_g$ . In particular, it has been observed for a

number of organic molecules that deposition onto substrates near  $0.85 T_g$  produces glasses with high density, low enthalpy and high kinetic stability as compared to the liquid-cooled glass.<sup>8-12, 57, 71, 77, 92-93, 99-101</sup>

$\alpha,\alpha,\beta$ -tris-naphthylbenzene ( $\alpha\alpha\beta$ -TNB) was the first system reported to show extraordinary stability for glasses vapor-deposited around  $0.85 T_g$  and several properties of its stable glasses have been reported.<sup>9-10, 71, 101-102</sup> A majority of that work utilized a substrate temperature of 296 K ( $0.85 T_g$ ) and a deposition rate of 0.2 nm/s. Differential scanning calorimetry showed that  $\alpha\alpha\beta$ -TNB glasses deposited under those conditions have an onset temperature 35 K higher than the ordinary glass (prepared by cooling the liquid at a few K per minute) and a fictive temperature that is 40 K lower.<sup>10, 71</sup> This indicates that these vapor-deposited glasses have high kinetic stability and low enthalpy, respectively. It is estimated that these glasses are 40% of the way toward the bottom of the amorphous portion of the potential energy landscape. As further evidence of the high kinetic stability of these vapor-deposited  $\alpha\alpha\beta$ -TNB glasses, bulk samples require times as long as  $10^6 t_a$  in order to transform into the supercooled liquid, where  $t_a$  is the liquid's structural relaxation time.<sup>102</sup> Vapor-deposited  $\alpha\alpha\beta$ -TNB glasses are also 1.3% more dense than the ordinary glass and have about 25% less free volume.<sup>101</sup>

Here we use alternating current (AC) nanocalorimetry to measure the heat capacity of vapor-deposited glasses of  $\alpha\alpha\beta$ -TNB. This study compliments the measurements that have already been performed on vapor-deposited  $\alpha\alpha\beta$ -TNB by providing information about the heat capacity difference between the stable and ordinary glasses. The heat capacity is

related to the vibrational density of states and thus contains information about the packing efficiency of glasses. Nanocalorimetry is well-suited for the investigation of thin films such as those produced by vapor deposition.<sup>13-15, 44, 77, 103-104</sup> In contrast to conventional calorimetry, the small addenda heat capacity of the sensor makes it possible to measure only nanograms of material. This sensitivity is ideal for vapor-deposited samples because thin films can be produced rapidly even when low deposition rates are utilized. In addition, thin films of vapor-deposited glasses are utilized technologically<sup>105-106</sup> and it is of interest to directly measure the properties of such films.

Recently nanocalorimetry has been employed to study the heat capacity<sup>12, 77-78, 87, 89, 92-93</sup> of a number of vapor-deposited glasses. Using nanocalorimetry, differences in heat capacity on the order of a few percent can be measured.<sup>12, 87, 89</sup> Such measurements are impossible to achieve with conventional differential scanning calorimetry. Vapor-deposited glasses of indomethacin<sup>87</sup>, toluene<sup>89</sup>, and ethylbenzene<sup>12</sup> have each been shown to exhibit lower heat capacity as compared to their respective glasses prepared by cooling the liquid. In the case of indomethacin, the heat capacity of the glass deposited at 265 K (0.84  $T_g$ ) was measured to be 4.5% lower than the heat capacity of the ordinary glass prepared by cooling from the liquid.<sup>87</sup> Recent *in situ* nanocalorimetry measurements by Ahrenberg et. al. reported that toluene glasses deposited at 113 K (0.97  $T_g$ ) have a 2.5% lower heat capacity as compared to the ordinary glass.<sup>89</sup> Using fast scanning nanocalorimetry, Rodriguez and coworkers measured 5% lower heat capacity for 100 nm vapor-deposited ethylbenzene glasses relative to the ordinary glass.<sup>12</sup> Simulations of trehalose glasses show that the

vapor-deposited glass has lower heat capacity than the glass cooled from the liquid.<sup>80</sup> Additionally, nanocalorimetry can be used to obtain information about the enthalpy of vapor-deposited glasses.<sup>12, 77, 93</sup> Rodriguez and coworkers report a thickness dependence in the properties of vapor-deposited glasses of toluene, with 4 nm films having the lowest onset temperature (kinetic stability) and also the lowest enthalpy and fictive temperature.<sup>77</sup>

In the experiments reported here, glasses of  $\alpha\alpha\beta$ -TNB are vapor-deposited directly onto the nanocalorimeters, which are held in a temperature controlled housing at  $0.85 T_g$  during deposition. The measurements are done in a differential apparatus outside of the vacuum chamber. Temperature scanning experiments are performed to determine the relative heat capacities of vapor-deposited glasses and glasses cooled from the liquid; isothermal experiments are performed to study the kinetic stability and transformation behavior of the as-deposited films. In particular, the thickness and temperature dependence of the transformation kinetics is probed.

We find  $\alpha\alpha\beta$ -TNB glasses deposited at  $0.85 T_g$  have a  $4 \pm 1\%$  lower heat capacity than the glass cooled from the liquid. In contrast, glasses deposited at  $T_g$  have heat capacities that are almost identical to the ordinary glass. The low heat capacity glasses prepared at  $0.85 T_g$  also show enhanced kinetic stability, with transformation times for thick films approaching  $10^5$  times the structural relaxation time  $\tau_\alpha$ . For thin films, the transformation time increases linearly with film thickness, consistent with surface-initiated transformation via a growth front.<sup>76, 78</sup> Transformation times for thick films ranged from

$10^4 \tau_\alpha$  to  $10^5 \tau_\alpha$ , values that substantially exceed those reported for any conventionally aged glass. Similar results have previously been reported for indomethacin glasses vapor-deposited around  $0.85 T_g$ .<sup>78, 87</sup> Our new results in combination with those previously reported<sup>12, 80, 87, 89</sup> indicate that low heat capacity is likely to be a general feature of the highly stable organic glasses prepared by vapor-deposition near  $0.85 T_g$ .

## 2.3 Experimental

### 2.3.1 Materials

The synthesis of 1,3-bis-(1-naphthyl)-5-(2-naphthyl)benzene, or  $\alpha\alpha\beta$ -TNB ( $T_g = 345 K$ <sup>71</sup>), has been described elsewhere.<sup>107</sup> The melting temperature of this material, as measured by DSC, agreed with the literature value to within 1 K.<sup>71</sup>

### 2.3.2 Vapor deposition

$\alpha\alpha\beta$ -TNB films with thicknesses from 75 nm to 4  $\mu m$  were prepared by physical vapor deposition.  $\alpha\alpha\beta$ -TNB was deposited directly onto the nanocalorimeters (Xensor Integration, XEN-39321), which were held at 296 K ( $0.85 T_g$ ). Temperature control was performed as previously described.<sup>87</sup> The rate of deposition was  $0.20 \pm 0.03$  nm/s and was monitored with a quartz crystal microbalance (QCM) (Sycon). Films deposited under similar conditions and measured with ellipsometry demonstrated that the absolute thickness was within 10% of the value reported by the QCM for films less than 1  $\mu m$  in thickness. The pressure in the vacuum chamber was  $\sim 5 \times 10^{-8}$  torr prior to the deposition.

### 2.3.3 AC nanocalorimetry

The details of the AC nanocalorimetry analysis have been described elsewhere<sup>14, 87</sup> and only the main features will be reviewed here. The nanocalorimeters consist of a micromachined SiN<sub>x</sub> membrane with integrated heaters and thermopiles; the active area is 60 μm × 60 μm. Measurements are performed in a differential set-up with a reference and a sample nanocalorimeter. A lock-in amplifier (model 7265, Signal Recovery) supplies an AC voltage to the heaters, which imparts a small temperature oscillation on the membrane of each nanocalorimeter. The frequency of the temperature oscillation in these experiments was 20 Hz with an amplitude of ~0.25 K. The thermopile on the nanocalorimeter membrane measures the amplitude of the temperature modulation. All experiments were performed in a dry nitrogen atmosphere (~ 0.7 bar) and thus the descriptions of an AC calorimeter where heat losses through the surrounding gas dominate are applicable.<sup>14, 45</sup> In the thin film limit (approximately < 300 nm), the signal amplitude is proportional to the sample heat capacity. For thicker samples the signal amplitude is proportional to  $1/C_o - 1/(C_o+C_s)$ , where  $C_o$  is the complex heat capacity of the empty nanocalorimeter sensor including the losses to the surrounding and  $C_s$  is the sample heat capacity.<sup>87</sup> By referencing the observed signal changes to the signal rise at the dynamic glass transition ( $\Delta C_p$ ) for the ordinary glass<sup>108</sup>, we can obtain the difference in  $C_p$  between stable and ordinary glasses, even for films thicker than 300 nm.

The temperature program for the experiments reported here was as follows. After the sample and reference nanocalorimeters were loaded into the temperature controlled housing, the temperature was ramped to the annealing temperature at a rate of ~8 K/min.

The housing temperature was maintained isothermally at the annealing temperature until the as-deposited sample transformed into the supercooled liquid. During this time, the membrane temperature is slightly oscillating around the housing temperature and thus the measurement is actually quasi-isothermal. After the transformation was complete, the housing temperature was decreased at a rate of 1 K/min to 313 K and then ramped to 378 K at 1 K/min. The temperature ramps were repeated two more times. Temperature was calibrated with the liquid crystal 4'-(octyloxy)-4-biphenylcarbonitrile<sup>109</sup> and is known to within  $\pm 1$  K.

## 2.4 Results

### 2.4.1 Heat capacity of vapor-deposited glasses

Nanocalorimetry not only provides for the measurement of small amounts of material, but the sensitivity of the technique allows very small differences in heat capacity to be observed. Figure 2.1 shows  $\alpha\beta$ -TNB glasses vapor-deposited at (a)  $0.85 T_g$  and (b)  $0.99 T_g$ . In panel a, the as-deposited sample was ramped at  $\sim 8$  K/min to the annealing temperature of 353 K. The sample was held quasi-isothermally at the annealing temperature until it completely transformed into the supercooled liquid. Then the housing temperature was ramped down to 313 K and then heated up to 378 K (all at 1 K/min) to obtain the heat capacity curve for the ordinary glass. Here we use the term ordinary glass to refer to the glass prepared by cooling the liquid at 1 K/min while stable glass designates



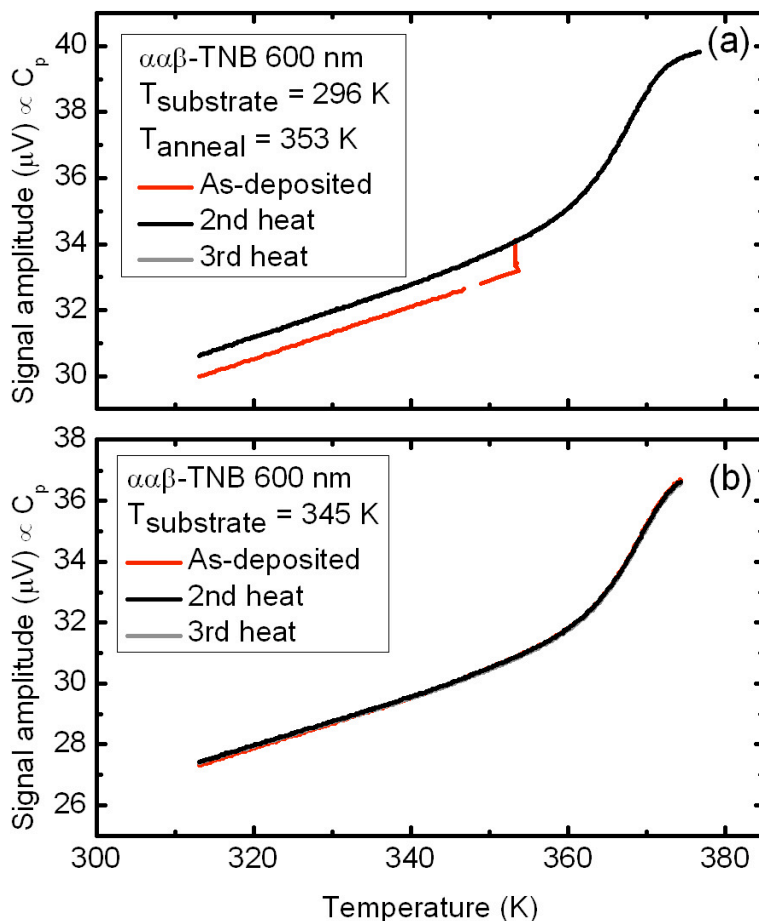


**Figure 2.1.** Effect of substrate temperature on the heat capacity  $C_p$  of  $\alpha\alpha\beta$ -TNB glasses vapor-deposited at 0.2 nm/s. (a) Reversing heat capacity of the glass deposited at  $T_{\text{sub}} = 296 \text{ K}$  ( $0.85 T_g$ ). The vapor-deposited glass (red) is heated to the annealing temperature of 353 K and allowed to isothermally transform to the supercooled liquid. The sample is then cooled into the glass and temperature scanned to produce the ordinary glass curves (black and gray).  $C_p$  is lower in the as-deposited glass (red) than the glass cooled from the liquid (black and gray). (b) Reversing heat capacity of the glass deposited at  $T_{\text{sub}} = 345 \text{ K}$  ( $0.99 T_g$ ). The vapor-deposited glass (red) was heated to 374 K and then cooled into the ordinary glass. The temperature ramps were repeated twice more to produce the ordinary glass curves (black and gray). The as-deposited glass (red) and the glass prepared by cooling the liquid (black and gray) have essentially the same  $C_p$ . In both panels, data for the third heating scan lies beneath the data for the second scan.

a glass deposited at a substrate temperature of  $0.85 T_g$  (296 K). In Figure 2.1(a), the as-deposited stable glass has a heat capacity that is  $\sim 4\%$  lower than the heat capacity of the ordinary glass. Upon isothermal annealing, the as-deposited glass transforms to the supercooled liquid and the heat capacity increases during transformation. The similarity between the second and third heating demonstrates that all structural features associated with the as-deposited glass are erased by the thermal treatment. In the experiment shown in panel b, a glass deposited at  $0.99 T_g$  was heated at 1 K/min to 378 K and then cooled at 1 K/min to form an ordinary glass. This procedure was repeated twice more on the ordinary glass. Glasses deposited at  $0.99 T_g$  (Figure 2.1 (b)) are nearly identical to the ordinary glass prepared by cooling from the liquid, with heat capacities that differ by no more than 0.6%.

The heat capacities of  $\alpha\alpha\beta$ -TNB films vapor-deposited at  $0.85 T_g$  with thicknesses ranging from 75 nm to 4000 nm were investigated here. For each sample, the heat capacity of the stable glass was compared to that of the ordinary glass by taking the ratio of their  $\Delta C_p$ 's at 333 K, where the liquid heat capacity was linearly extrapolated to 333 K and  $\Delta C_p = C_{p, \text{liquid}}(333 \text{ K}) - C_{p, \text{glass}}(333 \text{ K})$ . The ratio of  $\Delta C_p$ 's was determined at 333 K because at this temperature the ordinary glass and stable glass are completely responding as solids at the modulation frequency. Figure 2.2 shows the ratio of  $\Delta C_p$  values as a function of film thickness. The difference between the two  $\Delta C_p$ 's is  $\sim 20\%$  of  $\Delta C_p(\text{OG})$ . Using the values of 683 J/mol K and 553 J/mol K as the liquid and glass heat capacity, respectively, at 333 K for  $\alpha\alpha\beta$ -TNB<sup>108</sup>, we calculate that the stable glass  $C_p$  is lower than that of the ordinary glass by about 26 J/mol K. [Note that ref<sup>108</sup> identifies this substance as 1,3,5-tri- $\alpha$ -naphthylbenzene

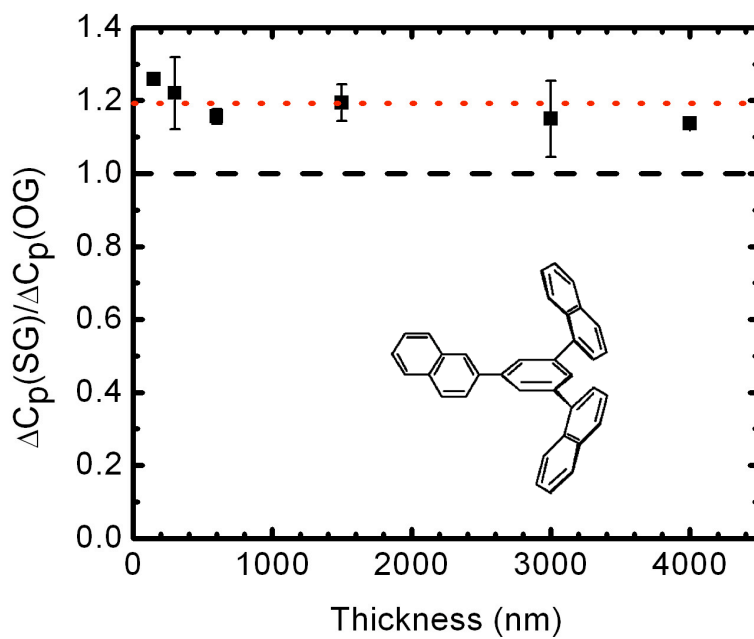


**Figure 2.2.** Comparison of the heat capacity of stable glasses (deposition at  $0.85 T_g$ ) and ordinary glasses of  $\alpha\alpha\beta$ -TNB as a function of sample thickness, expressed as a ratio of  $\Delta C_p$  calculated at 333 K. The red dotted line represents the average ratio across all thicknesses. Error bars indicate the standard deviations characterizing the range of values obtained from two to eleven samples. Inset shows the structure of  $\alpha\alpha\beta$ -TNB.

but Whitaker and McMahon established that the material was  $\alpha\alpha\beta$ -TNB.<sup>107]</sup> Using the absolute value of  $C_p$  for the ordinary glass at 333 K, this indicates that the stable glass has a heat capacity that is  $4 \pm 1\%$  lower than the ordinary glass. Over the thickness range that was examined, the heat capacity of the stable glass, relative to the ordinary glass, does not depend systematically on film thickness.

AC nanocalorimetry experiments only measure the reversing heat capacity of the sample and thus irreversible features, such as the enthalpy overshoot that is associated with the glass transition in conventional calorimetry<sup>110</sup>, are not seen. In addition, the enthalpy of the as-deposited glass cannot be measured. Since AC measurements probe the dynamic response of the sample at the modulation frequency, the observed  $C_p$  curves show the dynamic glass transition at this frequency. Thus the curves for the ordinary glasses in Figure 2.1 appear shifted to higher temperature with respect to the glass transition measured with DSC at conventional heating and cooling rates.

#### **2.4.2 Transformation kinetics of stable glasses**

The experiments described above also allow for the characterization of the kinetic stability of as-deposited glasses. Samples of vapor-deposited  $\alpha\alpha\beta$ -TNB were quickly heated from room temperature to the annealing temperature and then held quasi-isothermally until the transformation was complete. As illustrated in Figure 2.3(a), once the annealing temperature is attained, the differential nanocalorimetry signal begins with a value associated with the heat capacity of the stable glass. In the stable glass, molecules do not have the mobility to rearrange at the frequency of the temperature oscillation; under

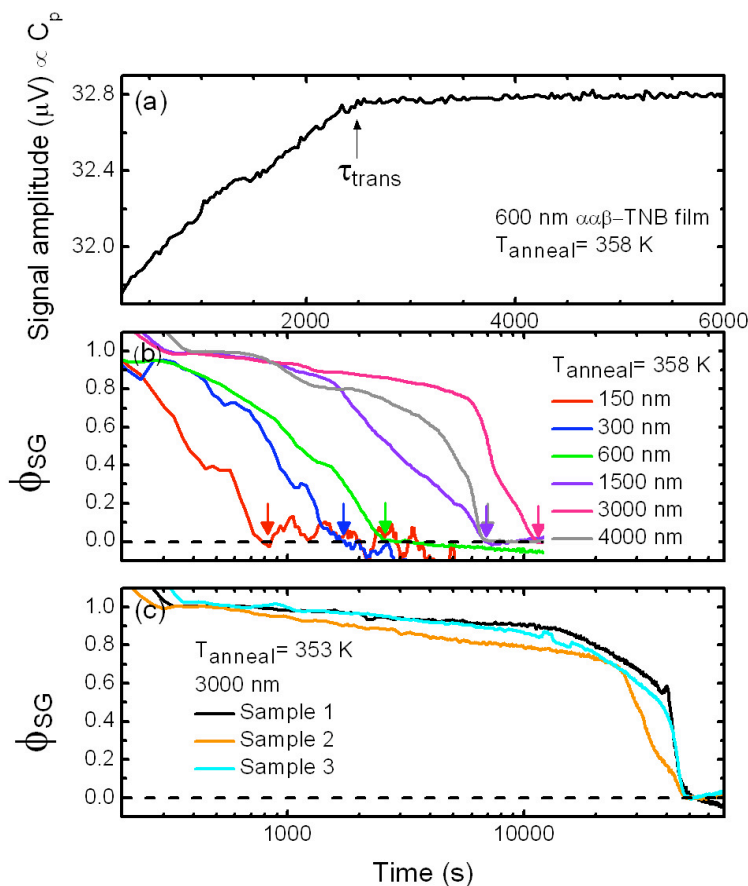


**Figure 2.3.** Isothermal transformation of stable glasses. (a) Isothermal  $C_p$  measurement of a 600 nm  $\alpha\beta$ -TNB film during annealing at 358 K. The signal increases as the heat capacity of the sample rises to the heat capacity of the supercooled liquid. (b) Normalized transformation curves of  $\alpha\beta$ -TNB films of a range of thicknesses, all annealed at 358 K.  $\Phi_{SG} = 1$  represents a sample that is untransformed and  $\Phi_{SG} = 0$  is 100% supercooled liquid. Arrows mark the end of the transformation. (c) Transformation curves of three different 3000 nm  $\alpha\beta$ -TNB films annealed at 353 K.

these conditions, the heat capacity is purely a result of vibrational motions. As shown in Figure 2.3(a), the heat capacity increases with time as the sample transforms from stable glass to supercooled liquid; molecules in the supercooled liquid rearrange on the timescale of the temperature oscillation and these configurational degrees of freedom also contribute to the heat capacity. When the sample is completely transformed, the signal stops changing and is characteristic of the heat capacity of the supercooled liquid at the annealing temperature. As shown in Figure 2.1(a), we confirmed the complete transformation to the supercooled liquid by cooling the film and then heating through the glass transition, recovering the behavior of the ordinary glass.

Stable glasses of  $\alpha\alpha\beta$ -TNB not only show extremely long transformation times (see discussion), but there is also a thickness dependence to the transformation time for the thinner films, as shown in panel b of Figure 2.3. We use the parameter  $\Phi_{SG}$  to define the fraction of the sample that remains in the stable glass state at any point in time;  $\Phi_{SG}$  varies linearly with heat capacity.<sup>86</sup> At the start of the isotherm  $\Phi_{SG} = 1$  because the sample is entirely in the glassy state.  $\Phi_{SG}$  decreases over time as the stable glass evolves into the supercooled liquid and finally at  $\Phi_{SG} = 0$ , no stable glass remains and the transformation is complete. The time when  $\Phi_{SG}$  reaches 0 and becomes constant is defined as the transformation time. Presenting the data as  $\Phi_{SG}$  allows for the easy comparison of films of different thicknesses. Figure 2.3(b) shows  $\Phi_{SG}$  curves for films covering the thickness range 150 nm to 4  $\mu\text{m}$ , with the transformation time increasing by more than one order of magnitude as the thickness increases.

The transformation time is a robust feature from sample to sample while the shapes of the  $\Phi_{SG}$  curves are somewhat variable. Figure 2.3(c) shows three different  $\alpha\beta$ -TNB samples that were 3000 nm in thickness and annealed at 353 K. The three samples have transformation times that agree within 3% but the shapes of the curves are less consistent. We have observed with optical microscopy that cracks can appear in the as-deposited films upon heating due to thermal expansion mismatches between the vapor-deposited films and the underlying substrate.<sup>101</sup> Cracking during isothermal transformation could influence the shape of the curve and the exact location of the cracks, e.g. in the center of the active area vs. only partially in the area of active measurement, could cause the shape to vary from sample to sample. The excellent agreement in transformation times suggests that the variability that we associate with cracking does not affect our ability to measure the transformation times of these samples with reasonable accuracy.

Our data show that  $\alpha\beta$ -TNB stable glasses thinner than 1  $\mu\text{m}$  exhibit a thickness-dependent transformation time, which increases linearly with film thickness. Transformation times, as determined by the time when  $\Phi_{SG} = 0$ , are plotted in Figure 2.4 for two different annealing temperatures. As discussed below, the features of the data are consistent with the transformation of thin stable glass films through a mechanism of surface-initiated growth fronts,<sup>76</sup> and with previously reported nanocalorimetry experiments on indomethacin stable glasses<sup>78, 87</sup>. Secondary ion mass spectrometry (SIMS) measurements of the growth front velocities for  $\alpha\beta$ -TNB provide values of 0.013 nm/s and 0.09 nm/s at 353 K and 358 K, respectively, and growth fronts were observed to

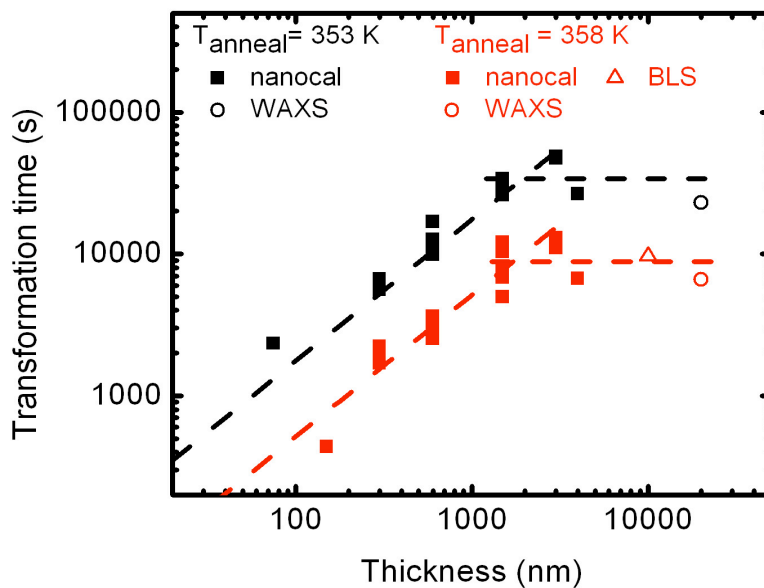


**Figure 2.4.** Thickness dependence of the stable glass transformation time.  $\alpha\beta$ -TNB films were annealed at 353 K (black) or 358 K (red). The dashed lines are fits to the data. For films thinner than one micron the slopes were constrained to one and for thicker films the slope was constrained to zero. The squares were obtained using nanocalorimetry; circles and triangles were obtained using WAXS<sup>102</sup> and BLS<sup>72</sup>, respectively.



originate both at the free surface and from the substrate.<sup>76</sup> In the SIMS measurements, the surface-initiated growth fronts were observed to proceed at a constant velocity, while the progress of the growth front from the substrate was more variable. If we assume that two growth fronts transform the nanocalorimetry samples and that they both move at the same rate, we estimate that the growth front rates for the data in Figure 2.4 are approximately 0.03 nm/s at 353 K and 0.1 nm/s at 358 K. These values are in reasonable agreement with those reported in ref<sup>76</sup>. For films thicker than 1  $\mu\text{m}$ , the transformation time becomes independent of film thickness and equal to the bulk transformation time, as measured by wide-angle X-ray scattering (WAXS)<sup>102</sup> and Brillouin light scattering spectroscopy (BLS)<sup>72, 102</sup>. This observation holds true for both annealing temperatures employed in these experiments.

The kinetic stability of  $\alpha\alpha\beta$ -TNB stable glass films can be quantified by comparing the transformation time to the structural relaxation time of the supercooled liquid,  $\tau_\alpha$ . The structural relaxation time is approximately equal to the transformation time of an ordinary glass. Figure 2.5 shows the temperature dependence of the transformation time for all film thicknesses. Transformation times increase not only with increasing thickness (up to 1  $\mu\text{m}$ ), but also with decreasing annealing temperature, as expected. When the stable glass transformation times are compared to the  $\tau_\alpha$  value at the annealing temperature, thick films take on the order of  $10^5\tau_\alpha$  to transform, indicating very significant kinetic stability.

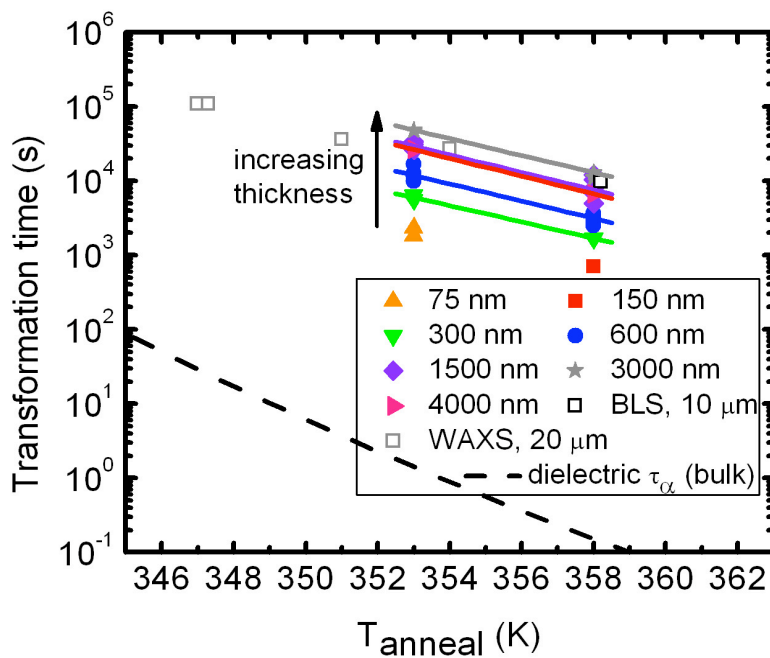


**Figure 2.5.** Temperature dependence of the stable glass transformation time for  $\alpha\beta$ -TNB. Solid symbols are from nanocalorimetry and open symbols are from WAXS and BLS. Solid lines are fits to the nanocalorimetry data. The dashed line is the structural relaxation time  $\tau_\alpha$  for the supercooled liquid of  $\alpha\beta$ -TNB obtained by dielectric spectroscopy.<sup>111</sup>

## 2.5 Discussion

We have shown here that vapor deposition at  $\sim 0.85 T_g$  produces glasses of  $\alpha\alpha\beta$ -TNB with heat capacities that are significantly lower than for the ordinary glass prepared by cooling the liquid at 1 K/min. In this section, we first describe how the deposition process influences the properties of a glass, in particular the heat capacity. Next the role of growth fronts in the transformation of highly stable glasses will be presented along with some perspectives on the absolute transformation times.

### 2.5.1 Heat capacity of vapor-deposited glasses

In this work it has been shown that  $\alpha\alpha\beta$ -TNB glasses vapor-deposited at  $0.85 T_g$  have a  $4 \pm 1\%$  lower heat capacity than the glass prepared by cooling the liquid, while the glass deposited around  $T_g$  is nearly identical to its liquid-cooled counterpart. When a film is deposited near  $0.85 T_g$ , there is a driving force for the depositing molecules to rearrange to optimize their packing towards that of the equilibrium supercooled liquid at the deposition temperature. There is also enough molecular mobility at the surface for such rearrangements to take place. Due to the nature of vapor deposition, each molecule in the final glass film was part of the mobile surface region for some period of time before being buried into the bulk. This allows all the molecules an opportunity to rearrange towards equilibrium during deposition and to build an efficiently packed glass from the bottom up. These stable glasses, deposited around  $0.85 T_g$  have low enthalpy, high density and high kinetic stability.<sup>8-12, 57, 71, 77-78, 92-93, 99-101</sup> This is the first report of low heat capacity  $\alpha\alpha\beta$ -TNB glasses.

The magnitude of the heat capacity decrease of these vapor-deposited glasses is remarkably large. This can be shown through a comparison with physical aging, which is another route by which the heat capacity of a glass can be decreased. The most relevant comparison is to the aging experiments of Bestul and coworkers.<sup>112-115</sup> They performed adiabatic calorimetry on glasses of diethyl phthalate, cis-1,4-polyisoprene, *ortho*-terphenyl and selenium that were aged for several days at temperatures around  $T_g - 10$  K. The aged glasses were observed to have molar heat capacities  $\sim 1$  J/(mol K) lower than for the ordinary glass. Here we report vapor-deposited  $\alpha\alpha\beta$ -TNB glasses with heat capacities that are  $\sim 26$  J/(mol K) lower than the ordinary glass. The results reported here are qualitatively similar to observations that have been made for vapor-deposited glasses of ethylbenzene<sup>12</sup>, toluene<sup>89</sup> and indomethacin<sup>87</sup>, and a simulated vapor-deposited glass of trehalose<sup>80</sup>. In this respect and in others, stable glasses obtained by vapor deposition appear to be “super-aged”.

Goldstein argued that the heat capacity of a glass can be influenced by changes in the vibrational density of states, the anharmonicity of the vibrational motions, and possibly by secondary relaxations.<sup>116</sup> The information available for stable glasses of  $\alpha\alpha\beta$ -TNB does not allow us to determine which of these is primarily responsible for the lower  $C_p$  values of stable glasses. At present, we assume that changes in the vibrational density of states are the primary factor. Ellipsometry experiments on  $\alpha\alpha\beta$ -TNB glasses deposited under similar conditions indicate that the stable glasses are about 1.3% more dense than the ordinary glass.<sup>101</sup> We imagine that, as a result of the more efficient packing of the stable glass, low

frequency vibrations are shifted to higher frequencies, consistent with a lower heat capacity. The ellipsometry measurements also indicate that stable glasses experience more harmonic potential energy minima than ordinary glasses as indicated by a lower thermal expansion coefficient. It is possible that this also contributes to the difference in heat capacity between stable and ordinary glasses. Dielectric relaxation experiments show that neither  $\alpha\alpha\beta$ -TNB<sup>111</sup> nor indomethacin<sup>117</sup> exhibit pronounced  $\beta$ -relaxations at ambient pressure.

Neutron scattering experiments, heat conductivity measurements and heat capacity measurements as a function of temperature have the capability to sort out the various contributions to the heat capacity of stable and ordinary glasses.  $\alpha\alpha\beta$ -TNB has a relatively simple molecular structure and this makes it an attractive target for neutron scattering experiments. It might be possible to identify specific molecular processes that contribute to the heat capacity of ordinary glasses more significantly than to stable glasses.

### **2.5.2 Stable glass transformation mechanism and kinetics**

The difference in heat capacity between the stable glass and ordinary glass allows us to observe the transformation of the stable glass. By holding the as-deposited glass at a temperature above the glass transition temperature we can watch the evolution of the stable glass to supercooled liquid. For films less than 1 micron in thickness, we observe that the transformation time increases linearly with film thickness and the transformation curves are close to linear in time. Both of these features are consistent with the view that films of stable glasses of  $\alpha\alpha\beta$ -TNB transform into the supercooled liquid as a result of

surface-initiated growth fronts. Stable glasses of  $\alpha\alpha\beta$ -TNB are apparently so well-packed that molecules in the interior of the film do not become unjammed as a result of local rearrangements but rather wait until mobility arrives from a considerable distance.

Evidence supporting stable glass transformation via growth fronts is found elsewhere in the literature. Swallen et al. reported secondary ion mass spectrometry (SIMS) measurements that directly show the presence of a growth front in  $\alpha\alpha\beta$ -TNB, initiated at the free surface, and propagating into the stable glass at constant (and very slow) velocity.<sup>76</sup> Leonard et al. used the facilitated kinetic Ising model to represent vapor-deposited glasses such as those described here. These model calculations also show that relaxation during annealing was propagated by a front moving in from the surface at a constant velocity.<sup>82</sup> This model was also able to reproduce the low fictive temperatures that are reported for vapor-deposited  $\alpha\alpha\beta$ -TNB glasses.<sup>10</sup> Sepulveda et al. studied the transformation of vapor-deposited glasses of toluene to the ordinary glass with fast-scanning nanocalorimetry.<sup>94</sup> The calorimetric traces for partially transformed samples exhibited two peaks; one for the highly stable as-deposited glass and one for a less stable glass fast-cooled from the supercooled liquid. The evolution of the peaks with annealing at  $T_g + 7$  K and  $T_g + 11$  K was consistent with a growth front mechanism.

The transformation times for  $\alpha\alpha\beta$ -TNB stable glasses thicker than 1 micron are independent of film thickness and agree reasonably well with the transformation times for thick samples measured by BLS and WAXS. Similar results also obtained using nanocalorimetry have previously been reported for indomethacin stable glass films.<sup>78, 87</sup>

For both indomethacin and  $\alpha\alpha\beta$ -TNB, one micron was the upper limit for films that showed thickness-dependent transformation times associated with a surface-initiated growth front mechanism. In ref<sup>78</sup>, it was postulated that a distance of  $\sim 1$  micron separates transformation initiation sites inside the bulk film and that growth fronts propagate radially away from these sites at the same rate observed for fronts near the free surface. This idea is in agreement with the theory of thermal rejuvenation of aged glasses put forward by Wolynes. This theory describes highly mobile regions in a (highly aged) bulk glass that serve to initiate radially propagating fronts.<sup>118</sup> The similarity of the indomethacin and  $\alpha\alpha\beta$ -TNB results suggest that this scenario will be a feature common to glasses prepared by physical vapor deposition at  $\sim 0.85 T_g$ , although it seems unlikely to us that a 1 micron length scale will control transformation in all bulk stable glasses. While we do not expect the nature of the substrate to affect the observed length scale<sup>8</sup>, it would be interesting to explore the effect of the substrate temperature, which influences the stability of the vapor-deposited glass.

We emphasize that these stable glasses of  $\alpha\alpha\beta$ -TNB transform into the supercooled liquid much more slowly than does an ordinary glass. Figure 2.5 shows a comparison of the transformation times to the structural relaxation time  $\tau_\alpha$  of the supercooled liquid<sup>111</sup> at the annealing temperature. All of the transformation times are orders of magnitude longer than  $\tau_\alpha$  and those of the bulk films are  $\sim 10^5 \tau_\alpha$ . To put this in context, Kovacs aged poly(vinyl acetate) glasses for two months and less than  $10^2 \tau_\alpha$  was required to return the aged glasses to equilibrium on heating.<sup>119</sup> Interestingly, the transformation times that we

observe seem to have a weaker temperature dependence than the structural relaxation time; this is consistent with a recent report that  $\tau_{\text{trans}} \sim \tau_{\alpha}^{0.60}$  for indomethacin and TNB bulk stable glasses.<sup>102</sup>

## 2.6 Summary

AC nanocalorimetry has been used to measure the reversing heat capacity of vapor-deposited glasses of  $\alpha,\alpha,\beta$ -tris-naphthylbenzene. The sensitivity of this technique allowed us to measure the difference in heat capacity between the as-deposited glass and the ordinary glass cooled from the liquid at 1 K/min. The glasses deposited at  $0.85 T_g$  have a  $4 \pm 1\%$  lower heat capacity than the ordinary glass. The kinetic stability of these films was investigated by measuring the heat capacity increase that occurs during the isothermal transformation into the supercooled liquid. Transformation times approaching  $10^5 \tau_{\alpha}$  demonstrate the very high kinetic stability of the as-deposited glasses. The transformation times for films up to 1 micron in thickness depend linearly on the thickness of the film, consistent with transformation via a surface-initiated growth front.

Work by a number of groups has established that stable glass formation is remarkably general for organic glasses vapor-deposited near  $0.85 T_g$ .<sup>12, 57, 71, 99-100</sup> The work reported here, together with previous work on indomethacin, establishes that the heat capacity of stable glasses is lower than that of ordinary glasses by  $\sim 4\%$ . Studies on other organic molecules<sup>12, 80, 89</sup> support the idea that stable glasses will generally have lower heat capacity than ordinary glasses. Clearly it is of interest to understand the structural origin of the lower heat capacity and whether it results from a shift in the vibrational density of



states or an absence of secondary relaxation or more harmonic vibrational motion. Neutron scattering experiments and computer simulations should be able to provide important insight into these questions.

## **2.7 Acknowledgments**

We gratefully acknowledge funding from the US National Science Foundation (CHE-0724062 and CHE-1012124) and the German Science Foundation (DFG-SCHI 331 14-1).

## Chapter 3

### Highly stable glasses of *cis*-decalin and *cis/trans*-decalin mixtures

Katherine R. Whitaker, Daniel J. Scifo, and M. D. Ediger

Department of Chemistry, University of Wisconsin–Madison, Madison, Wisconsin 53706

Mathias Ahrenberg and Christoph Schick

Institute of Physics, University of Rostock, Rostock, 18051 Germany

Reprinted with permission from Journal of Physical Chemistry B. Copyright 2013 American  
Chemical Society.

### 3.1 Abstract

*In situ* AC nanocalorimetry was used to measure the reversing heat capacity of vapor-deposited glasses of decahydronaphthalene (decalin). Glasses with low heat capacity and high kinetic stability, as compared to the corresponding liquid-cooled glass, were prepared from *cis*-decalin and from several *cis/trans*-decalin mixtures. This is the first report of highly stable glass formation for molecular mixtures. The 50/50 *cis/trans*-decalin mixture is the highest fragility material reported to produce an ultrastable glass. The 50/50 mixture exhibited high kinetic stability, with an  $\sim 500$  nm film deposited at 116 K ( $0.86 T_g$ ) displaying a transformation time equivalent to  $10^{4.4}$  times the structural relaxation time of the supercooled liquid at the annealing temperature. *cis*-Decalin and the decalin mixture formed stable glasses that had heat capacities as much as 4.5% lower than the liquid-cooled glass.

### 3.2 Introduction

Glasses are an interesting class of solids that can be formed from organic, inorganic, polymeric, colloidal, and metallic components.<sup>97, 120</sup> While the irregular local packing of glasses is sometimes perceived as a drawback of these materials, it is precisely this feature that allows the properties of glasses to be tuned significantly by changing the composition. This tunability is responsible for much of the technological impact of glasses. Another important difference between glasses and crystals is that the properties of a glass can depend significantly upon its preparation history. For example, a glass formed by rapid cooling from the liquid will generally be less stable than a glass formed by slow cooling, and

both of these glasses will typically be different from glasses formed by physical vapor deposition.

Glasses produced by physical vapor deposition can exhibit extraordinary properties in comparison with liquid-cooled glasses. Glasses with high kinetic stability and high density can be prepared<sup>8-12</sup> by depositing at low rates onto substrates at temperatures near  $0.85 T_g$ ; here  $T_g$  is the conventional glass transition temperature. Such an enhancement of properties would be expected if a glass were prepared by very slow cooling from the liquid state or by aging below  $T_g$  for long times<sup>121-122</sup>. The observed properties for vapor-deposited glasses though are equivalent to those expected for glasses aged for one thousand to one million years. These unique glasses also have low enthalpy<sup>8, 10, 12</sup>, low heat capacity  $C_p$ ,<sup>12, 80, 87-88, 90</sup> low water vapor uptake<sup>74</sup>, high mechanical moduli<sup>72-73</sup>, and can be anisotropic<sup>75</sup>. It is hypothesized that these materials can form because strongly enhanced mobility at the glass surface allows molecules to find efficient packing arrangements before they are buried by further deposition.<sup>9</sup> This mechanism is supported by theoretical work<sup>118, 123</sup>, by computer simulations<sup>81-83</sup>, and by direct measurements of surface mobility<sup>66</sup>.

The formation of highly stable glasses by physical vapor deposition appears to be quite general, with more than a dozen organic molecules reported to show this behavior to date. Vapor-deposited stable glasses have been formed from larger molecules including the family of tris-naphthylbenzene isomers<sup>71</sup> and the pharmaceuticals indomethacin and nifedipine<sup>8, 10, 57</sup>, as well as smaller molecules such as toluene and ethylbenzene<sup>12, 77, 90, 93</sup>,

<sup>100</sup>. Much work has been done to investigate and characterize these unusually stable glasses in the last five years, but two avenues that remain unexplored are high fragility glassformers and mixtures. Both of these are investigated here for the first time.

Fragility is a topic that has received much attention in the field of supercooled liquids and glasses.<sup>5</sup> Fragility describes the temperature dependence of the viscosity or structural relaxation time as a material is cooled towards  $T_g$ . The kinetic fragility can be characterized by the steepness index  $m$ .<sup>96</sup> Glassformers that exhibit Arrhenius behavior have small values of  $m$  and are termed "strong"; glassformers that exhibit strongly non-Arrhenius behavior have large  $m$  values and are considered "fragile".<sup>5, 95</sup> Fragility provides a means of classifying glassformers and has been found to be correlated to the boson peak<sup>124</sup> and the shape of the potential energy landscape<sup>125-126</sup>. The relationship between fragility and the heat capacity jump at  $T_g$  has also been extensively investigated.<sup>127-129</sup> Up to this point, all the systems shown to form stable glasses have intermediate fragility. Recently, it was reported that glycerol (the organic glassformer with the lowest fragility) does not form a stable glass when vapor-deposited near  $0.85 T_g$ .<sup>130</sup> In two recent studies, water (which is often considered to be a low fragility liquid at low temperature) was vapor-deposited at different substrate temperatures and measured with fast scanning calorimetry;<sup>131-132</sup> stable glass features were observed in neither study. These results raise the question as to whether stable glass formation is possible across the range of known fragilities or if it might be restricted to a subset of fragilities.

Here we report experiments in which we vapor-deposit thin glassy films of *cis*-decalin and *cis/trans*-decalin mixtures over a range of substrate temperatures  $T_{\text{sub}}$  and analyze the properties of these glasses with *in situ* AC nanocalorimetry. Kinetic stability is quantified by comparing the onset temperature  $T_{\text{onset}}$  for the reversing heat capacity of the as-deposited glass to that of the liquid-cooled glass. For the 50/50 *cis/trans*-decalin mixture, the kinetic stability was further investigated by performing isothermal annealing experiments. Nanocalorimetry also enables us to measure the difference between the heat capacity of an as-deposited glass and the glass cooled from the liquid;  $C_p$  for stable glasses can be significantly less than that for liquid-cooled glasses. These experiments on *cis*-decalin and *cis/trans*-decalin mixtures allow us to test whether stable glasses can be formed from molecular mixtures and also whether they can be formed from highly fragile glassformers. The 50/50 *cis/trans*-decalin mixture has the highest reported fragility among molecular glassformers.<sup>133-134</sup>

We show here that *cis/trans*-decalin mixtures with a wide range of compositions form stable glasses when vapor-deposited. The as-deposited glasses of the 50/50 mixture are up to 2.5% lower in heat capacity and have onset temperatures up to 7 K higher than that of the glass prepared by cooling from the liquid. The transformation time for a thin film ( $\sim 500$  nm) was  $10^{4.4}$  times the structural relaxation time of the supercooled liquid at the annealing temperature. *cis*-Decalin forms stable glasses with up to 4.5% lower heat capacity for glasses deposited around  $0.73 T_g$ . Relative to the ordinary glass, the onset temperature of *cis*-decalin glasses can be increased 8 K by depositing between  $0.84$ - $0.94 T_g$ .

Efforts to prepare a stable glass of *trans*-decalin were not successful, presumably due to crystallization during deposition.

This is the first report of a stable glass formed from a mixture and also establishes that very high fragility systems can form stable glasses. Stable glass mixtures could be technologically relevant in organic electronics<sup>106, 135</sup> or amorphous pharmaceuticals<sup>136-137</sup>.

### **3.3 Experimental Methods**

#### **3.3.1 Materials**

*cis*-Decahydronaphthalene (*cis*-decalin) and *trans*-decahydronaphthalene (*trans*-decalin) were purchased from Sigma (St. Louis, MO) with a purity of 99%. Both were used without further purification. Figure 3.1 shows the molecular structures of the geometric isomers.

#### **3.3.2 Sample preparation**

*cis*-Decalin and *cis/trans*-decalin mixture films were prepared by physical vapor deposition. The liquid material was placed in crucibles maintained at room temperature outside of the vacuum chamber and a leak valve was used to control the flow of gaseous material into the chamber. The vapor pressure of the liquids is high enough that no heating of the crucibles was required to achieve the desired deposition rate.

Decalin and decalin mixtures were deposited directly from the vapor phase onto the nanocalorimeters (Xensor Integration, XEN-39391), which were held in a temperature-

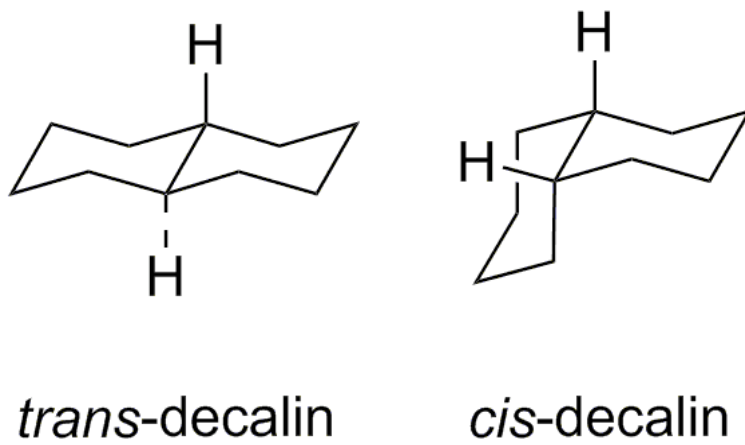


**Figure 3.1.** Structures of *trans*-decalin (left) and *cis*-decalin (right).



controlled housing. The temperature was measured with a surface resistance temperature detector (RdF Corporation) epoxied to the surface of the housing. Temperature was maintained by heating a cartridge heater against liquid nitrogen cooling. The temperature calibration is described below. The copper housing contained two nanocalorimeters; one calorimeter (the reference calorimeter) was completely enclosed by the housing while the other (the sample calorimeter) was located 2.8 mm below a 1.6 mm diameter opening that allowed deposition onto the active area. A mechanically rotatable shield located inside the vacuum chamber controlled deposition onto the sample calorimeter. For the measurements reported here, three different sample/reference calorimeter pairs were used. Similar results were achieved with all three pairs.

Prior to deposition, the pressure in the chamber was  $10^{-10}$  torr. To deposit, the leak valve was opened until the ion gauge pressure (Granville-Phillips 274 Nude Bayard-Alpert Ionization Gauge) increased to  $4.0 \times 10^{-6}$  torr. [Note that this is the nitrogen equivalent pressure. Based on the deposited thickness, the actual decalin pressure is estimated to be approximately a factor of three lower than the pressure read from the gauge.] After the pressure stabilized, the shield was rotated to allow deposition onto the sample sensor. Since deposition occurs through a small opening, the molecules can only approach the nanocalorimeter substrate at a cone of angles within  $15^\circ$  of normal; previous work has shown that the properties of vapor-deposited glasses can depend upon the angle at which the molecules approach the substrate.<sup>98</sup> The distance between the opening and the point where molecules enter the chamber through the leak valve is 20.5 cm. There is a line of

sight from the leak valve to the calorimeter substrate and a portion of the molecules directly deposit in this manner. The lock-in amplifier signal (see below) was monitored during the deposition and once the desired increase in signal was observed, the shield was raised to end the deposition.

The absolute thickness of the film on the nanocalorimeter was determined by comparison with *in situ* ellipsometry measurements. For this comparison only, a completely exposed nanocalorimeter was placed adjacent to a silicon wafer. Simultaneous calorimetry and ellipsometry measurements were performed during several depositions. The relationship between the calorimetry signal and the thickness in these calibration experiments was then used to determine the film thickness for deposition through the 1.6 mm hole. For the results discussed in this paper, the *cis*-decalin and decalin mixture films were  $570 \pm 60$  nm in thickness and deposited at a rate of  $0.2 \pm 0.1$  nm/s.

The *cis/trans*-decalin mixture films were produced by co-deposition. *cis*-Decalin and *trans*-decalin were in separate crucibles, each with a leak valve. To deposit the 50/50 mixture, first the leak valve connected to the *cis*-decalin crucible was opened until the ion gauge pressure read  $2.0 \times 10^{-6}$  torr. Then the leak valve of the *trans*-decalin crucible was opened until the total pressure came to the standard deposition pressure of  $4.0 \times 10^{-6}$  torr; under these conditions, the gas phase composition in the chamber was 50% *cis*-decalin and 50% *trans*-decalin. Finally, the shield was positioned to allow deposition onto the nanocalorimeters. Since the deposition rate can be controlled within 3%, we assume the composition condensing on the calorimeters matches the intended composition within 3%,

i.e., for the mixture above,  $(50 \pm 3)\%$  of the molecules on the nanocalorimeter are *cis*-decalin. Other compositions were achieved by changing the deposition pressures of each component accordingly.

### 3.3.3 *In situ* AC nanocalorimetry

Our *in situ* AC nanocalorimetry measurements on decalin glasses closely follow those described previously.<sup>89</sup> Here we use the commercially available sensors XEN-39391 (Xensor Integration, The Netherlands) in an electrical set-up similar to references<sup>14, 138</sup>. A digital lock-in amplifier (SR7265, Signal Recovery) measures the amplitude and phase of the complex differential thermopile signal. The complex amplitude of the differential thermopile signal is directly proportional to the reversing heat capacity of the sample. A differential set-up is used here for increased sensitivity and to minimize the influence of the addenda heat capacity.<sup>139</sup> To account for imbalances between the two sensors, an empty scan was performed prior to the measurements under the same conditions and subtracted in the complex plane from the sample measurement.

Nanocalorimetry measurements were performed during sample deposition and during subsequent temperature scanning. A thermal frequency of 20 Hz was used in the AC nanocalorimetry measurements to maximize sensitivity. In each experiment, the sample was deposited at the desired substrate temperature and then the temperature was changed at 2 K/min to 105 K. A 2 K/min heating ramp was then performed to obtain the heat capacity curve of the as-deposited glass (Figures 3.2, 3.3 and 3.4). Immediately after the dynamic glass transition was complete, the liquid was cooled at 2 K/min to form the liquid-

cooled glass (also described herein as the “ordinary glass”). All the systems studied here were prone to crystallization so a rapid transition from heating to cooling was necessary and temperature scans could only be performed to a temperature just past the dynamic glass transition. Heating and cooling ramps at 2 K/min were then repeated a second time. Generally, the heat capacities observed during the second heating and the two cooling cycles were in excellent agreement; in these cases, the second heating curve was used as the reference curve for the liquid-cooled glass. In some experiments, particularly on pure *cis*-decalin samples, samples began to crystallize near the end of the second heating curve; in these cases, the first cooling curve was used as the reference for the liquid-cooled glass.

For the 50/50 *cis/trans*-decalin mixture, quasi-isothermal AC nanocalorimetry experiments were also performed. In these experiments, the sample was deposited at the desired substrate temperature and then the temperature was ramped at 5 K/min to the annealing temperature. The sample was held quasi-isothermally ( $\sim 0.5$  K temperature oscillation at 20 Hz) at the annealing temperature until the heat capacity of the sample was observed to stop changing. Subsequent temperature ramping experiments verified that this final state was the equilibrium supercooled liquid.

As a result of small thickness differences, the ordinary glass reference curves for different samples differ in amplitude by as much as 11%. To simplify the visual comparison of different samples in Figure 3.3, the ordinary glass curves were scaled to coincide at 119.5 K. The same small adjustments were also applied to the corresponding as-deposited glass  $C_p$  values. Small vertical shifts were also applied to the data in Figure 3.4. The

deposited film can cause small amounts of stress in the nanocalorimeter membrane, which in turn causes a change in the sample heater resistance. This effect was carefully measured and the reported heat capacities have been corrected for this.

### 3.3.4 Temperature calibration

We utilized the resistance of the heater on the nanocalorimeter membrane in order to determine the membrane temperature. Following ref <sup>89</sup>, we calibrated the heater resistance using cyclopentane and toluene. Cyclopentane has three phase transitions in the relevant temperature range: 122.23 K (crystal—plastic crystal II), 138.35 K (plastic crystal II—plastic crystal I) and 178.59 K (plastic crystal I—liquid).<sup>140</sup> Ahrenberg et al.<sup>89</sup> have shown that the dynamic glass transition of toluene measured with AC nanocalorimetry is in good agreement with the dielectric relaxation data of Hatase et al.<sup>141</sup> and thus it can be used for temperature calibration.

As a check on the temperature calibration procedure, we make use of dielectric relaxation data for the supercooled 50/50 *cis/trans*-decalin mixture.<sup>133</sup> Using the temperature calibration described above, our nanocalorimetry measurements show that the 20 Hz dynamic glass transition temperature for the supercooled liquid of this mixture is on average 140.8 K, which is in good agreement with the value of 140.2 K reported in the dielectric work. The run-to-run variation of the dynamic glass transition of the supercooled liquid in our measurements is about 1 K. All ordinary glass reference curves were horizontally shifted to correct for these run-to-run variations and the same shift was

applied to the corresponding as-deposited glass. For pure *cis*-decalin,  $T_{g,dyn}(20\text{ Hz})$  was determined to be 147.5 K, with similar run-to-run variation.

A further check on the nanocalorimeter temperature calibration can be made by a comparison with differential scanning calorimetry (DSC) experiments. DSC (Perkin Elmer Pyris 1 DSC) experiments utilizing scanning rates of 1 K/min to 5 K/min were performed on *cis*-decalin and the 50/50 decalin mixture. The onset temperatures for the glass transition from these experiments were slightly extrapolated to obtain the 10 K/min values of 141.0 K and 134.8 K, respectively; these values are denoted as  $T_g$  in this paper. The temperature differences between the glass transition temperatures measured with DSC and at 20 Hz with nanocalorimetry are in good agreement for the two systems, as would be expected if the fragility of *cis*-decalin is similar to that of the 50/50 mixture. In the DSC measurements, crystallization of the *cis*-decalin sample was avoided by fast-quenching the sample from room temperature; this was done by placing the room temperature DSC pan containing *cis*-decalin on the cold block of the DSC. The DSC was modified for liquid nitrogen cooling and the cold block was maintained at 113 K. Similar DSC experiments were attempted for pure *trans*-decalin but were unsuccessful due to crystallization.

## 3.4 Results

### 3.4.1 Reversing $C_p$ during temperature ramping

Vapor-deposited glasses can be equivalent to ordinary glasses or they can be highly stable, depending on the deposition temperature. This is illustrated for the 50/50 *cis/trans*-

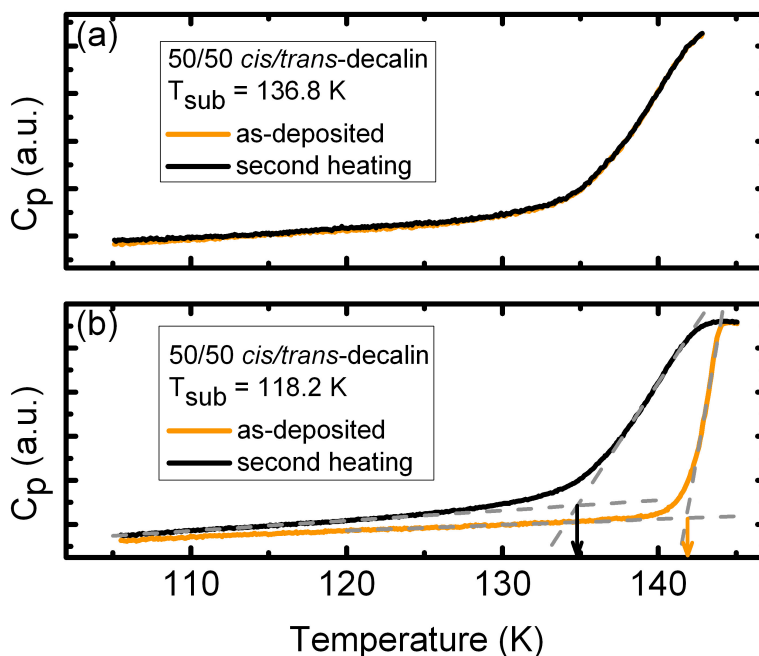


**Figure 3.2.** Effect of substrate temperature on the heat capacity of vapor-deposited 50/50 *cis/trans*-decalin mixture glasses. (a) Reversing heat capacity of the glass deposited at  $T_{\text{sub}} = 136.8 \text{ K}$  ( $1.01 T_g$ ). The as-deposited glass (orange) has the same heat capacity as the glass prepared by cooling the liquid (black). (b) Reversing heat capacity of the glass deposited at  $T_{\text{sub}} = 118.2 \text{ K}$  ( $0.88 T_g$ ). The as-deposited glass (orange) is lower in heat capacity and has a higher onset temperature than the glass cooled from the liquid (black). For both samples the scanning rate was 2 K/min and the thermal frequency was 20 Hz. The gray dotted lines indicate the tangent method used to determine the onset temperatures; the vertical arrows point to the  $T_{\text{onset}}$  values. The films were  $570 \pm 60 \text{ nm}$  thick and were deposited at  $0.2 \pm 0.1 \text{ nm/s}$ .

decalin mixture in Figure 3.2. Here we show the reversing heat capacity curves of decalin mixture glasses deposited at  $1.01 T_g$  and  $0.88 T_g$ . In AC nanocalorimetry, the signal is proportional to the reversing heat capacity and thus non-reversing features such as the enthalpy overshoot are not observed. Figure 3.2(a) shows that the glass deposited near  $T_g$  has the same heat capacity as the glass cooled from the liquid at 2 K/min; this can be seen by comparing the as-deposited glass (orange curve) and the ordinary glass (black curve). As seen in Figure 3.2(b), the *cis/trans*-decalin mixture glass deposited at  $0.88 T_g$  exhibits properties of a highly stable glass: low heat capacity and high onset temperature (high kinetic stability). The heat capacity of the as-deposited glass is 1.8% lower than the liquid-cooled glass and the onset temperature is 7 K higher. Upon heating, the as-deposited glass transforms into the supercooled liquid. The sample was subsequently cooled and reheated; the second heating curve shows the properties of the liquid-cooled glass for comparison.

As shown in Figure 3.3, glasses of *cis*-decalin were deposited over a range of substrate temperatures from 101.3 K to 141 K, or  $0.72$  to  $1.00 T_g$ . The properties of the vapor-deposited glasses are significantly affected by the deposition temperature. For clarity, Figure 3.3 has been divided into three panels each of which shows the behavior of the liquid-cooled glass for comparison. The arrows indicate the direction of increasing substrate temperature. Figure 3.3(a) shows glasses deposited from  $0.72$  to  $0.79 T_g$ . In this range, the onset temperature of the as-deposited glass increases with substrate temperature. The heat capacity has the lowest values of all substrate temperatures but no trend is observed between the experiments shown within the error of the measurement. In



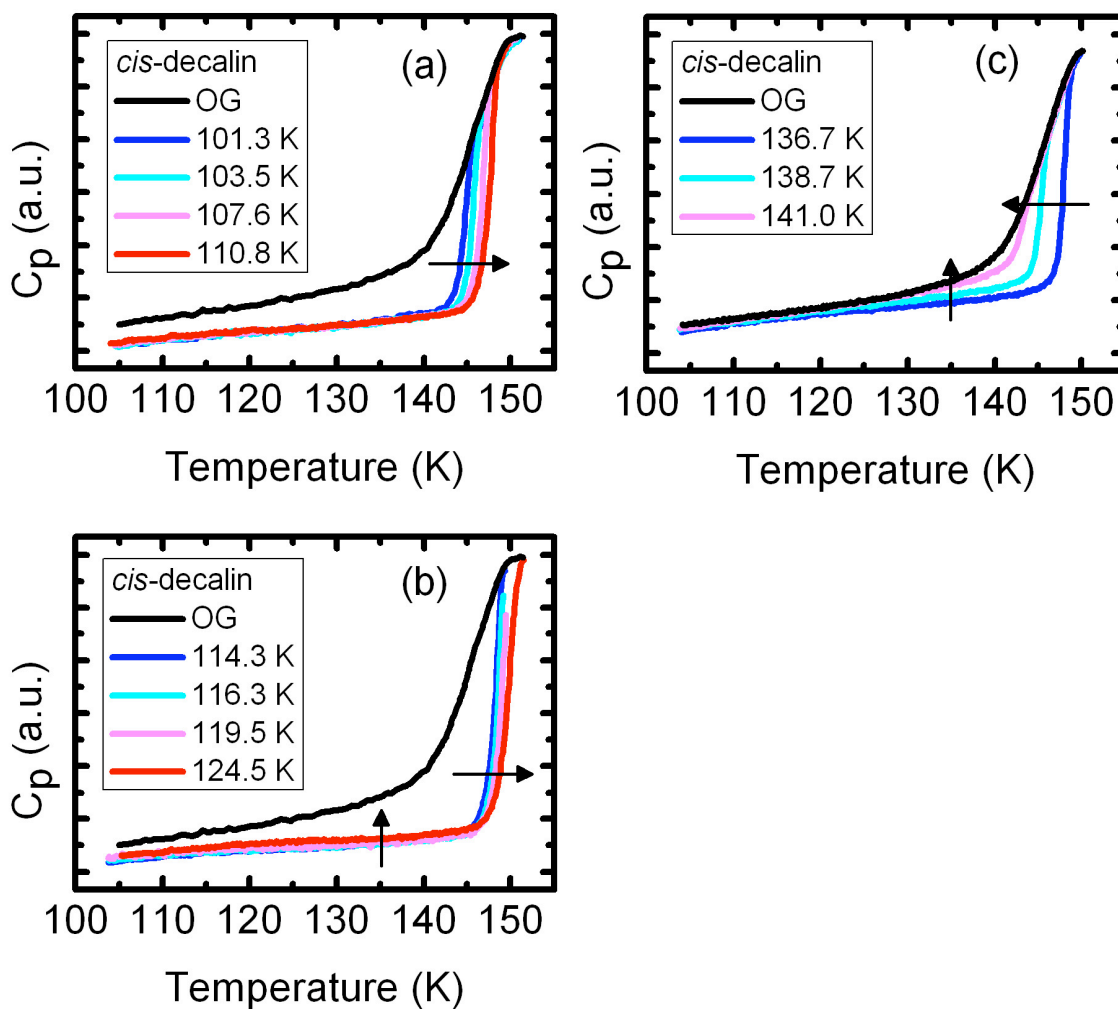


**Figure 3.3.** Effect of substrate temperature on the reversing heat capacity for vapor-deposited glasses of *cis*-decalin at substrate temperatures of (a)  $0.72$  to  $0.79 T_g$  (b)  $0.81$  to  $0.88 T_g$  and (c)  $0.97$  to  $1.00 T_g$ . For comparison, the black line in each panel shows the heat capacity of the ordinary glass prepared by cooling the liquid. The arrows indicate the direction of increasing substrate temperature. For all samples the thermal frequency was 20 Hz and the scanning rate was 2 K/min. The *cis*-decalin films were deposited at  $0.2 \pm 0.1$  nm/s at the substrate temperature specified in the legend and the thickness was  $570 \pm 60$  nm.

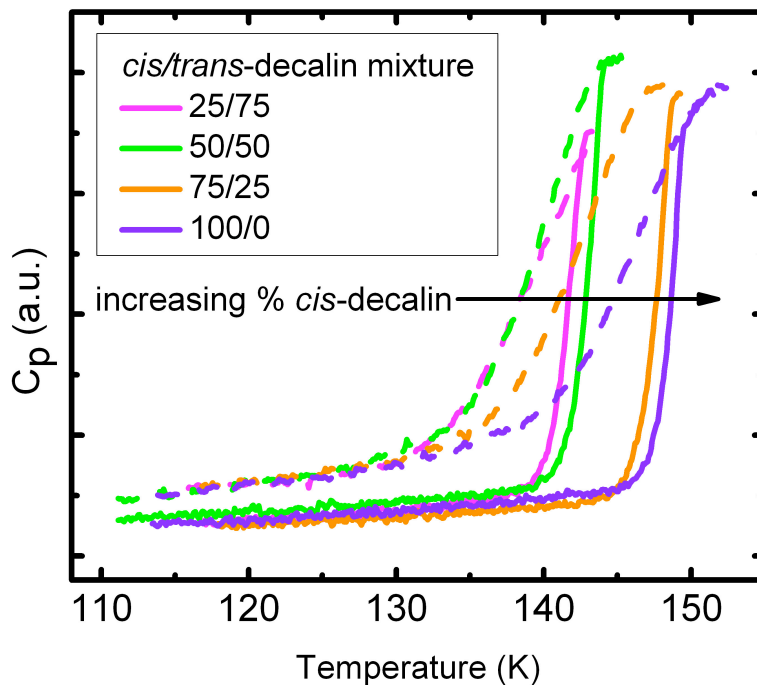


**Figure 3.4.** Effect of composition on the reversing heat capacity of *cis/trans*-decalin mixtures. Solid lines are heating curves of the as-deposited glasses and dotted lines are cooling curves of the corresponding liquid-cooled glass. The magenta curves are a 25/75 *cis/trans*-decalin mixture (deposited at 115.1 K), the green curves are a 50/50 mixture (deposited at 108.9 K), orange curves are a 75/25 mixture (deposited at 117.4 K) and the purple curves are pure *cis*-decalin (deposited at 113.0 K).

the middle of the substrate temperature range (Figure 3.3(b), 0.81 to 0.88  $T_g$ ) the onset temperature continues to increase with substrate temperature and is maximized in this range. The heat capacity increases with substrate temperature. Figure 3.3(c) shows these same trends continue for glasses deposited from 0.97 to 1.00  $T_g$ . *cis*-Decalin is not a good glassformer and these measurements are the first report of the glass transition of a completely amorphous sample. A similar series of experiments was performed on the 50/50 *cis/trans*-mixture. The primary data showed the same qualitative features as those shown in Figure 3.3 and a summary of the results is presented below.

Two other compositions of *cis/trans*-decalin were vapor-deposited and observed to form stable glasses. Figure 3.4 shows the as-deposited heating curves and the first cooling curves for 25/75, 50/50, 75/25 and 100/0 *cis/trans*-decalin vapor-deposited glasses. Each as-deposited glass has a lower heat capacity and a higher onset temperature than the corresponding liquid-cooled glass, indicating that a highly stable glass has been obtained. The glass transition temperature is seen to increase with increasing proportions of *cis*-decalin.

### 3.4.2 Dependence of glassy $C_p$ and kinetic stability upon substrate temperature

Vapor-deposited glasses of decalin can have lower heat capacity than the liquid-cooled glass. Figures 3.2 and 3.3 demonstrate this for the 50/50 *cis/trans*-decalin mixture and *cis*-decalin, respectively. In order to quantify this difference in heat capacity between the as-deposited and ordinary glasses, we use the quantity  $C_{p,AD}/C_{p,OG} - 1$ , determined at 0.85  $T_g$  (119.5 K and 114.5 K for *cis*-decalin and the 50/50 *cis/trans*-decalin mixture, respectively). The heat capacity difference is calculated at this temperature because the

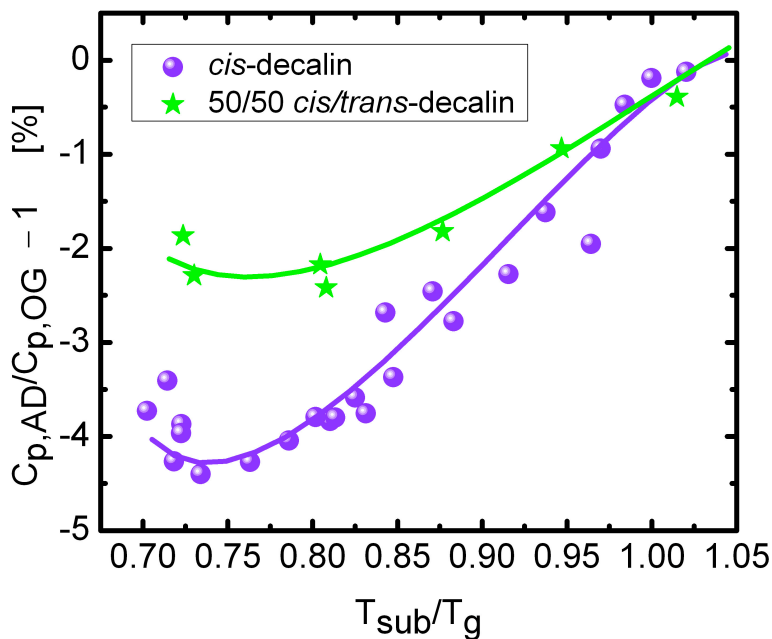


**Figure 3.5.** Heat capacity of as-deposited glasses (AD) of decalin, expressed as a percentage change relative to the ordinary glass (OG) prepared by cooling the liquid. The heat capacities used in the calculation were determined at  $0.85 T_g$  and the substrate temperature is normalized to  $T_g$ . The purple spheres are *cis*-decalin data and the green stars are 50/50 decalin mixture data. The solid lines are guides to the eye.

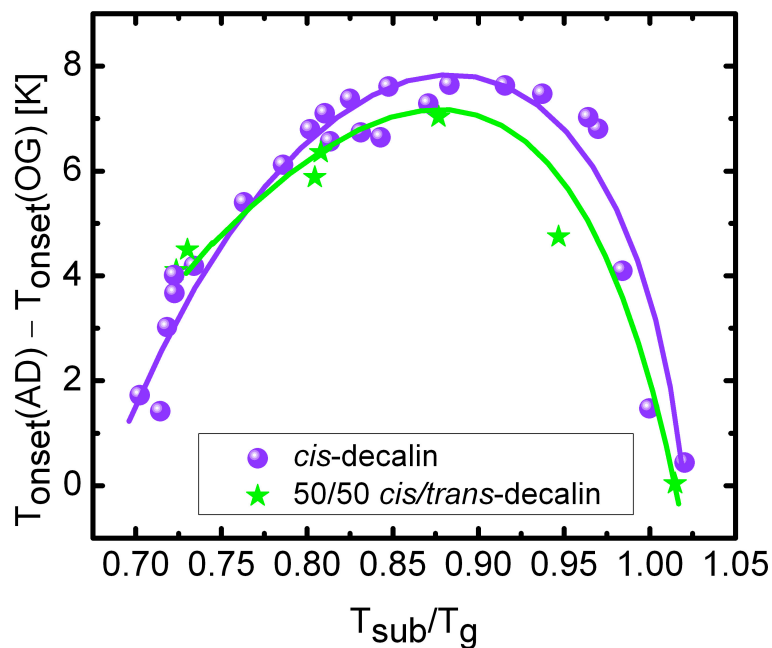


**Figure 3.6.** The onset temperatures for the as-deposited decalin glasses (AD) as a function of substrate temperature, relative to the ordinary glass (OG) cooled from the liquid. Purple spheres are *cis*-decalin data and green stars are decalin mixture data. The substrate temperature is normalized to  $T_g$ . Heating ramps were done at 2 K/min and the onset temperatures were determined by the tangent method, as shown in Figure 3.2(b). The solid lines are guides to the eye.

response here comes purely from the glassy solid (at the modulation frequency of 20 Hz). Figure 3.5 shows the fractional  $C_p$  decrease as a function of substrate temperature during deposition. The substrate temperature is scaled by  $T_g$  of the corresponding supercooled liquid. *cis*-Decalin and the decalin mixture show qualitatively similar trends. At substrate temperatures close to  $T_g$  the heat capacities of the as-deposited glasses are almost equivalent to the corresponding liquid-cooled glasses, consistent with Figure 3.2(a). As the substrate temperature is decreased, the heat capacity of the as-deposited glass decreases. Near the lowest substrate temperatures used here, the fractional  $C_p$  decrease is  $4.5 \pm 1\%$  for *cis*-decalin and  $2.5 \pm 0.5\%$  for the *cis/trans*-decalin mixture.

The onset temperature of the as-deposited glass also depends upon the substrate temperature. The onset temperature is determined according to the tangent method shown in Figure 3.2(b). Figure 3.6 compares the onset temperatures of the as-deposited glass to that of the liquid-cooled glass, as a function of substrate temperature. The trends in onset temperature are very similar for *cis*-decalin and the 50/50 *cis/trans*-decalin mixture. Close to  $T_g$ , the onset temperatures are equal to those of the ordinary glass. Between  $0.84$  and  $0.94 T_g$ , the greatest increase of the onset temperature is seen and ranges up to  $8 \pm 1$  K for *cis*-decalin and  $7 \pm 1$  K for the decalin mixture. As the substrate temperature is further decreased, the onset temperature of the as-deposited glass begins to decrease.

### 3.4.3 Isothermal annealing experiments

Isothermal annealing experiments were performed to determine the kinetic stability of vapor-deposited *cis/trans*-decalin mixture glasses. AC nanocalorimetry is ideally suited

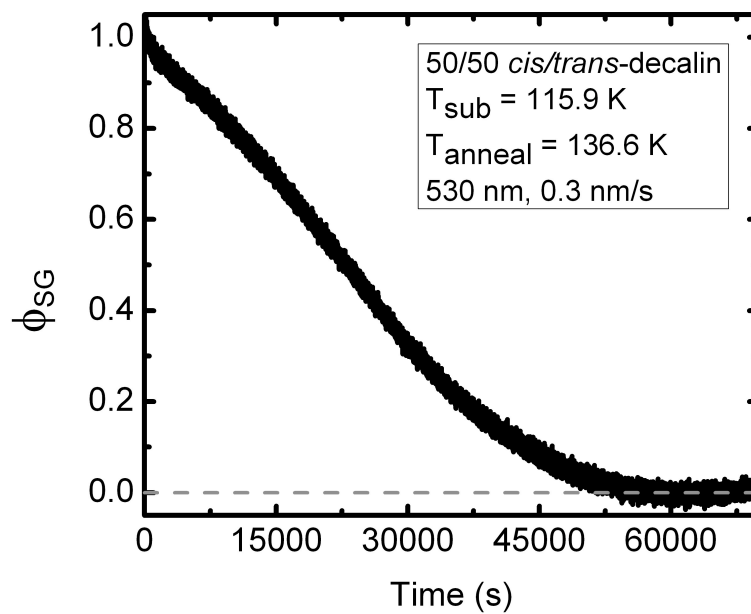


**Figure 3.7.** Isothermal annealing of a vapor-deposited 50/50 *cis/trans*-decalin mixture film (530 nm).  $\Phi_{\text{SG}}$  represents the fraction of stable glass remaining at any point in time. This sample was deposited at 0.3 nm/s at  $0.86 T_g$  and annealed at 136.6 K.

to study the isothermal transformation of a thin as-deposited glass to the supercooled liquid. A quasi-isothermal annealing experiment was carried out at 136.6 K on a 50/50 *cis/trans*-decalin mixture glass deposited at  $0.86 T_g$  (115.9 K). During annealing the heat capacity increases as the sample transforms from the glass to the supercooled liquid.  $\Phi_{SG}(t)$  is used to represent the fraction of the sample responding as a stable glass at any point in time.<sup>86</sup> At the start of the annealing measurements  $\Phi_{SG}(t = 0 \text{ s}) = 1$  and the sample is completely glassy. As the transformation proceeds,  $\Phi_{SG}(t)$  decreases until the sample is entirely supercooled liquid and  $\Phi_{SG}(t) = 0$ . The time when  $\Phi_{SG}(t)$  reaches zero is defined as the transformation time of the as-deposited glass. The transformation shown in Figure 3.7 took  $\sim 43,000 \text{ s}$  (determined by linear extrapolation), which is  $10^{4.4}$  times the structural relaxation time  $\tau_\alpha$  of the equilibrium supercooled liquid at the annealing temperature, as determined from dielectric spectroscopy.<sup>133</sup>

## 3.5 Discussion

### 3.5.1 Substrate temperature dependence of vapor-deposited glasses

During vapor deposition onto a substrate held near  $0.85 T_g$ , molecules condensing onto the sample surface find a sufficiently mobile environment such that they have the opportunity to explore the energy landscape and find stable configurations. As a result of the deposition process, each molecule is part of the mobile surface layer before being buried in the film. These glasses become well-packed<sup>9</sup> from the bottom up.



The efficient packing that occurs during deposition near  $0.85 T_g$  gives rise to glasses that are kinetically stable and have low heat capacity. In order for thin films of these glasses to transform into the supercooled liquid, a growth front moves in from the free surface, providing the mobility needed for further transformation as it progresses.<sup>76, 82, 118</sup> With nanocalorimetry, this growth front is most directly observed in isothermal experiments on thin films; a growth front results in a transformation curve that is approximately linear in time and there is a linear thickness dependence to the transformation time.<sup>78, 88</sup> Both of these features are consistent with the surface-initiated growth front mechanism observed with secondary ion mass spectrometry.<sup>76</sup> Highly stable vapor-deposited glasses have low heat capacity<sup>12, 80, 87-88, 90</sup> and it has been suggested that the higher packing efficiency of the stable glass shifts some of the vibrational modes to higher frequencies<sup>88</sup>. The resulting difference in the vibrational density of states (VDOS) would lead to the observed lower heat capacity of the stable glass. Simulations and experiments qualitatively support this idea. Mossa et al. showed for the Lewis-Wahnstrom model of *ortho*-terphenyl that the VDOS of higher density glasses was shifted to higher frequency.<sup>142</sup> Experimental work on a mineral glass showed that high fictive temperature glasses have VDOS shifted to lower frequency.<sup>143</sup> As stable glasses are characterized by higher density and lower fictive temperature relative to ordinary glasses, both of these observations are consistent with the VDOS of stable glasses being shifted to higher frequency and thus having a lower heat capacity.

The two preceding paragraphs provide the context needed to understand the properties of as-deposited decalin glasses as a function of substrate temperature. At substrate temperatures near  $T_g$ , the onset temperature is nearly the same as that of the ordinary glass (see Figure 3.6). Although there is adequate mobility at the glass surface to allow rapid configurational sampling,<sup>66</sup> the temperature is sufficiently high that equilibration does not result in highly efficient packing. As the substrate temperature is lowered, the glasses become more kinetically stable until the substrate becomes so cold that the molecules lack the mobility to sample different packing arrangements. For both *cis*-decalin and the *cis/trans*-decalin mixture, maximum kinetic stability is observed 0.84-0.94  $T_g$ . These results are similar to what Ahrenberg et al.<sup>90</sup> observed with AC nanocalorimetry for ethylbenzene and toluene and those reported by Kearns et al.<sup>8</sup> in DSC experiments on indomethacin.

The heat capacity of the vapor-deposited glasses follows a somewhat different trend than the onset temperature over the range of substrate temperatures studied (see Figure 3.5). Similar to the onset temperature, the heat capacity is equal to that of the liquid-quenched glass at substrate temperatures closest to  $T_g$ , but below this region, the heat capacity decreases significantly (Figure 3.5). Near the lowest substrate temperatures, the heat capacity has a maximum decrease of ~2.5% and ~4.5% for the 50/50 *cis/trans*-decalin mixture and *cis*-decalin, respectively. We expect that if we were able to access even lower deposition temperatures, we would see the heat capacity increase again, as was observed for toluene and ethylbenzene.<sup>90</sup> The data in Figure 3.5 suggests an increase in

heat capacity would occur just beyond the lower end of our accessible temperature range. At very low substrate temperatures, molecules do not have time to find more stable configurations so the heat capacity should increase. Consistent with this view, Suga and coworkers<sup>51-54</sup> showed that the enthalpy of a glass vapor-deposited at very low temperatures is higher than the enthalpy of the liquid-cooled glass.

For vapor-deposited toluene and ethylbenzene glasses, Ahrenberg et al.<sup>90</sup> examined the relationship between the heat capacity and the onset temperature over a range of substrate temperatures. For both systems, the two quantities were anti-correlated down to  $\sim 0.80 T_g$ , with increasing onset temperatures associated with decreasing heat capacity. At lower substrate temperatures, this anti-correlation is lost as both the onset temperature and the heat capacity decrease. These qualitative observations for toluene and ethylbenzene are consistent with the results presented here for *cis*-decalin and the 50/50 *cis/trans*-decalin mixture. This behavior is not understood and merits further exploration. In this context, we note that decalin is the first molecule without an aromatic ring in its structure to be shown to form stable glasses.

### 3.5.2 Stable glasses and fragility

Table 3.1 provides a compilation of some of the properties of vapor-deposited stable glasses, including results from the literature and those reported here. In order to compare the kinetic stability of different materials, we tabulate  $t_{\text{trans}}$  for a 500 nm stable glass film; this is the time required for the stable glass to transform into the supercooled liquid at a temperature where the structural relaxation time of the supercooled liquid  $\tau_\alpha$  is about 1.5

**Table 3.1: Vapor-deposited glasses measured with AC nanocalorimetry**

System	$T_g$ (K)	fragility <sup>a</sup>	%C <sub>p</sub> decrease <sup>b</sup>	$t_{\text{trans}}/\tau_\alpha^c$	references
indomethacin	315	83	$4.5 \pm 2$	$10^{4.1}$	10, 85, 87, 117, 144
$\alpha,\alpha,\beta$ -tris- naphthylbenzene	348	86	$4 \pm 1$	$10^{4.4}$	10, 85, 88, 144
toluene	117	104	$4 \pm 0.5$	$10^{3.8}$	90, 144-145
ethylbenzene	115	97	$4 \pm 0.5$	$10^{3.7}$	90, 144-145
<i>cis</i> -decalin	141	-	$4.5 \pm 1$	-	this work
50/50 <i>cis/trans</i> -decalin	135, 137	145, 147	$2.5 \pm 0.5$	$10^{4.4}$	133-134, this work

<sup>a</sup> The fragility column reports  $m = \left. \frac{d \log \tau}{d(T_g/T)} \right|_{T=T_g}$

<sup>b</sup>  $(1 - C_{p,AD}/C_{p,OG}) \times 100\%$

<sup>c</sup>  $t_{\text{trans}}$  is the transformation time for a 500 nm film at the temperature where  $\tau_\alpha \approx 1.5$  s for the supercooled liquid.

s.  $t_{\text{trans}}$  is expressed as a ratio relative to  $\tau_{\alpha}$ ; to a first approximation, this ratio expresses the factor by which the stability of the stable glass exceeds that of an ordinary liquid-cooled glass. Table 3.1 also shows the heat capacity decrease for the stable glass as compared to the ordinary liquid-cooled glass. For each of these quantities, results are shown for the deposition conditions that maximize the tabulated property. For one case,  $\alpha,\alpha,\beta$ -tris-naphthylbenzene, the value of  $t_{\text{trans}}/\tau_{\alpha}$  shown in the table was obtained by interpolation of the published data.

Stable glass formers cover a range of fragilities, as can be seen in Table 3.1. The 50/50 *cis/trans*-decalin mixture has the highest fragility of molecular glassformers. As determined by calorimetry and dielectric relaxation spectroscopy, the values of “ $m$ ” characterizing the kinetic fragility are 145<sup>134</sup> and 147<sup>133</sup>, respectively. Since surface mobility is a key factor in the formation of stable glasses, we can infer from Table 3.1 that organic glasses show substantial surface mobility across a wide range of fragilities, including very fragile systems.

### 3.5.3 Stable glasses of mixtures

These are the first experiments to show that stable glasses can be formed from mixtures. Figure 3.4 shows vapor-deposited glasses of decalin mixtures over a range of possible compositions. For each composition, the as-deposited glass has a lower heat capacity and a higher onset temperature than the corresponding liquid-cooled glass, demonstrating that a stable glass is formed. The ability to continuously tune the properties of glasses by changing composition is one of the key features that make glasses

technologically useful. An important element of the current work is the demonstration that stable glasses can also show this versatility. If the properties that we associate with stable glasses, such as low heat capacity<sup>12, 80, 87-88, 90</sup>, high density<sup>9</sup> and an extra peak in the wide-angle X-ray scattering<sup>102, 146</sup> were somehow a result of nanocrystals rather than a truly amorphous system, this new result would be difficult to understand. While mixed molecular crystals can be formed in some cases, they are uncommon especially if the molecules are not superimposable<sup>147</sup> and a mixed crystal of *cis*- and *trans*-decalin has not been reported. Thus Figure 3.4 strongly argues against the idea that nanocrystals are responsible for the extraordinary features of vapor-deposited glasses. Additional arguments also support this view.<sup>146</sup>

The mixed stable glasses of *cis*- and *trans*-decalin have properties that are distinct from the pure components. Stable glasses of *cis*-decalin and the 50/50 *cis/trans*-decalin mixture have different heat capacity decreases at low substrate temperature, with *cis*-decalin achieving a larger heat capacity decrease (see discussion below). Additionally, Table 3.1 shows that among the systems investigated, the mixed decalin stable glass has the smallest heat capacity decrease, relative to the ordinary glass. While it was not possible to form glasses from vapor-deposited *trans*-decalin, stable glasses could be formed that contained up to 75% *trans*-decalin in the mixture. This illustrates the possibility to incorporate the molecules of a very poor glassformer into stable glasses at quite high concentration. This opportunity might be relevant in organic electronics<sup>106</sup> or for fast-crystallizing drug molecules.<sup>136-137</sup>

Can any mixture form a stable glass? The mixture of two geometric isomers of decalin is quite simple; the two molecules have the same chemical functionality and the glass transition temperatures differ by only about 5%. It will be interesting to see if stable glasses can also be formed from molecules that differ more significantly, e.g., in terms of glass transition temperatures. Perhaps for molecules of quite different sizes, stable glass formation might still be possible in a limited composition window. A key component of stable glass formation is molecular mobility during deposition. When the glass transition temperatures are different enough, it may not be possible to find a substrate temperature where both components have sufficient mobility to support stable glass formation. It may also be interesting to investigate whether the ability to form a stable glass of a given mixture will be hindered or facilitated by the degree of intermolecular attractions between the components.

#### **3.5.4 Stability of *cis*-decalin vs. decalin mixture glasses**

The kinetic stability, as determined by onset temperature, is quite similar for *cis*-decalin and 50/50 *cis/trans*-decalin glasses but the heat capacity decrease is markedly different. As seen in Figure 3.6 both *cis*-decalin and the decalin mixture show a maximum onset temperature increase of 7-8 K at substrate temperatures around 0.88  $T_g$ . Moreover, across the entire substrate temperature range the onset temperatures and thus kinetic stability are comparable. The fractional  $C_p$  decrease of *cis*-decalin and the 50/50 mixture, however, begin to deviate at substrate temperatures below 0.95  $T_g$  (Figure 3.5). At the lowest substrate temperatures, the *cis*-decalin glasses show almost twice the decrease in

heat capacity as compared to the ordinary liquid-cooled glass as the decalin mixture. Considering that the heat capacity and onset temperature do not appear to be correlated for a single substance as deposition conditions are varied, it is reasonable that the kinetic stability of the two systems can be similar while the fractional  $C_p$  decreases differ. It is interesting that the decalin mixture has a smaller decrease in heat capacity than any of the materials shown in Table 3.1. We anticipate that investigations of additional systems will reveal which factors control the observed heat capacity drop. For reference, we note that physical aging has previously been shown to lower  $C_p$  for glasses, but aging on the order of days only lowers  $C_p$  by  $\sim 1\%$  or less.<sup>112-115</sup>

### 3.5.5 The generality of stable glass formation

Stable glass formation is not limited to good glassformers. *cis*-Decalin is a very poor glassformer and for this reason few reports on glasses or supercooled liquids of the pure component can be found in the literature. Prior to the DSC results that we report here, the glass transition temperature was only measured on a sample that was more than 95% crystalline.<sup>148</sup> Our measurements provide the first reported glass transition temperature of pure *cis*-decalin for a completely amorphous sample. *cis*-Decalin joins  $\beta\beta\beta$ -TNB<sup>71</sup> in the ranks of poor glassformers that can be vapor-deposited to form stable glasses. However, we also attempted to vapor-deposit glasses of pure *trans*-decalin, which based on our lack of success in DSC measurements, is an even poorer glassformer. A *trans*-decalin film could be formed on the calorimeter by vapor-deposition but the signal changes that occurred upon heating were not consistent with transformation into the supercooled liquid; we



interpret this result to mean that the as-deposited film was already largely crystalline or crystallizes in the vicinity of  $T_g$ .

Crystallization during deposition represents one way in which stable glass formation can fail. A recent paper by Capponi et al.<sup>130</sup> describes another route by which stable glass formation can fail. These authors vapor-deposited glycerol onto substrates near  $0.88 T_g$  at a rate of 0.03 nm/s. Based upon previous work, as summarized in Table 3.1, stable glass formation would be expected under these conditions. In contrast, Capponi et al. did not obtain a stable glass. When they heated their as-deposited glass above  $T_g$  it transformed relatively quickly into a liquid with unusually large dipolar order; this liquid persisted for an extremely long time. Qualitatively similar behavior was observed by these authors when they vapor-deposited threitol and xylitol. In light of the range of fragility of these molecules, we are inclined to interpret their behavior in terms of the dense network of hydrogen bonds formed by these liquids. In view of this, the failure of water to form stable glasses<sup>131-132</sup> could also be seen as a result of its hydrogen bonding network. Why liquids with a strong network of hydrogen bonds might behave systematically different than the substances listed in Table 3.1 is a matter for future investigation. One possibility is that these liquids do not have highly mobile surfaces. In any case, it remains an open question as to whether any moderately strong organic glassformer can form a highly stable glass via vapor-deposition.

### 3.6 Conclusions

*In situ* nanocalorimetry has been used to measure the heat capacity of glasses of *cis*-decalin and *cis/trans*-decalin mixtures vapor-deposited across a range of substrate temperatures. For all systems investigated, glasses deposited very near  $T_g$  had properties identical to those of the corresponding liquid-cooled glasses. For both *cis*-decalin and 50/50 *cis/trans*-decalin mixtures, the heat capacity of the as-deposited glass decreased with decreasing substrate temperature. The largest differences were seen near the lowest deposition temperatures ( $\sim 0.75 T_g$ ), and were equal to a  $4.5 \pm 1\%$  decrease for *cis*-decalin and a  $2.5 \pm 0.5\%$  decrease for the decalin mixture. These vapor-deposited glasses exhibited increased kinetic stability as evidenced by increases in the onset temperature of up to almost 8 K relative to the liquid-cooled glass. Glasses deposited between 0.84 and 0.94  $T_g$  had the highest onset temperatures. Extremely long isothermal transformation times ( $10^{4.4} \tau_\alpha$  for  $\sim 500$  nm film) were observed when 50/50 *cis/trans*-decalin glasses were annealed above  $T_g$ .

These results extend our knowledge of stable glass formation in at least two important directions. We have shown that extremely fragile glassformers can form stable glasses. Combined with previous results, stable glass formation has now been demonstrated for systems with intermediate and high fragility. Our results also show that mixtures of organic molecules can form stable glasses and that extremely poor glassformers can form stable glasses if mixed with  $\sim 25\%$  of a second component. The ability to tune properties by changing composition is an important characteristic of glasses that enables many technological applications. Our results show that stable glasses also

have this flexibility with regard to composition and this may facilitate applications of stable glasses. Amorphous mixtures are found, for example, in organic electronics and in pharmaceuticals in the form of drug-excipient mixtures that stabilize the drug. Stable glasses could potentially be useful in these applications and elsewhere that mixtures play a role. For fundamental studies, dyes or other probes could be incorporated into stable glasses to track the dynamics in the system. In addition, the formation of stable glasses from mixtures implies that nanocrystalline order likely plays no role in the enhanced stability observed in these vapor-deposited glasses.

### **3.7 Acknowledgements**

We would like to thank Gilbert Nathanson and Ranko Richert for helpful discussions. We would like to thank Prof. Richert in particular for suggesting the implications of these results for the hypothesis of nanocrystalline order. We thank Shakeel Dalal for performing the *in situ* ellipsometry measurements and Yeong Zen Chua for support regarding temperature calibration. We gratefully acknowledge funding from the US National Science Foundation (CHE-0724062 and CHE-1012124) and the German Science Foundation (DFG-SCHI 331 14-1).

## Chapter 4

### Reversing heat capacity of vapor-deposited glasses of *o*-terphenyl

Katherine R. Whitaker, Mike Tylinski, and M. D. Ediger

Department of Chemistry, University of Wisconsin–Madison, Madison, Wisconsin 53706

Mathias Ahrenberg, Christoph Schick

Institute of Physics, University of Rostock, Rostock, 18051 Germany

To be submitted to:

Journal of Chemical Physics

## 4.1 Abstract

The reversing heat capacity of vapor-deposited *o*-terphenyl glasses as a function of deposition temperature was determined using *in situ* AC nanocalorimetry. Glasses were deposited at substrate temperatures ranging from  $0.39 T_g$  to  $T_g$ . For substrate temperatures up to  $\sim 0.5 T_g$ , the heat capacity of the vapor-deposited glass was greater than the heat capacity of an ordinary liquid-cooled glass at the same temperature. At higher substrate temperatures, the as-deposited heat capacity was lower than that of the ordinary glass and reached a maximum fractional heat capacity decrease of  $(1 \pm 0.4)\%$  near  $0.85 T_g$ . The other systems studied thus far have shown 3-4% maximum fractional heat capacity decreases, making the value of  $\sim 1\%$  reported here for *o*-terphenyl the smallest decrease to date. The kinetic stability of vapor-deposited glasses of *o*-terphenyl was maximized near  $0.80 T_g$  and a 460 nm film required  $\sim 10^{4.5}$  times the structural relaxation time of the equilibrium supercooled liquid to transform from the stable glass. The stable glass to supercooled liquid transformation time was thickness-dependent, consistent with previous reports for indomethacin and  $\alpha,\alpha,\beta$ -tris-naphthylbenzene.

## 4.2 Introduction

Glasses are kinetically frozen, non-equilibrium systems in which the properties of the material can significantly depend of the preparation method.<sup>9, 28</sup> One of the most common ways of preparing glasses is by cooling from the liquid. If crystallization is avoided when the liquid is cooled below the melting point, the material becomes a supercooled liquid. As temperature is further decreased, molecular motion slows down and the system

falls out of equilibrium. The temperature where this occurs is known as the glass transition temperature  $T_g$ . However, the observed glass transition temperature depends on the cooling rate of the liquid, as does the enthalpy and volume. Glasses can also be prepared by physical vapor deposition (PVD). Using PVD, glasses with an even wider range of enthalpies and volumes can be made. Deposition onto cold substrates produces glasses with high enthalpy and low density,<sup>11, 51-54</sup> while deposition onto substrates held near  $0.85 T_g$  produces glasses with properties characteristic of exceptionally stable materials such as low enthalpy, high density, low water vapor uptake, and high mechanical moduli.<sup>8-9, 12, 72-74</sup> Stable glasses were first reported less than a decade ago, but over one dozen vapor-deposited systems have already demonstrated similar extraordinary properties.<sup>10, 12, 57, 71, 91</sup>

*o*-Terphenyl (OTP) is one of the most well-studied molecular glassformers,<sup>114, 149-153</sup> however, stable glasses of OTP have yet to be examined. Prior to the first report of stable glasses, anomalously slow diffusion was observed in vapor-deposited glasses of *o*-terphenyl.<sup>154</sup> Considering those glasses were deposited between  $0.8$  and  $0.9 T_g$ , a temperature range where stable glass formation is commonly reported, it is possible this was a result of the vapor-deposited glasses having enhanced stability. Among the myriad of data available for *o*-terphenyl is high quality heat capacity data. In the early 1970's, Chang and Bestul used adiabatic calorimetry to measure the heat capacity of a number of glass forming systems, including OTP.<sup>112-115</sup> The heat capacity of the liquid, crystal, and glass of OTP, as well as an annealed glass, was measured and then used to calculate the enthalpy and entropy. The Chang and Bestul data has been used to test various theories associated

with the glass transition, including that of Adam and Gibbs.<sup>114, 116, 155-156</sup> Studying the heat capacity of vapor-deposited glasses of *o*-terphenyl provides an opportunity to add a new facet to the substantial body of literature that exists for OTP.

A number of organic glassformers have been shown to have 3-4% lower heat capacity when vapor-deposited, as compared to the liquid-cooled glass at the same temperature.<sup>12, 87-88, 90-91</sup> This difference in heat capacity between the two types of glasses has been attributed to a shift in the vibrational density of states (VDOS); stable vapor-deposited glasses are better packed and some of the vibrational modes could be shifted to higher frequencies, resulting in a lower heat capacity.<sup>88</sup> In accordance with this, simulations on the Lewis-Wahnstrom model of OTP showed the VDOS shifted to higher frequency for higher density glasses.<sup>142</sup> Since stable vapor-deposited glasses have been associated with both higher density and lower heat capacity, it seems likely that vapor-deposited glasses of OTP will also exhibit lower heat capacity than the ordinary glass. The reversing heat capacity of vapor-deposited glasses of OTP is presented here to explore this hypothesis.

In these experiments, OTP was vapor-deposited from  $0.39 T_g$  to  $T_g$  and the reversing heat capacity of the as-deposited glasses was measured using AC nanocalorimetry. The heat capacities of glasses deposited at different temperatures are compared to one another as well as to the heat capacity of the liquid-cooled glass. Furthermore, the relative kinetic stability is determined by comparing the onset temperatures of the glasses. Higher onset temperatures indicate greater kinetic stability, as the molecules require higher

temperatures to be dislodged from the glass. Isothermal annealing experiments were performed to determine the transformation time of the stable glass; this is a metric that can be used to compare the kinetic stability of OTP vapor-deposited glasses to other stable glass forming systems. The transformation behavior is also examined as a function of film thickness.

We find that the substrate temperature during deposition influences the heat capacity of the vapor-deposited glass relative to the ordinary glass. For deposition between  $\sim 0.4$ - $0.5 T_g$ , the heat capacity of the vapor-deposited glass is greater than that of the liquid-cooled glass at the same temperature. As the substrate temperature is increased towards  $0.85 T_g$ , the heat capacity decreases to a maximum fractional  $C_p$  decrease of  $\sim 1\%$ . With further increase of the substrate temperature, the as-deposited heat capacity increases until it is equivalent to the heat capacity of the ordinary glass for a deposition temperature of  $T_{\text{sub}} = T_g$ . The kinetic stability, using the onset temperature of the as-deposited glass as a metric, also depends on the substrate temperature and was maximized near  $0.8 T_g$ . Isothermal annealing experiments showed the kinetic stability of OTP is comparable to that previously reported for indomethacin and  $\alpha,\alpha,\beta$ -tris-naphthylbenzene.<sup>78, 85, 88</sup> Thickness dependent transformation times are observed for thin films of OTP; this result is also consistent with the indomethacin and  $\alpha,\alpha,\beta$ -tris-naphthylbenzene data.<sup>31, 34-35</sup>

## 4.3 Experimental

### 4.3.1 Materials



*o*-Terphenyl ( $T_g = 246$  K)<sup>157</sup> was obtained from Sigma (St. Louis, MO) with a purity of 99% and used without further purification.

#### 4.3.2 Sample preparation

Physical vapor deposition was used to prepare the *o*-terphenyl glasses. The details of the set-up are presented elsewhere<sup>89, 91</sup> and only the main points will be covered here. Prior to deposition, the pressure in the chamber was  $10^{-10}$  torr; during deposition, the pressure was  $\sim 4 \times 10^{-6}$  torr which corresponded to a deposition rate of  $0.15 \pm 0.05$  nm/s. The crucible containing *o*-terphenyl had to be heated in order to achieve this deposition rate. To prevent direct deposition from the source, a baffle was utilized. Both calorimeters were in the same temperature controlled housing, set to the deposition temperature. The material was only deposited onto the sample calorimeter; the reference calorimeter is completely enclosed in the housing. XEN-39391 nanocalorimeters (Xensor Integrations) were used for the measurements. A quartz crystal microbalance (QCM) was used to monitor the deposition. For each deposition, a predetermined amount of *o*-terphenyl was deposited onto the QCM and the sample calorimeter. When the desired amount had been deposited as measured by the QCM, a shield was raised to stop the deposition. Immediately following the deposition, the chamber was backfilled to 220 torr with dry nitrogen gas for the measurement.

The thickness of the films was determined by *in situ* ellipsometry, as has been previously described.<sup>91</sup> Glasses deposited at substrate temperatures below 225 K were  $800 \pm 20$  nm thick. When deposition temperatures above 225 K were used, the sticking

coefficient of the molecules impinging on the surface of the nanocalorimeter housing was less than one. As a result of this, material could desorb from the housing and also contribute to the deposition; thus glasses deposited at substrate temperatures above 225 K were  $\sim 1000$  nm thick. We have confirmed that the thickness of the films does not significantly affect the resulting onset temperature or the observed heat capacity difference between the as-deposited and liquid-cooled glasses within the error of the measurement. The second route of deposition became important for films deposited below 225 K during the sample measurement. When the temperature was ramped to above 262 K, molecules could again leave the calorimeter housing and deposit onto the nanocalorimeter membrane, increasing the thickness of the film during the measurement. Multiple ordinary glass scans showed that during a pair of heating and cooling ramps, the signal increased by  $\sim 0.2$   $\mu\text{V}$  due to additional material being deposited. This is equivalent to a 1% increase in film thickness. To correct for this effect, the ordinary glass heating and cooling scans were averaged and 0.2  $\mu\text{V}$  was subtracted from the average curve. Ordinary glass curves shown herein are the corrected average curves.

### 4.3.3 *In situ* AC nanocalorimetry

The reversing heat capacity was measured with *in situ* AC nanocalorimetry. The setup of the device has been described elsewhere.<sup>14, 89</sup> The nanocalorimeters consist of a chip with a one micron thick silicon nitride membrane, with integrated thermopiles and heaters. The active area of the particular device used here (XEN-39391) is 60 x 60  $\mu\text{m}$ . A lock-in amplifier supplies a 20 Hz thermal oscillation to the heaters and the complex differential

thermopile amplitude is directly proportional to the reversing heat capacity. The vapor pressure of OTP is high near  $T_g$ , so the vacuum chamber was backfilled to 220 torr with dry nitrogen gas to prevent loss of the OTP films during the measurement scans. Prior to the measurement, background scans were performed under the same conditions and the background was subtracted from the measurement in the complex plane to account for the asymmetry between the sample and reference sensors. Three different calorimeter pairs were employed for the measurements; variations in the data between calorimeters are within the reported error. The data was corrected for the effect of stress on the calorimeter membrane.<sup>91</sup>

Depending on the deposition temperatures, the as-deposited glasses were heated or cooled to 207 K, then heated from 207 K to 268 K at a rate of 2 K/min. Subsequent cooling at the same rate produced the ordinary glass. The ordinary glass was also heated from 207 K to 268 K at a rate of 2 K/min. Because the reversing heat capacity is measured, irreversible kinetic events such as the enthalpy overshoot peak are not observed in AC nanocalorimetry measurements. Multiple heating and cooling scans were performed on the ordinary glass to quantify the change in the signal due to additional deposition (see above for details).

Quasi-isothermal experiments were also done on films with thicknesses from 80 nm to 1370 nm. The glasses for these measurements were all deposited at 206 K ( $0.84 T_g$ ) at a rate of  $0.15 \pm 0.05$  nm/s. Following the deposition, the glasses were heated at a rate of 2 K/min from 206 K to the annealing temperature of 255 K. The sample was held at the

annealing temperature until the reversing heat capacity become constant, signifying the end of the transformation from the stable glass to the supercooled liquid.

## 4.4 Results

### 4.4.1 Reversing heat capacity of as-deposited glasses

The reversing heat capacity of vapor-deposited glasses of OTP depends on the deposition temperature of the glass. Glasses were deposited at substrate temperatures from  $\sim 0.4 T_g$  to  $T_g$ ; Figure 4.1 shows heat capacity curves that are representative of different substrate temperature regions. In Figure 4.1a, the glass was deposited at  $0.39 T_g$  and then heated at a rate of 5 K/min to 207 K. At 207 K, the heating rate was changed to 2 K/min and heating was continued to a temperature of 268 K. The ordinary liquid-cooled glass was then prepared by cooling at a rate of 2 K/min to 207 K. Reheating at the same rate to above  $T_g$  yielded the ordinary glass heat capacity curve. Due to the AC nature of the experiment, the dynamic glass transition is measured at the frequency of the oscillation. All measurements reported herein utilized a thermal frequency of 20 Hz. Glasses prepared at the lowest deposition temperatures in this study ( $0.39 T_g$ ) had as-deposited heat capacity higher than the heat capacity of the ordinary liquid-cooled glass. At 230 K, the heat capacity of the low substrate temperature vapor-deposited glasses was  $\sim 1\%$  higher than that of the ordinary glass. The curves in Figure 4.1b were produced by a temperature profile similar to that described above, except the glass was deposited at  $0.64 T_g$ . For this substrate temperature, the heat capacities of the glasses are comparable but the onset temperature of the as-deposited glass is enhanced with respect to the ordinary glass. In Figure 4.1c, the

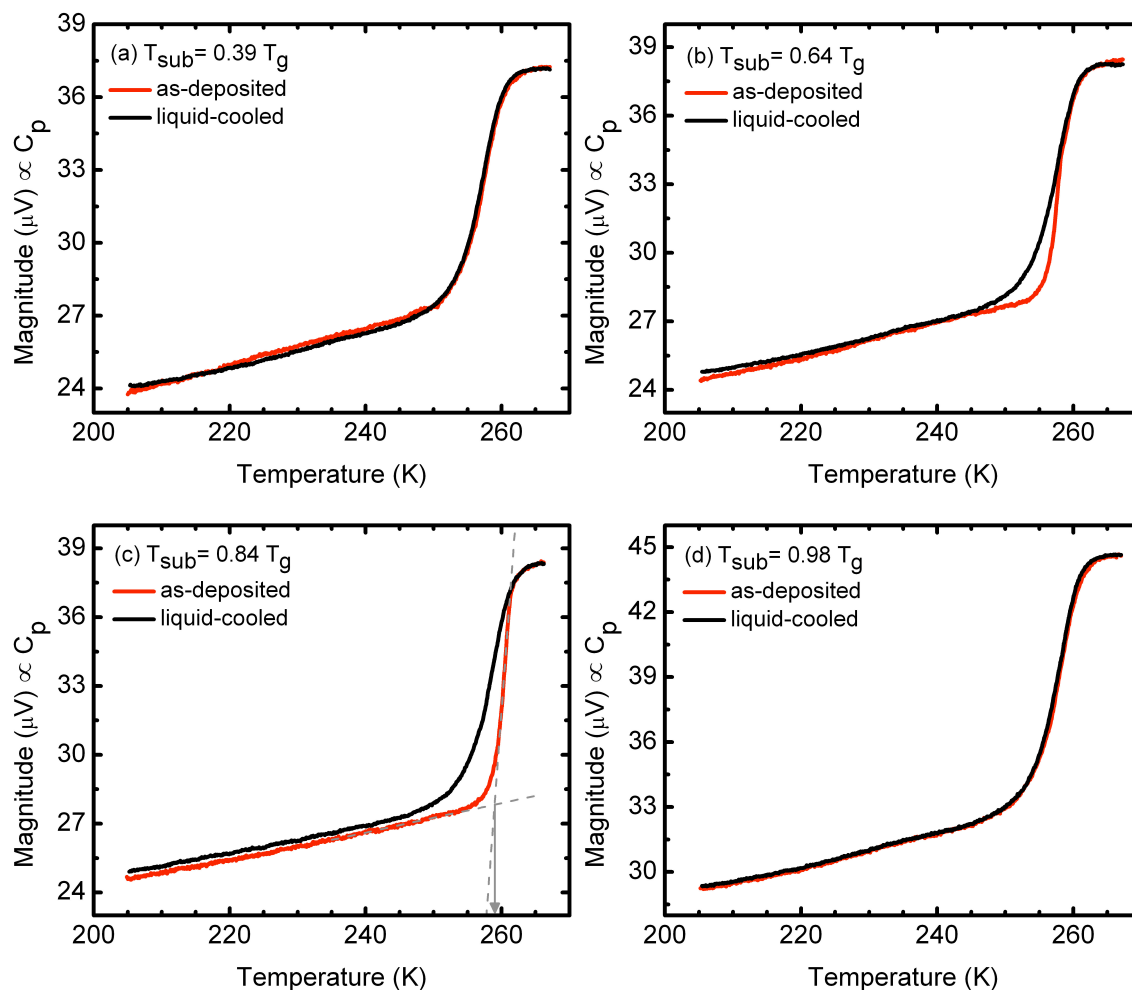


**Figure 4.1.** Effect of substrate temperature on the reversing heat capacity of vapor-deposited glasses of *o*-terphenyl. The glasses were deposited at (a) 95.7 K, (b) 156.9 K, (c) 206.3 K and (d) 240.3 K. In each panel the red curve is the as-deposited glass and the black curve is the ordinary liquid-cooled glass prepared by cooling at a rate of 2 K/min. The dashed gray lines in panel (c) demonstrate the tangent method used to determine the onset temperature.

glass was deposited at  $0.84 T_g$ . The heat capacity of the as-deposited glass is 1% lower than the heat capacity of the liquid-cooled glass. With an onset temperature increase of  $\sim 4$  K over the liquid-cooled glass, this glass shows even greater kinetic stability than the glass deposited at  $0.64 T_g$ . A glass deposited at  $0.98 T_g$  (Figure 4.1d) is essentially equivalent to the ordinary liquid-cooled glass.

#### 4.4.2 Effect of substrate temperature on the reversing heat capacity

The difference in heat capacity between vapor-deposited glasses and liquid-cooled glasses of *o*-terphenyl depends on the temperature at which the glass was deposited. Figure 4.2 summarizes the heat capacity difference between the as-deposited glass and the liquid-cooled glass at 230 K for all of the substrate temperatures measured. The difference was evaluated at 230 K because at this temperature the response of the material to a 20 Hz modulation frequency comes exclusively from the glass. At deposition temperatures close to  $T_g$ , the heat capacities of the vapor-deposited and liquid-cooled glasses are comparable. However, as the deposition temperature is decreased, the heat capacity of the vapor-deposited glass decreases with respect to the liquid-cooled glass. Near  $0.85 T_g$ , the as-deposited glass heat capacity is minimized and the heat capacity is  $\sim 1\%$  lower than the heat capacity of the ordinary glass cooled from the liquid. The heat capacity of the as-deposited glass is lower than the ordinary glass heat capacity for substrate temperatures  $>0.5 T_g$ . Glasses deposited at temperatures below  $0.5 T_g$  have higher heat capacity than the ordinary glass. The heat capacity of the crystal relative to the ordinary glass (data taken

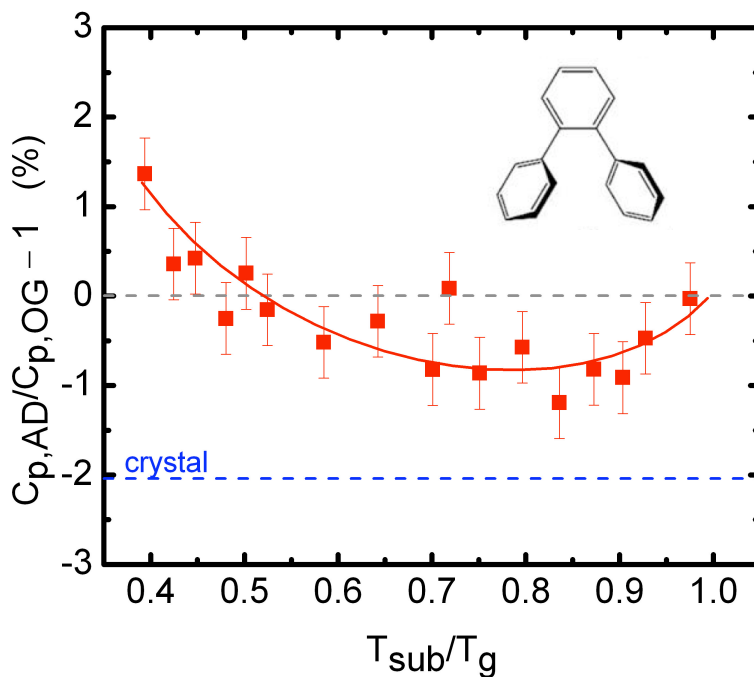


**Figure 4.2.** Fractional decrease of the heat capacity of as-deposited *o*-terphenyl glasses, relative to a glass cooled at a rate of 2 K/min. The blue dashed line represents the heat capacity of crystalline *o*-terphenyl relative to the liquid-cooled glass, as measured by Chang and Bestul with adiabatic calorimetry.<sup>114</sup> All of the heat capacity comparisons are made at 230 K. The substrate temperature is scaled by  $T_g$  and the red line is a guide to the eye. Data points represent one to six experiments and the error bars are equal to the average standard deviation. The molecular structure of OTP is shown in the top right corner.

from Chang and Bestul<sup>114</sup>) is also shown for comparison. The crystal heat capacity is 2% lower than the liquid-cooled glass at 230 K.

#### 4.4.3 Effect of substrate temperature on the kinetic stability

As a metric of the kinetic stability, the onset temperatures of the vapor-deposited and liquid-cooled glasses are compared. A higher onset temperature corresponds to greater kinetic stability because higher temperatures are required to dislodge the molecules from the glass. The onset temperature was determined by the tangent method, as illustrated in Figure 4.1c. The difference between the as-deposited glass and the ordinary glass onset temperatures as a function of substrate temperature is summarized in Figure 4.3. When the deposition temperature is below  $\sim 0.55 T_g$ , the onset temperature of the as-deposited glass is very similar to that of the liquid-cooled glass. As the deposition temperature is increased, the onset temperature of the as-deposited glass increases as well. Between  $\sim 0.7-0.9 T_g$ , the greatest increase in kinetic stability, as quantified by the onset temperature, is achieved. In this substrate temperature range, the onset temperatures of the vapor-deposited glasses and the ordinary liquid-cooled glass are separated by  $\sim 4$  K. For glasses deposited at temperatures near  $T_g$  little difference between the onset temperatures is observed.

#### 4.4.4 Isothermal transformation kinetics

The kinetic stability of vapor-deposited glasses can also be quantified through isothermal transformation experiments, which measure the time required to transform the



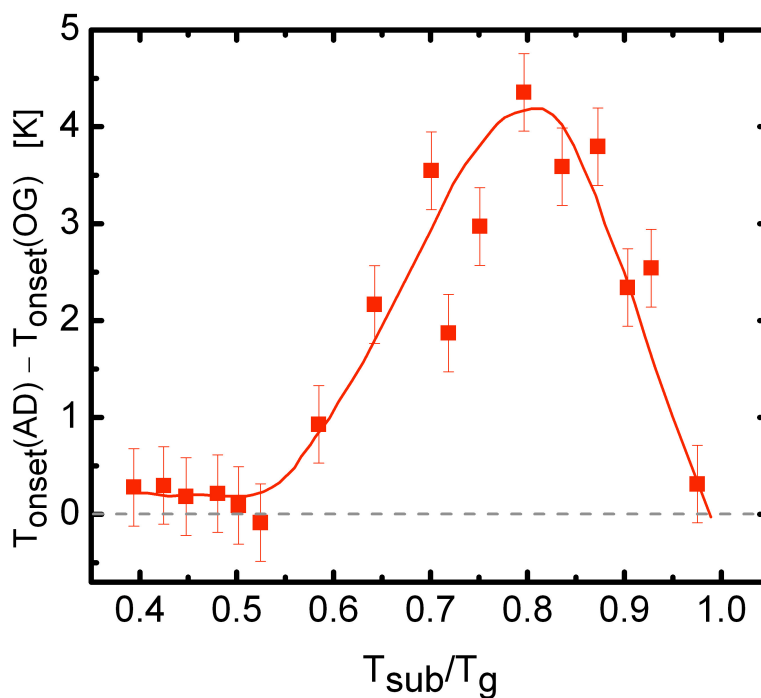


**Figure 4.3.** Effect of substrate temperature on the onset temperature of vapor-deposited glasses of *o*-terphenyl. The onset temperature of the as-deposited glass is compared to the onset temperature of the ordinary glass. The onset temperature was determined by the tangent method as shown in Figure 4.1c. The substrate temperature is scaled by  $T_g$  and the red line is a guide to the eye. Data points represent one to six experiments and the error bars are equal to the average standard deviation.

stable vapor-deposited glass into the supercooled liquid. For such measurements, OTP glasses were deposited at 206 K ( $0.84 T_g$ ) with thicknesses ranging from 80 nm to  $\sim 1400$  nm. The glasses were heated at a rate of 5 K/min from the deposition temperature to the annealing temperature of 255 K. Using quasi-isothermal AC nanocalorimetry, the evolution of the heat capacity from that of the as-deposited stable glass to that of the supercooled liquid can be observed as a function of time. As previously defined<sup>86</sup>, the parameter  $\phi_{SG}$  is used to normalize curves of different thicknesses for comparison.  $\phi_{SG}$  represents the fraction of stable glass remaining in the film at any point in time and the stable glass to supercooled liquid transformation is complete when  $\phi_{SG}$  is equal to zero. Figure 4.4 shows  $\phi_{SG}$  curves for glasses with thicknesses from 80 nm to 1370 nm. For films that are  $\leq 460$  nm in thickness,  $\phi_{SG}$  is linear with respect to time. For thicker films, the curves have a more complicated profile with time. The 460 nm thick stable glass film required  $\sim 2000$  s to transform into the supercooled liquid. To put this in context, the structural relaxation time  $\tau_\alpha$  of the supercooled liquid at 255 K is  $\sim 0.06$  s;<sup>158</sup> thus the transformation time of a 460 nm thick *o*-terphenyl glass deposited at  $0.84 T_g$  is  $10^{4.5} \tau_\alpha$ .

## 4.5 Discussion

### 4.5.1 Heat capacity of *o*-terphenyl

The effect of substrate temperature on the stability of vapor-deposited glasses is now well-documented.<sup>8, 11-12, 65, 90</sup> It also seemingly well-understood based on the role of surface mobility during deposition.<sup>9, 66</sup> For deposition at temperatures near  $T_g$ , the depositing molecules have enough mobility to rapidly sample configurations and

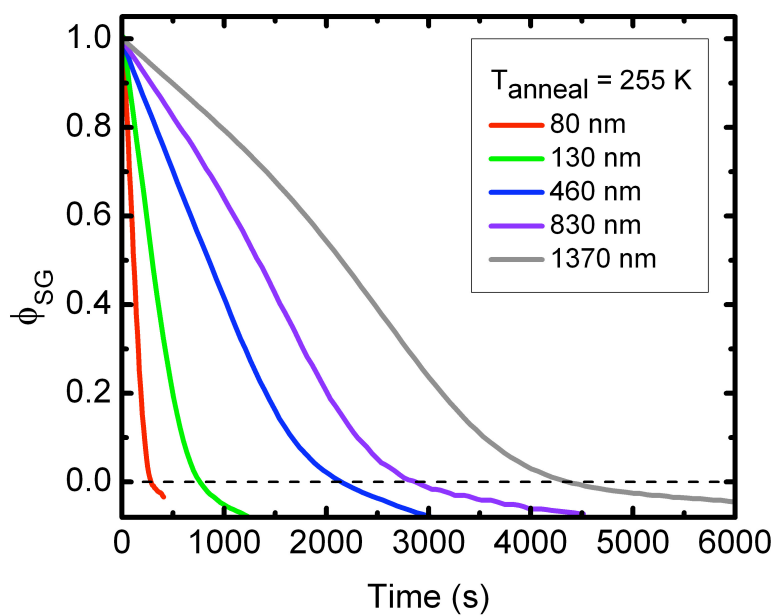


**Figure 4.4.** Isothermal transformation behavior of stable glasses of *o*-terphenyl. Glasses were deposited at 206 K and 0.2 nm/s.  $\phi_{SG}$  is a parameter used to define the fraction of the film that remains stable glass at any point in time. The data has been smoothed to more clearly show the transformation process.

equilibrate. Since each molecule spends some amount of time in the mobile surface layer before becoming buried in the bulk by newly depositing molecules, the entire film has had an opportunity to equilibrate. For deposition onto cold substrates, there is a large driving force to find a more stable packing, but the mobility is lacking. When deposition temperatures near  $0.85 T_g$  are utilized, the conditions are optimized for the molecules to explore the energy landscape, which results in exceptionally stable glasses.<sup>8</sup> In this respect, the results obtained here for vapor-deposited glasses of *o*-terphenyl are not surprising. Similar to the reports for other systems, *o*-terphenyl glasses exhibit maximum stability when they are deposited near  $0.85 T_g$ . Qualitatively as well as quantitatively, the kinetic stability of *o*-terphenyl glasses is on par with other stable glass formers (see section 4.5.2 for more details).<sup>90-91</sup>

On the other hand, the heat capacity results presented here are somewhat different than the previous results for other systems. Based on the other systems studied thus far, one might have expected the heat capacity of vapor-deposited glasses of OTP to be 3-4% lower than the heat capacity of the ordinary glass.<sup>12, 87-88, 90-91</sup> This was not the case though; vapor-deposited glasses of *o*-terphenyl only show at most a 1% fractional  $C_p$  decrease. Why might the heat capacity difference between vapor-deposited glasses and the ordinary glass be so much smaller for OTP compared to the other systems? One possible explanation is that the ordinary glass is already well-packed and further stabilization of the packing is difficult to achieve. The heat capacity of the ordinary glass is only  $\sim 2\%$  greater than the heat capacity of the crystal in the temperature range of interest. Perhaps this small

difference in heat capacity between the disordered and ordered solids indicates the packing of the ordinary glass is already fairly optimized. It is possible that even through vapor-deposition, more stable configurations are hard to access. *cis*-Decalin vapor-deposited glasses were at the other end of the spectrum. Of the stable glass forming systems studied thus far with nanocalorimetry, *cis*-decalin showed one of the largest fractional  $C_p$  decreases with a value of 4.5%.<sup>91</sup> Neutron scattering experiments on *cis*-decalin exhibited anharmonicity in the ordinary glass, which can be interpreted as poor packing<sup>159</sup>. *cis*-Decalin has a poorly packed ordinary glass and a large fractional  $C_p$  decrease for the vapor-deposited glass while *o*-terphenyl seems to have a well-packed ordinary glass and the vapor-deposited glass has a relatively small fractional  $C_p$  decrease.

The efficient packing of *o*-terphenyl ordinary glasses is further supported by aging experiments. Numerous reports exist demonstrating that aging glasses lowers their heat capacity.<sup>112-115, 160</sup> When Chang and Bestul measured the heat capacity of OTP, they also measured the heat capacity of a quenched glass that had been annealed at 230 K ( $T_g - 16$  K) for 3 days. Over that time period, the annealed glass heat capacity decreased  $\sim 0.15\%$  with respect to the quenched glass heat capacity in the temperature range of interest. The logarithmic timescale associated with aging implies it would take  $\sim 10^{13}$  years to decrease the heat capacity of an ordinary glass by 1% through aging. Since the vapor-deposited *o*-terphenyl glass has  $(1 \pm 0.4)\%$  lower heat capacity than the ordinary glass, the equivalent age of the vapor-deposited glass would be at least  $10^8$  years based on the heat capacity.

Compared to other organic glassformers, the heat capacity change observed for the annealed *o*-terphenyl glass is relatively small. Diethyl phthalate glasses aged at  $T_g - 10$  K for 16 hours showed a heat capacity decrease of  $\sim 0.3\%$ ,<sup>112</sup> while aging a glass of sucrose at  $T_g - 15$  K for 12 hours decreased the heat capacity  $\sim 1.2\%$  with respect to the liquid-cooled glass<sup>160</sup>. By comparison, much longer time at a similar relative aging temperature had a far weaker effect on lowering the heat capacity of an *o*-terphenyl glass.

Differences in the vibrational density of states (VDOS) of liquid-cooled and stable vapor-deposited glasses are thought to be responsible for the observed difference in heat capacity between the glasses. Bestul and coworkers performed heat capacity comparisons similar to those done for *o*-terphenyl on five additional systems: diethyl phthalate, *cis*-1,4-polyisoprene, selenium, polyethyl methacrylate and polyvinyl chloride.<sup>112-116</sup> Goldstein analyzed the quenched glass and annealed glass entropies available from this data to determine which factors between the vibrational density of states and changes in anharmonicity or secondary relaxational degrees of freedom provide contributions to  $\Delta C_p$ .<sup>116</sup> In every system except *o*-terphenyl, anharmonicity or secondary relaxational degrees of freedom were determined to be a significant cause for the decrease in the entropy difference between the quenched glass and annealed glass on cooling. However, the OTP data was consistent with mainly changes in the vibrational frequencies. The heat capacity difference between the stable vapor-deposited glass and the ordinary glass cooled from the liquid has also been interpreted as a change in the VDOS, with some of the vibrational modes shifted to higher frequency in the vapor-deposited glass.<sup>88</sup> Perhaps in

OTP stable glasses, the main contribution to the heat capacity difference is a change in the vibrational frequencies but the heat capacity of stable glasses of other materials are additionally affected by changes in anharmonicity or secondary relaxational degrees of freedom.

Besides the relatively small fractional  $C_p$  decrease measured here, this is also one of the only systems where the heat capacity of a vapor-deposited glass is reported to be *greater* than that of the ordinary glass. A vapor-deposited glass of 1-pentene had higher heat capacity than a liquid-cooled 1-pentene glass in the temperature range 12-30 K, which is far below the reported  $T_g$  of 70 K. The heat capacity of *o*-terphenyl glasses deposited at temperatures near  $0.4 T_g$  is higher than the ordinary glass almost all the way to the dynamic glass transition temperature. In the measurements on toluene and ethylbenzene, the heat capacity of the vapor-deposited glass started to increase toward the ordinary glass heat capacity for substrate temperatures below  $0.65 T_g$ , but a crossover to heat capacity higher than that of the liquid-cooled glass was not seen.<sup>90</sup> The rarity of such an observation may be partially attributable to the fact that conventional calorimetry techniques may not be sensitive to 1% differences in heat capacity.

Vapor-deposition of glasses with high heat capacity relative to the ordinary glass can also be interpreted in terms of the VDOS. At low substrate temperatures, poorly packed glasses are formed and the vibrational density of states can be shifted to lower frequency. Experiments on a mineral glass with high fictive temperature showed the VDOS shifted to

lower frequency.<sup>143</sup> Since high fictive temperatures are commonly associated with glasses vapor-deposited onto cold substrates,<sup>51, 53</sup> that report is consistent with this explanation.

#### 4.5.2 Kinetic stability of *o*-terphenyl glasses

The kinetic stability of vapor-deposited glasses of *o*-terphenyl was quantified in two ways: onset temperature and isothermal transformation time. The onset temperature of the most kinetically stable glasses (deposited at  $\sim 0.8 T_g$ ) was 259 K, which is 13 degrees higher than  $T_g$  (246 K). To put this in perspective, an ordinary glass of OTP aged for 10 hours at 233 K showed an onset temperature only 5 K greater than  $T_g$ .<sup>161</sup> Based on an extrapolation of that data, it would be necessary to age an ordinary glasses at 233 K for  $\sim 20,000$  years to achieve an onset temperature comparable to that of the most stable vapor-deposited glass of OTP.

While the onset temperature provides a means of comparing the age of glasses of the same material, measurement of the isothermal transformation time allows the kinetic stability of glasses of different materials to be compared. A 460 nm thick OTP glass that was deposited at  $0.84 T_g$  and annealed at 255 K required  $\sim 2000$  s to transform into the supercooled liquid. At 255 K, the structural relaxation time of the equilibrium supercooled liquid is  $\sim 0.06$  s, indicating  $\sim 10^{4.5}$  structural relaxation times were necessary to relax the stable glass. Vapor-deposited glasses of indomethacin and  $\alpha,\alpha,\beta$ -tris-naphthylbenzene showed similar stability against heating.<sup>78, 88</sup> While the stability of vapor-deposited glasses of OTP is comparable to other stable glasses, it should be stressed that these glasses are



still quite remarkable compared to liquid-cooled OTP glasses and among some of the most kinetically stable glasses ever produced in the laboratory.

Similar to other vapor-deposited glasses with high kinetic stability, OTP glasses exhibited thickness-dependent transformation times. For all of the samples measured here, the transformation time increased with thickness. For the thinnest films (up to  $\sim 450$  nm), the transformation proceeds linearly in time. This result is consistent with the transformation being controlled by a surface-initiated growth front.<sup>76</sup> The thicker films initially transform linearly in time but then become faster. The presence of the initial linearity indicates that they may begin to transform via a growth front before some other mechanism becomes favorable. For indomethacin, it was postulated that transformation initiation sites exist within the bulk.<sup>78</sup> For thick films, these sites primarily control the transformation process and the transformation time will be thickness independent. It appears for the OTP films measured here even the thickest films ( $\sim 1400$  nm) do not yet display completely bulk transformation behavior. This is a testament to the kinetic stability of the vapor-deposited glass; bulk transformation is highly suppressed in these films.

#### **4.6 Summary**

Glasses of *o*-terphenyl were vapor-deposited at substrate temperatures from  $0.39 T_g$  up to  $T_g$ . Within this wide range of substrate temperatures, the heat capacity of the vapor-deposited glasses varied from  $\sim 1\%$  greater than that of the ordinary liquid-cooled glass to  $\sim 1\%$  less. The glasses deposited onto the coldest substrates had the highest relative heat capacity and the glasses deposited at temperatures near  $0.85 T_g$  had the lowest relative

heat capacity. Vapor-deposition at temperatures near  $T_g$  produced glasses with heat capacity equivalent to that of the ordinary glass. Compared to the other materials that have been studied, the maximum fractional heat capacity decrease of 1% observed for *o*-terphenyl vapor-deposited glasses is relatively small. However, ordinary liquid-cooled glasses of OTP may already be particularly well-packed, making further enhancement difficult. It is estimated that  $10^8$ - $10^{13}$  years of aging would be required to obtain the same decrease in heat capacity.

The kinetic stability of OTP vapor-deposited glasses is both qualitatively and quantitatively similar to previously studied molecules. The maximum kinetic stability, as determined by the onset temperature, was observed near  $0.85 T_g$ . Roughly 20,000 years of aging would be necessary to increase the onset temperature of an ordinary glass by a similar amount. Comparable to other stable vapor-deposited glasses, the isothermal transformation time of a 460 nm thick *o*-terphenyl stable glass was  $10^{4.5} \tau_\alpha$ . In agreement with measurements on indomethacin and  $\alpha,\alpha,\beta$ -tris-naphthylbenzene, a thickness-dependent transformation time was observed.

#### **4.7 Acknowledgements**

The isothermal annealing measurements were performed by Mike Tylinksi. We gratefully acknowledge funding from the U.S. National Science Foundation (CHE-0724062 and CHE-1012124) and the German Science Foundation (DFG-SCHI 331 14-1).

## Chapter 5

# High heat capacity of low temperature vapor-deposited glasses of *o*- terphenyl

Katherine R. Whitaker and M. D. Ediger

Department of Chemistry, University of Wisconsin–Madison, Madison, Wisconsin 53706

Yeong Zen Chua and Christoph Schick

Institute of Physics, University of Rostock, Rostock, 18051 Germany

To be submitted to:

Journal of Physical Chemistry Letters

## 5.1 Abstract

The reversing heat capacity of vapor-deposited glasses of *o*-terphenyl was measured using *in situ* AC nanocalorimetry. The calorimetric signal for glasses deposited near  $0.38 T_g$  was ~50% higher than that of the ordinary liquid-cooled glass. This large feature was irreversibly erased on heating, with a majority of the difference between the glasses vanishing once the vapor-deposited glass was heated above ~150 K. Glasses with deposition temperatures up to  $0.48 T_g$  also showed initially large signals near the deposition temperature though to a lesser extent.

## 5.2 Introduction, Results and Discussion

If crystallization is avoided when a liquid is cooled below its melting point, it is known as a supercooled liquid. As cooling is continued, a point is reached where the molecules are no longer able to reconfigure on the timescale of the measurement and the material becomes a kinetically frozen glass. The temperature where this occurs is known as the glass transition temperature  $T_g$ . Glasses have the mechanical properties of solids but lack long-range order. Non-crystalline solids can also be prepared by other methods including physical vapor deposition (PVD) or disruption of the crystalline structure, e.g. through ball milling.<sup>19, 28</sup>

In the 1960's Suga and coworkers used adiabatic calorimetry to show that amorphous materials prepared by PVD demonstrate a glass transition at temperatures similar to those of the liquid-cooled glasses.<sup>58-60</sup> However, despite the similarity of the glass

transition temperatures, the two glasses were not identical in other regards. Glasses of 1-pentene and butyronitrile vapor-deposited at  $\sim 0.6 T_g$  and  $\sim 0.41 T_g$ , respectively, exhibited large configurational enthalpy, which decreased with heating.<sup>51-54</sup> This restructuring of the vapor-deposited glasses occurred at temperatures far below  $T_g$  where molecular motion is inhibited in ordinary liquid-cooled glasses. Additionally, near 13 K the vapor-deposited 1-pentene glass had  $\sim 18\%$  higher heat capacity than the ordinary glass. Consistent with that result, inelastic neutron scattering experiments showed that a propene glass deposited at  $0.36 T_g$  was more disordered and less dense than an annealed glass.<sup>64</sup>

Structural relaxation far below  $T_g$  has also been reported for vapor-deposited glasses of 1,2-dichloroethane.<sup>162</sup> In the liquid and gas phases of 1,2-dichloroethane, trans and gauche conformational isomers coexist, but in different ratios, with the gauche conformer dominating in the liquid. Vapor-deposited glasses prepared at low substrate temperatures were comprised of the conformers in proportions similar to that present in the gas phase. As the samples were heated, irreversible structural relaxation occurred and the mole fraction of gauche conformers increased to a larger value, characteristic of the liquid. Similar to the results described above, such restructuring in the glass is only observed in glasses deposited at low substrate temperatures; the liquid-cooled glass is completely immobile at similar temperatures.

In this letter, we report high calorimetric signals for vapor-deposited glasses of the canonical glassformer *o*-terphenyl. Previous studies on vapor-deposited organic glassformers have shown that glasses deposited around  $0.85 T_g$  have 3-4% lower heat

capacity than the liquid-cooled glass.<sup>87-88, 90-91</sup> In contrast, we present here a detailed investigation of *o*-terphenyl glasses deposited around  $0.4 T_g$  that show *higher* reversing heat capacity than the ordinary glass. The as-deposited signature of these glasses at temperatures  $\sim 140$  K below the glass transition temperature is almost 50% larger than that of the liquid-cooled glass. Similar to the structural relaxations described above, this large difference is irreversibly erased upon heating. Glasses deposited at substrate temperatures up to  $\sim 0.48 T_g$  also show this feature. We tentatively interpret the calorimetric signal as the heat capacity of the *o*-terphenyl film. As will be discussed below, possible adsorption of nitrogen molecules into the vapor-deposited glasses could contribute to the measured heat capacity as well.

The reversing heat capacity of a glass of *o*-terphenyl deposited at 96.6 K ( $0.39 T_g$ ) is shown in Figure 5.1. The sample was deposited directly onto a nanocalorimeter and a differential AC nanocalorimetry measurement was carried out *in situ*, as has been described previously.<sup>14, 89, 91</sup> To prevent desorption of the film during the measurement, the vacuum chamber was backfilled to 220 torr with dry nitrogen gas. In the measurement, an applied AC voltage results in a temperature oscillation on the calorimeters and the complex differential amplitude is proportional to the reversing heat capacity. Since only the reversing heat capacity is measured, non-reversible features such as the enthalpy overshoot peak are not observed. Also, due to the AC nature of the experiment the dynamic glass transition at the frequency of the AC voltage oscillation (20 Hz) is measured. The as-deposited glass was heated at a rate of 2 K/min to 269 K (red curve) and then cooled to 106

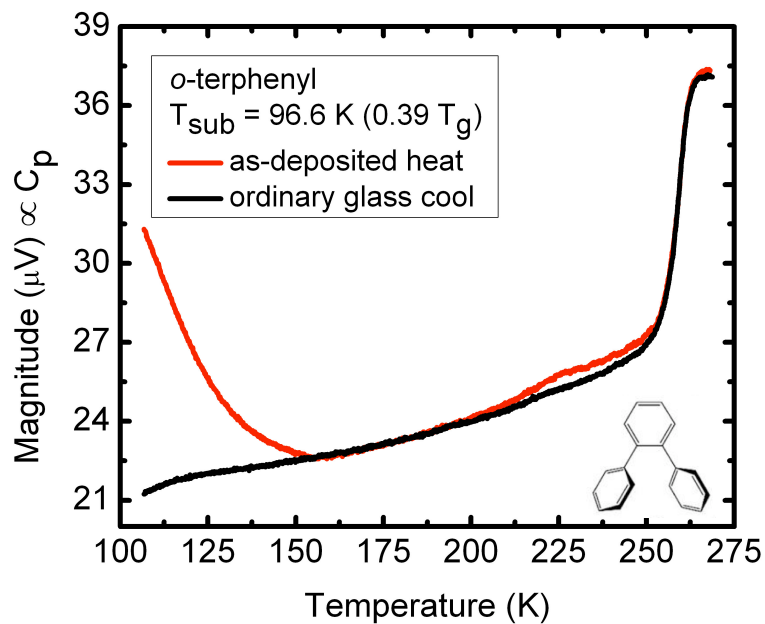


**Figure 5.1.** Reversing heat capacity of a low substrate temperature vapor-deposited *o*-terphenyl glass. A glass was deposited at a substrate temperature of 96.6 K ( $0.39 T_g$ ) and then heated above the dynamic glass transition temperature (red). The sample was then cooled into the glass, producing the ordinary glass curve (black). The molecular structure of *o*-terphenyl is shown in the bottom right hand corner.

K to measure the ordinary liquid-cooled glass (black curve). The ordinary glass behaves as expected based on the other AC calorimetry measurements; in the glass the supplied heat only contributes to vibrations, then as the temperature is increased into the liquid state molecules can also rearrange in response to the temperature oscillation, increasing the heat capacity.<sup>87-88</sup>

The behavior of the as-deposited glass, however, is different than that of the ordinary glass and also quite surprising. Near the deposition temperature, the as-deposited signal is almost 50% higher than that of the liquid-cooled glass. As the temperature is increased towards  $\sim 150$  K, the large signal difference is diminished and the curves become similar. In the temperature range of  $\sim 200$ -253 K, the curves again diverge before coinciding for the remainder of the temperature range measured.

Qualitatively an observation of high heat capacity for a vapor-deposited glass is not completely unprecedented, but quantitatively the effect here is much larger. As mentioned above, adiabatic calorimetry was used to measure a 1-pentene glass ( $T_g = 70$  K) vapor-deposited between 38 and 47 K.<sup>53</sup> At 13 K, the vapor-deposited glass had a heat capacity  $\sim 18\%$  higher than the liquid-cooled glass. By 30 K, the heat capacities of the samples were virtually identical. However, similar measurements were also done on butyronitrile glasses ( $T_g = 97$  K) vapor-deposited onto substrates maintained at 0.41 and 0.72  $T_g$  and essentially no difference in heat capacity was observed between the vapor-deposited and liquid-cooled samples.<sup>54</sup> Here we report what is potentially a 50% difference in heat capacity between the vapor-deposited and liquid-cooled samples of *o*-terphenyl. This is 2.5 times



larger than the heat capacity difference reported for 1-pentene and this interpretation requires careful consideration.

Besides heat capacity, the configurational enthalpy of the vapor-deposited glasses of 1-pentene and butyronitrile was also reported.<sup>53-54</sup> The initial enthalpy of the vapor-quenched samples of 1-pentene and butyronitrile was up to 0.9 and 1.2 kJ/mol, respectively, higher than that of the corresponding liquid-cooled glass. In the butyronitrile measurements, two different substrate temperatures were utilized and the lower substrate temperature glass had a higher configurational enthalpy than the glass deposited at the higher substrate temperature. Once the glasses were heated above the deposition temperature, the configurational enthalpy began to decrease and changes were continually observed until the glass transition temperature was reached. When cold substrate temperatures are utilized for vapor-deposition, the arriving molecules are quickly locked into place and unstable structures can result. As the temperature is increased, the unstable structure can relax. Though it has not been presented quantitatively, vapor-deposited glasses of carbon tetrachloride and propene have also been noted to show behavior similar to that described for 1-pentene and butyronitrile.<sup>163-164</sup>

Only the reversing portion of the heat capacity is measured here and thus the enthalpy is inaccessible, but the structural relaxation has instead been quantified by performing progressively higher temperature ramps and observing the resulting decrease of the calorimetric signal. Figure 5.2a shows heating and cooling curves for a glass deposited at  $0.38 T_g$  and challenged in this manner. The glass was heated to the

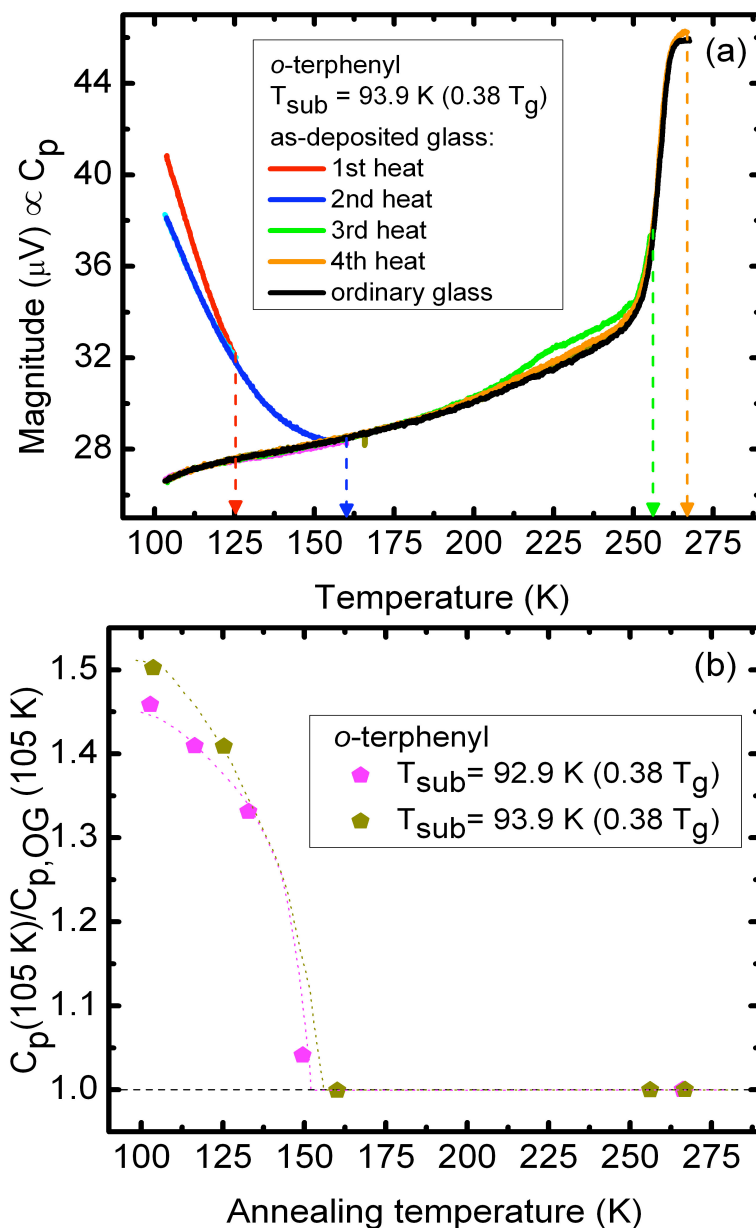


**Figure 5.2.** Structural relaxation of vapor-deposited glasses. (a) The as-deposited glass was heated to progressively higher temperatures, as denoted by the arrows, before returning to 103 K. The cooling curves are buried beneath the heating curve that succeeds them. (b) The initial magnitude and the magnitude after each heating scan are determined at 105 K and are compared to the value of the ordinary glass, also at 105 K. The abscissa indicates the highest temperature the glass reached during a given heating scan. The dark yellow points correspond to the data in (a).

temperature indicated by the arrow, cooled back down to  $\sim 103$  K and then heated to the next temperature indicated by an arrow and so on. The cooling curves coincide with their subsequent heating curves and are difficult to see. The black curve is an ordinary liquid-cooled glass. The magnitude of the ordinary glass, the initial magnitude and the magnitude following each heating scan were determined at 105 K. Figure 5.2b shows the comparison of the heat capacities at 105 K as a function of the highest temperature the glass reached on heating. Results are shown for the data in Figure 5.2a, as well as another *o*-terphenyl glass deposited at a similar temperature.

In each heating scan the calorimetric signal is irreversibly decreased. When the as-deposited sample is returned to low temperature, the large heat capacity is somewhat diminished. The irreversible change in heat capacity is interpreted as an irreversible change in the glass structure. This behavior is consistent with and similar to the irreversible changes in configurational enthalpy in 1-pentene and butyronitrile<sup>53-54</sup> and also the conformational changes in 1,2-dichloroethane<sup>162</sup>. Glasses deposited onto cold substrates can experience molecular restructuring at low temperatures that is not possible in ordinary glasses. Once heated above  $\sim 150$  K, the low temperature feature of the vapor-deposited glass is completely erased, though the higher temperature heat capacity difference still remains until the glass is heated above  $\sim 255$  K. Even though it appears the structure has relaxed, the material is still not equivalent to the ordinary glass, as evidenced by the lingering heat capacity difference between the two glasses in the temperature range  $\sim 200$ -250 K.

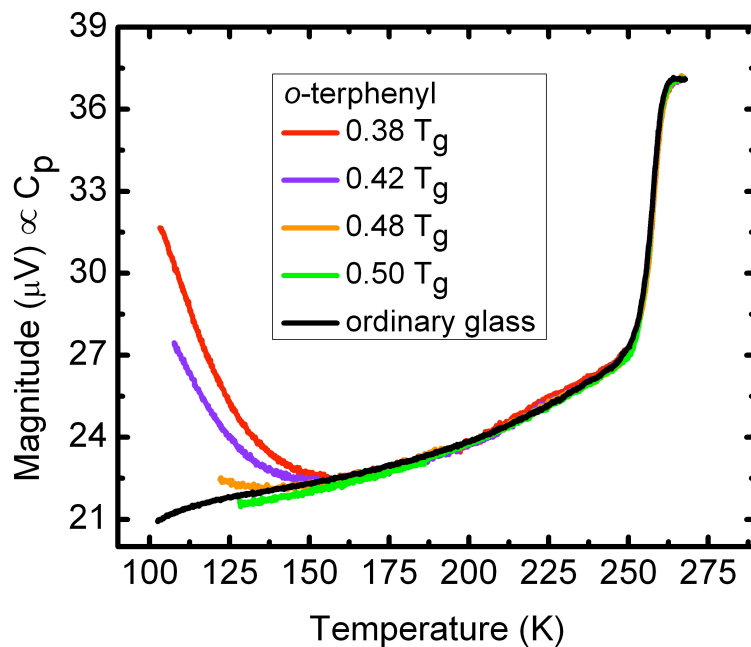


**Figure 5.3.** Effect of substrate temperature on the as-deposited magnitude. *o*-Terphenyl glasses were deposited at substrate temperatures of  $0.38 T_g$  (red),  $0.42 T_g$  (violet),  $0.48 T_g$  (orange) and  $0.50 T_g$  (green). An ordinary liquid-cooled glass (black) is shown for comparison.

Glasses with deposition temperatures up to  $0.48 T_g$  showed higher as-deposited calorimetric signals than the corresponding liquid-cooled glass at the same temperature. Figure 5.3 shows the as-deposited curves of glasses deposited at 94.5, 104.5, 118.2 and 123.5 K. The glasses were heated at a rate of 5-10 K/min from the deposition temperature to  $\sim 190$  K and then a heating rate of 2 K/min was used to temperatures above the glass transition. The black curve shows an ordinary glass heated at a rate of 2 K/min across the same temperature range. Except for the glass deposited at the highest temperature (123.5 K or  $0.50 T_g$ ), all of the glasses were deposited with higher heat capacity than the liquid-cooled glass at the same temperature. Furthermore, as the deposition temperature increased, the as-deposited difference became smaller.

The signal of the vapor-deposited glasses is strongly influenced by the deposition temperature. Based on the data in Figure 5.3, it seems that as the deposition temperature is increased, better packed, lower heat capacity glasses are produced. For the organic glassformers toluene, ethylbenzene and *cis*-decalin, the effect of substrate temperature on glass stability was studied in the temperature range of  $\sim 0.6 T_g$  to  $T_g$ .<sup>90-91</sup> For those materials the as-deposited heat capacity was nearly equivalent to the heat capacity of the ordinary glass for depositions close to  $T_g$ , but became up to  $\sim 4\%$  lower as the substrate temperature was decreased. In toluene and ethylbenzene, the as-deposited heat capacity was minimized until  $\sim 0.7 T_g$ ; for even lower substrate temperatures the heat capacity increased again towards that of the ordinary glass, but was never higher. *o*-Terphenyl vapor-deposited glasses shown here exhibit higher heat capacity than the ordinary glass

for substrate temperatures between 0.38-0.48  $T_g$ . Preliminary results on ethylbenzene indicate that similar results would be achieved for the other molecules if lower substrate temperatures were utilized.

When glasses are vapor-deposited, the amount of time the depositing gas molecules have to explore configurations is dictated by the substrate temperature.<sup>9, 50</sup> If the substrate is very cold, the molecules are almost immediately frozen into place. This is an efficient strategy for avoiding crystallization during deposition and indeed depositing glasses, but as noted above those glasses have high enthalpy with respect to the liquid-cooled glass. Alkylbenzene glasses vapor-deposited at low substrate temperatures show much greater molar volume than the extrapolated supercooled liquid, indicating low density for such glasses as well.<sup>11</sup> Inelastic neutron scattering experiments on low substrate temperature propene glasses were also consistent with vapor-deposited glasses having lower density relative to the liquid-cooled glass.<sup>64</sup>

The nanocalorimetry results presented here are in agreement with deposition onto a cold substrate producing a poorly packed glass. Preliminary *in situ* ellipsometry results for similarly prepared *o*-terphenyl glasses indicate the as-deposited glass is considerably lower in density than the ordinary glass and also showed irreversible changes on heating. In a loosely packed, porous glass, some of the vibrational modes could be shifted to lower frequency, which would result in a higher heat capacity.<sup>142</sup> We interpret Figure 5.2 as the poorly packed structure of the as-deposited glass collapsing as the temperature is increased. The irreversibility of the heat capacity change is consistent with this idea. The

density of states while approaching the jamming transition, or onset of rigidity, in granular materials has been reported to show interesting behavior. In simulations of soft spheres, as the packing fraction is incrementally lowered towards the jamming threshold, large changes in the density of states of the system are observed.<sup>165-166</sup> It was concluded that it is necessary for weakly connected amorphous solids to have an excess density of vibrational states. Perhaps the seemingly large heat capacity measured in this molecular glassformer is a related phenomenon.

It is possible that the high heat capacity observed here is not exclusively from the vapor-deposited *o*-terphenyl glass. As described above, it is reasonable to believe that the as-deposited glass is highly porous. Kay and coworkers<sup>98, 167-168</sup> have demonstrated that highly porous vapor-deposited glasses of water absorb nitrogen and other gases. Since our measurements were performed under a nitrogen atmosphere to prevent desorption of the film, it is possible nitrogen gas is also adsorbed here into the potentially porous glasses. If this is indeed the case, the adsorbed nitrogen would contribute to the measured heat capacity and cause it to be artificially high. Preliminary experiments performed under vacuum indicate the as-deposited heat capacity is affected by the nitrogen backfill. Further experiments with other gases such as helium can shed some light on this issue.

In summary, physical vapor deposition is a method of producing glassy materials, but the properties of the glass will depend on the deposition temperature. Low substrate temperatures are known to produce high enthalpy glasses, while substrate temperatures near  $0.85 T_g$  are known to produce highly stable glasses.<sup>8-9, 51-54</sup> It was demonstrated here

that glasses of *o*-terphenyl deposited between 0.38 and 0.48  $T_g$  have calorimetric signals up to ~50% higher than the glass cooled from the liquid. Prior to this, there was only one report of a vapor-deposited glass with marginally higher heat capacity.<sup>53</sup> Heating the as-deposited glass irreversibly erases the large heat capacity, as would be expected for a structural relaxation. Deposition at the higher substrate temperatures used here yielded glasses with increasingly smaller, but still positive, as-deposited heat capacity differences.

### 5.3 Experimental

*o*-Terphenyl ( $T_g = 246$  K)<sup>157</sup> was purchased from Sigma (St. Louis, MO) and used without further purification. *o*-Terphenyl was vapor-deposited directly onto the sample nanocalorimeter (Xensor Integrations, XEN-39391) as previously described.<sup>89, 91</sup> The deposition was monitored by a quartz crystal microbalance (QCM); when a predetermined amount was deposited onto the QCM, the deposition was stopped. The deposition rate was  $0.15 \pm 0.05$  nm/s and the films were  $800 \pm 20$  nm thick. As has been reported elsewhere, *in situ* ellipsometry was used to determine the thickness of the films.<sup>91</sup> In order to achieve a measurable deposition rate, the crucible holding the material had to be heated.

The nanocalorimeters were held in a temperature-controlled housing which was set to the deposition temperature. The sample and reference calorimeters were contained in the same housing, but deposition was limited to the sample calorimeter. After the deposition, the chamber was backfilled to a pressure of 220 torr with dry nitrogen gas. This prevented loss of the sample due to desorption during heating scans.



The details of the *in situ* AC nanocalorimetry measurements can be found in references <sup>14, 89</sup>; the main points are summarized here. A temperature oscillation with a thermal frequency of 20 Hz was applied to the nanocalorimeter heaters. A thermopile is integrated into the nanocalorimeter membrane and the complex differential thermopile amplitude is directly proportional to the reversing heat capacity. The asymmetry of the reference and sample calorimeters is accounted for by subtracting an empty scan collected under the same conditions from the sample measurement in the complex plane. The vapor-deposited samples were heated from the deposition temperature to  $\sim 190$  K at a rate of 5 or 10 K/min and then heated with a rate of 2 K/min to  $\sim 269$  K. The material was then cooled and reheated to measure the ordinary glass at the same rate.

When the temperature is scanned above  $\sim 260$  K, small amounts of deposition occur on the sample calorimeter as a result of molecules leaving warmer parts of the chamber. This increases the thickness by  $\sim 1\%$ . The temperature scans have been corrected by averaging the ordinary glass heating and cooling scans and then subtracting the signal ( $\sim 0.2$   $\mu\text{V}$ ) due to the excess material. The heat capacity has also been corrected for the effect of stress on the calorimeter membrane.<sup>91</sup>

## Chapter 6

### Concluding Remarks

#### 6.1 Introduction

Physical vapor deposition can be used to prepare glasses with remarkable stability. Among the reported characteristics of stable glasses are low enthalpy, high density and high onset temperature with respect to the values for the glass cooled from the liquid.<sup>8-12, 65</sup> Through the use of nanocalorimetry, the heat capacity of stable vapor-deposited glasses has been investigated to a deeper level of detail and 'low heat capacity' was able to be added to the list of stable glass properties. The following is a broad overview of the main conclusions of the original work presented in this thesis. It aims to tie together the body of results and present them as a whole.

#### 6.2 Influence of substrate temperature on kinetic stability

The deposition temperature is a key factor in the stability of vapor-deposited glasses. From the first reports of glasses with high enthalpy and low density being deposited on cold substrates,<sup>51-54, 61</sup> to the more recent reports of glasses with enhanced kinetic stability being deposited near  $0.85 T_g$ ,<sup>8-9</sup> substrate temperature has played a role in the properties of vapor-deposited glasses. The effect of the deposition temperature on the kinetic stability of vapor-deposited glasses of three systems was reported in this thesis. *o*-Terphenyl, *cis*-decalin and 50/50 *cis/trans*-decalin glasses were vapor-deposited over a range of substrate temperatures and the onset temperatures of the as-deposited glasses were determined from the reversing heat capacity. Figure 6.1 provides a comparison of the

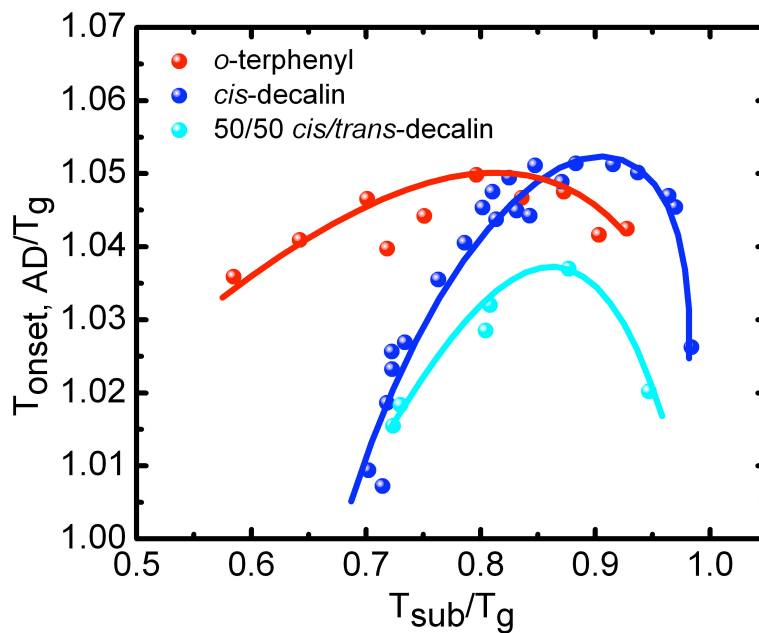


**Figure 6.1.** Comparison of the kinetic stability of vapor-deposited glasses as a function of substrate temperature. The onset temperature of the as-deposited glass is scaled by the glass transition temperature of the corresponding glassformer. The abscissa is also scaled by  $T_g$ . The solid lines are guides to the eye.

effect of the substrate temperature on the kinetic stability of the three systems. To fairly compare the different materials, the onset temperatures of the as-deposited glasses as well as the substrate temperatures are scaled by  $T_g$ .

In broad strokes, vapor-deposited glasses of *o*-terphenyl, *cis*-decalin and 50/50 *cis/trans*-decalin are similarly influenced by deposition temperature. For deposition near  $T_g$  the kinetic stability of vapor-deposited glasses (as indicated by the onset temperature) is no more than that of the ordinary glass, but as the substrate temperature is lowered the kinetic stability passes through a maximum. This is understood in terms of the mobility of depositing molecules: at intermediate substrate temperatures, surface mobility during deposition allows the molecules to find more efficient packing arrangements.<sup>9</sup> Since each molecule spends some amount of time in the mobile surface layer before being buried into the bulk by further deposition, stable glasses are built from the bottom up.

In detail, the behavior of *o*-terphenyl vapor-deposited glasses is different than the decalin glasses. Based on the scaled kinetic stability presented in Figure 6.1, the overall degree of kinetic stability is similar for the two systems, but vapor-deposited glasses of *o*-terphenyl exhibit high kinetic stability across a wider range of deposition temperatures. The kinetic stability of vapor-deposited glasses of decalin changes more sharply with substrate temperature. It is possible this is associated with the high fragility of decalin; the properties of fragile glassformers depend more strongly on temperature near  $T_g$ .

The measurements on decalin demonstrate that highly fragile glassformers and molecular mixtures can achieve enhanced kinetic stability through vapor-deposition.

Additionally, all compositions of *cis/trans*-decalin mixture vapor-deposited glasses exhibited higher onset temperatures than the corresponding liquid-cooled glasses. The tunability of stable glasses is a feature consistent with amorphous rather than crystalline solids, arguing against the idea that stable glass properties may be a result of nanocrystals.

### 6.3 Isothermal transformation behavior of vapor-deposited glasses

Quasi-isothermal AC nanocalorimetry measurements can be used to observe the stable glass to supercooled liquid transformation. Advantages of this measurement are that the transformation behavior can be directly monitored as a function of time and also a wide range of thicknesses in the thin film regime are measurable. Prior to the work in this thesis, conventional calorimetry had been used to study the heat capacity and enthalpy of  $\alpha\alpha\beta$ -TNB stable glasses.<sup>10</sup> The nanocalorimetry work here complimented the previous results by providing information about thin films of  $\alpha\alpha\beta$ -TNB. By studying films with thicknesses ranging from  $\sim 100$  nm to  $4 \mu\text{m}$ , two transformation mechanisms regimes were observed. Films thinner than one micron had transformation times that increased linearly with film thickness and the transformation curves were close to linear in time; these results are consistent with a surface-initiated growth front mechanism controlling the transformation behavior of thin films. The limited motions in the bulk of the glass do not allow the molecules to rearrange to the supercooled liquid; mobility has to arrive from the surface.<sup>76</sup> Thick films displayed thickness independent transformation times comparable to the bulk transformation times measured by other techniques. *o*-Terphenyl glasses with thicknesses

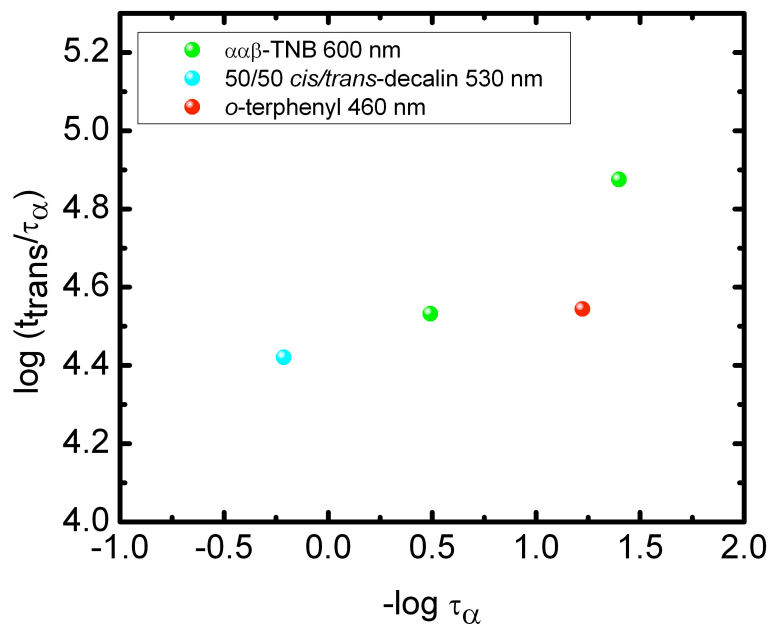


**Figure 6.2.** Stability of vapor-deposited glasses against isothermal annealing above the glass transition temperature.  $t_{\text{trans}}$  is the amount of time required to completely transform a stable vapor-deposited glass into the supercooled liquid. The thicknesses of the films are given in the legend.

ranging from  $\sim 100$  nm to  $\sim 1400$  nm showed similar behavior, but a purely bulk transformation mechanism was not yet apparent even in the thickest films measured.

The transformation times of vapor-deposited glasses are extremely long compared to what would be expected for an ordinary glass. The structural relaxation time  $\tau_\alpha$  of the equilibrium supercooled liquid is roughly equivalent to the time required for an ordinary glass to transform into the supercooled liquid, at a given temperature. Thus the ratio of the stable glass transformation time to  $\tau_\alpha$  gives the kinetic stability of the vapor-deposited glass relative to that of the ordinary liquid-cooled glass. Figure 6.2 summarizes this ratio for  $\alpha\alpha\beta$ -TNB, *o*-terphenyl and 50/50 *cis/trans*-decalin. Slight differences in thickness and relative transformation temperatures make a direct comparison of the systems somewhat unfair, but in each system the kinetic stability of the vapor-deposited glass exceeds that of the ordinary glass by at least a factor of 10,000. Regardless of the fragility, size or glass transition temperature of the organic glassformer studied, deposition near  $0.85 T_g$  produced glasses with comparable and immense kinetic stability.

#### **6.4 Heat capacity of vapor-deposited glasses**

Nanocalorimetry can be used to measure differences in heat capacity of less than 1%. This thesis presented a comparison of the heat capacity of vapor-deposited glasses and ordinary liquid-cooled glasses as a function of substrate temperature for three different systems: *o*-terphenyl, *cis*-decalin and 50/50 *cis/trans*-decalin. Figure 6.3a provides a qualitative summary of the heat capacity differences across the range of substrate temperatures. Though the scatter in the *o*-terphenyl data is much greater than in decalin, it

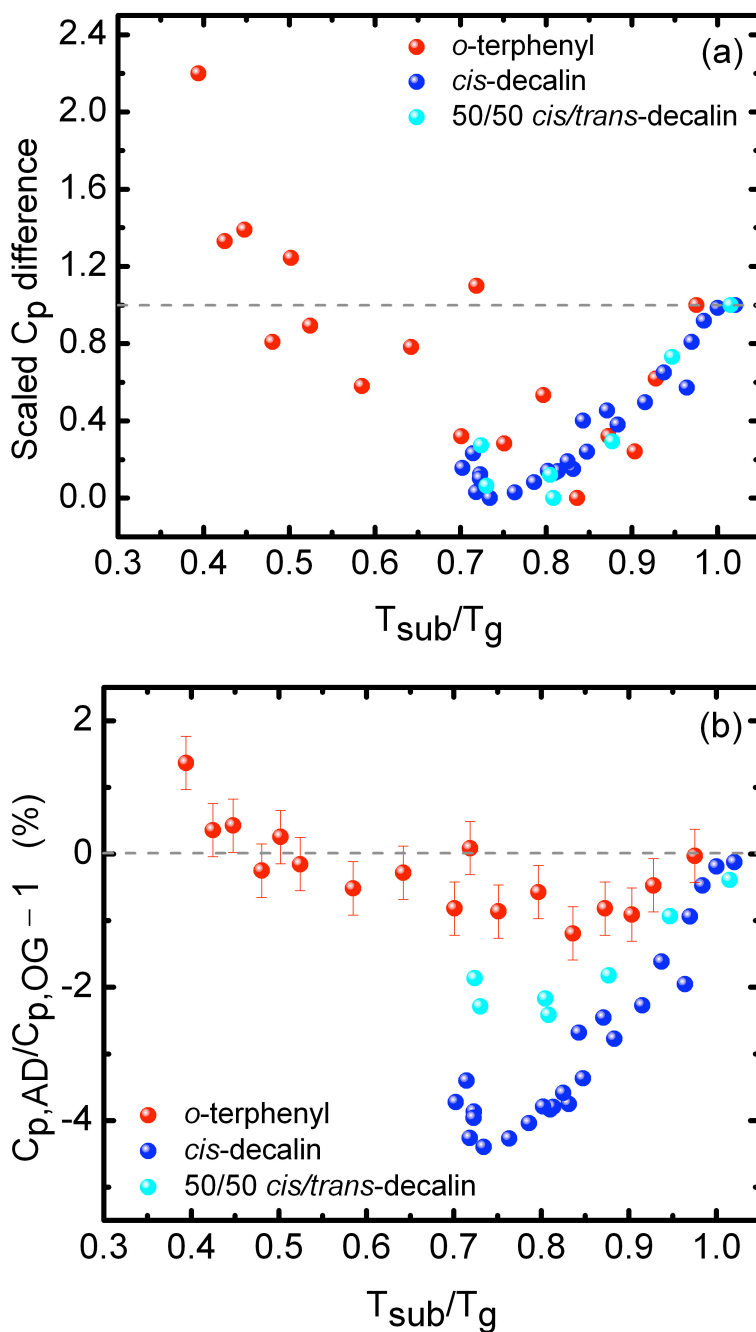


**Figure 6.3.** Scaled (a) and absolute (b) heat capacity differences between the vapor-deposited glasses and the ordinary liquid-cooled glass of the same system. In panel (a), one is equal to the heat capacity difference for a glass deposited near  $T_g$ , zero is the maximum fractional  $C_p$  decrease, and values greater than one indicate the degree to which the heat capacity of the vapor-deposited glass is larger than the ordinary glass.



is clear that the three systems show similar behavior with respect to scaled substrate temperature. As the deposition temperature is decreased away from  $T_g$ , the heat capacity of the vapor-deposited glass becomes lower than that of the ordinary glass. This has been interpreted in terms of the vibrational density of states.<sup>88</sup> Low frequency vibrational modes in well-packed, stable glasses are shifted to higher frequencies, which corresponds to a lower heat capacity. In the vicinity of 0.70-0.85  $T_g$ , the minimum heat capacity is attained; at lower substrate temperatures, the vapor-deposited glass heat capacity again begins to approach that of the liquid-cooled glass. The measurements on *o*-terphenyl were the first to utilize low enough substrate temperatures such that the heat capacity of the vapor-deposited glass was observed to become higher than that of the liquid-cooled glass. This result can be understood in an analogous way: the lack of mobility of molecules on cold substrates produces poorly packed glasses in which vibrational frequencies can shift to lower values, effectively increasing the heat capacity.

While the heat capacities of vapor-deposited glasses of organic molecules behave qualitatively similar as a function of substrate temperature, the degree to which the heat capacity can be decreased with vapor-deposition depends on the molecule. Figure 6.3b presents a quantitative summary of the heat capacity differences that exist between vapor-deposited glasses and liquid-cooled glasses of the systems investigated in this thesis. With fractional heat capacity decreases of  $\sim 1\%$  and  $\sim 4.5\%$ , respectively, *o*-terphenyl and *cis*-decalin represent opposite ends of the range of heat capacity differences reported thus

far.<sup>12, 87-88, 90-91</sup> Based on these two systems, it appears the inherent packing of the ordinary glass may play a role in the ability of vapor-deposited glasses to achieve low heat capacity.

### **6.5 Extremely high heat capacity at low temperature**

It is a well-known result in the field of vapor-deposited glasses that deposition onto cold substrates can produce glasses with high enthalpy and low density.<sup>51-54, 61</sup> Measurements reported herein on *o*-terphenyl demonstrated remarkably high heat capacity for glasses deposited at low substrate temperatures. Glasses deposited near  $0.4 T_g$  had initial heat capacities almost 50% higher than the heat capacity of the liquid-cooled glass at the same temperature. The large heat capacity difference was irreversibly erased by heating; this is consistent with structural collapse of a low density glass. Since these experiments were carried out in a nitrogen environment, it is possible that the as-deposited porous glass adsorbed nitrogen gas that contributed to the heat capacity.<sup>98</sup>

## Chapter 7

### Future Directions

#### 7.1 Introduction

Nanocalorimetry has proven to be a powerful tool for studying vapor-deposited glasses of small organic glassformers. Because films ranging in thickness from a few nanometers to a few microns can be accurately measured, thickness effects in stable glasses of indomethacin (IMC),  $\alpha,\alpha,\beta$ -tris-naphthylbenzene ( $\alpha\alpha\beta$ -TNB) and toluene have been able to be observed.<sup>77-78, 88</sup> The sensitivity of the technique has allowed for the difference in heat capacity between stable vapor-deposited glasses and ordinary liquid-cooled glasses to be measured for the first time. For most of the systems studied, the stable glass heat capacity is 3-4% lower than the ordinary glass heat capacity at the same temperature.<sup>12, 87-88, 90-91</sup> Nanocalorimetry has also been useful for investigating the deposition conditions that maximize kinetic stability for a number of organic glassformers and has extended the range of materials known to show stable glass forming ability to include mixtures and high fragility glassformers.<sup>12, 90-91</sup> One interesting result was that the deposition rate had a much weaker influence on the stability of the smaller molecules toluene and ethylbenzene, as compared to the effect that was observed for IMC and  $\alpha\alpha\beta$ -TNB vapor-deposited glasses.<sup>10, 12, 90</sup>

While nanocalorimetry has provided a wealth of information about the heat capacity and stability of vapor-deposited glasses, the results have also lead to many more questions. Can the heat capacity of a stable glass be lower than the heat capacity of the crystal? Why

do smaller molecules seem to have a weaker dependence on the deposition rate? What are the limitations for forming stable glasses of other molecular mixtures? This chapter will discuss these questions and suggest experiments that can be carried out to test potential resolutions, in particular those that can be performed in a high throughput manner.

## 7.2 Glass vs. crystal heat capacity

A number of examples exist in the literature where the heat capacity of the glass has been shown to be less than the heat capacity of a crystal of the same material. While no law of thermodynamics is violated by such an occurrence, the result is surprising. The first report appeared in 1919 for pyroxene and anorthite; between 300-800 K and 300-400 K, respectively, the heat capacity of the glass was lower than that of the crystal.<sup>169</sup> For pyroxene, the measured difference was 0.3%, which was on the order of the error of the measurement. For anorthite, however, the glass had a 0.9% lower heat capacity than the heat capacity of the crystal. As another example, the heat capacity of glassy dl-lactic acid was measured to be up to 3% lower than the crystal heat capacity over an eighty degree temperature range.<sup>170</sup> In 1957, the inorganic glassformers sodium tetraborate, boron trioxide and silicon dioxide were reported to have 1-3% lower heat capacity than their crystalline counterparts.<sup>171</sup> Ten years later, Bestul and coworkers at the National Bureau of Standards used adiabatic calorimetry to measure the heat capacity of diethyl phthalate crystal, glass and liquid.<sup>112</sup> Between 30 and 75 K, the liquid-cooled glass had a heat capacity up to 0.3% lower than the crystal and the annealed glass heat capacity was up to 0.6% lower.

Reversing heat capacity measurements on stable glasses have shown that the heat capacity of the stable glass is approaching the heat capacity of the crystal but have yet to definitively demonstrate a glass with lower heat capacity than the crystal. For both IMC and  $\alpha\beta$ -TNB, the heat capacity difference between the ordinary glass and stable glass is almost as large as the difference between the ordinary glass and the crystal.<sup>87-88</sup> However, the accuracy of the measurements limited the conclusions that could be drawn about the heat capacity. Since moving the nanocalorimetry measurements *in situ*, the error in the heat capacity determination has decreased by a factor of two and continues to improve. With *in situ* calorimetry, more meaningful conclusions regarding the relative heat capacities of the glass and the crystal are possible.

The organic molecule diethyl phthalate is a prime candidate to test whether vapor-deposited glasses can indeed have lower heat capacity than the crystal of the same material. Considering that the ordinary glass heat capacity has already been demonstrated to be lower than that of the crystal over a limited temperature range, vapor-deposited glasses of diethyl phthalate make for an interesting study. Based on the fact that stable glasses have characteristics you would expect for “super-aged” materials and that annealing has already been proven to further lower the heat capacity of the glass, it seems likely that if a stable glass can be made, it would also have lower heat capacity than the crystal. Furthermore the heat capacity of the vapor-deposited glass would be even lower with respect to the crystal than the liquid-cooled or aged glass.

The glass transition temperature of diethyl phthalate is  $\sim 180$  K and the vapor pressure at room temperature is  $\sim 10^{-3}$  torr.<sup>112, 172</sup> Based on these values, it is possible to vapor-deposit diethyl phthalate for *in situ* nanocalorimetry measurements. However, the interesting heat capacity observations were made at temperatures between 35 and 70 K, and our vacuum chamber is limited to temperatures above 90 K. At present, measurements of diethyl phthalate would have to take place in the lab of our collaborators, the Schick lab at the University of Rostock. Their *in situ* nanocalorimetry chamber is equipped with liquid helium cooling and can access the low temperature range of interest. Since Bestul and coworkers have already established the heat capacity relationship between the ordinary glass and the crystal, an ordinary glass of diethyl phthalate can be prepared under the same conditions and compared to the vapor-deposited glass. The relationship between the vapor-deposited glass and the crystal heat capacity can be transitively established to determine if the heat capacity of the vapor-deposited stable glass is lower than that of the crystal.

### **7.3 High throughput nanocalorimetry measurements**

The *in situ* vacuum chamber was designed to accommodate four nanocalorimetry stages. Each stage can be individually temperature controlled and contains two calorimeters in sample positions and one calorimeter in a reference position (i.e. blocked from deposition). Thus far, that setup has rarely been taken advantage of, but it has the potential to make short work of a variety of lingering questions.

#### **7.3.1 Stable glass deposition rate dependence**

Many properties associated with stable vapor-deposited glasses appear to be universal across various systems. Substrate temperature effects from material to material are fairly similar,<sup>8, 12, 90</sup> high density is commonly observed,<sup>11, 65, 101, 173</sup> and the transformations of thin films of a number of glassformers are consistent with a growth front process.<sup>76, 78, 88, 90, 94</sup> However, the effect of deposition rate on the stability of vapor-deposited glasses is much more variable. Conventional calorimetry experiments on IMC and  $\alpha\alpha\beta$ -TNB showed that varying the deposition rate from 15 nm/s to 0.2 nm/s increased the onset temperature by  $\sim 20$  K.<sup>10</sup> Two different studies have looked at the effect of deposition rate on toluene and ethylbenzene vapor-deposited glasses and a much less dramatic effect was observed for the smaller molecules. In one study thin films were deposited at rates of 0.001 to 0.1 nm/s and at a deposition temperature of 90 K.<sup>12</sup> Only very minor differences were noted between the glasses deposited at those rates. In the other study, 400 nm films were deposited at rates of 0.02 to 50 nm/s and a deposition temperature of 105 K.<sup>90</sup> The onset temperature of the glass deposited at the lowest rate was only a few degrees higher than that of the glass deposited at the fastest rate.

Two hypotheses were given to explain the difference in behavior between the larger molecules and smaller molecules.<sup>12, 90</sup> The first hypothesis considered the possibility of equilibration during deposition and the second took into account film thickness and the existence of different transformation mechanisms for thin films and bulk films. The deposition rate is postulated to provide no further enhance to the kinetic stability once equilibrated structures are produced during deposition. The smaller molecules toluene and

ethylbenzene may be able to sample the energy landscape faster than the larger molecules and thus reach equilibrated structures more rapidly. If nearly equilibrated samples were being deposited, then the deposition rate would have little to no effect on the stability of the glass. Since equilibration times increase with decreasing temperature, measuring the deposition rate dependence at lower temperatures could yield different results.

As to the second hypothesis, it is possible that the kinetic stability of only bulk films is affected by the deposition rate. Since DSC was used to measure the onset temperatures of the IMC and  $\alpha\alpha\beta$ -TNB vapor-deposited glasses, the films were necessarily  $\sim 20$   $\mu\text{m}$  in thickness, but the toluene and ethylbenzene experiments were done on films with thicknesses of only a few hundred nanometers. As the nanocalorimetry results on  $\alpha\alpha\beta$ -TNB presented in Chapter 2 have shown, thin films and thick films transform by different mechanisms. Furthermore, based on unpublished work, the growth front velocity, which controls the transformation of thin stable glass films, appears to be relatively independent of the deposition conditions. If this were the case, then the kinetic stability of thin films, which transform via growth fronts, would not show a rate dependence, but thick films would. Experiments that measure the deposition rate dependence of thin films and bulk films could yield different results and help to clarify this point.

High throughput measurements on vapor-deposited glasses of toluene or ethylbenzene are ideally situated to rapidly test these hypotheses. A set of experiments to examine the first hypothesis could focus on the effect of the deposition rate on thin vapor-deposited glasses produced at different substrate temperatures. Since it is possible in our



chamber to separately control four independent temperature stages, within a given deposition four different substrate temperatures can be utilized. Thus in only four depositions, four orders of magnitude in deposition rate can be explored for four different substrate temperatures. This is especially convenient for the lowest deposition rates, as these depositions require the longest amount of time. After the deposition, the heat capacity of the vapor-deposited samples can be measured in turn. Experience has shown that the nanocalorimetry stages are sufficiently isolated from one another and that the samples will remain at the programmed isothermal temperatures while neighboring stages are temperature ramped. If glasses deposited at different substrate temperatures exhibit different trends in the onset temperature with deposition rate, then the first hypothesis would be supported.

A second set of experiments can be performed on films that are known to display bulk transformation behavior. Isothermal transformation experiments on toluene have shown that 2500 nm thick films exhibit bulk transformation times. Such thicknesses are well within reach of nanocalorimetry measurements and thus the four depositions described above could be repeated for 2500 nm thick films. The advantage of high throughput depositions is twofold here because increased film thickness and decreased deposition rates combine for extremely lengthy depositions. Comparison of the first and second set of experiments would test the second hypothesis presented above.

Besides temperature scanning experiments, from which the onset temperature can be determined, isothermal annealing experiments can also be performed to gauge the

kinetic stability. With slight modifications to the electrical wiring outside of the chamber, four different samples could be simultaneously annealed. As annealing experiments can vary from a few hours to a day depending on the stability of the glass and the annealing temperature, this would significantly reduce the amount of experimental time. Depositions similar to those described above could be repeated, except the vapor-deposited samples would be isothermally annealed rather than temperature ramped after deposition.

### 7.3.2 Stable glasses of mixtures

As was demonstrated in Chapter 3 with *cis*- and *trans*-decalin, molecular mixtures can also form stable glasses when vapor-deposited. While the decalin result did serve as a proof of principle, the two geometric isomers are quite similar to one another and the simplicity of the mixture may have contributed to its ability to form a stable glass. This raises the question, how different can the molecular components be and still form stable glass mixtures? For glassformers with glass transition temperatures that differ by a wide margin, is there only a limited temperature range where stable glasses can be produced? These are questions that can be easily and rapidly explored with high throughput nanocalorimetry measurements.

Within one day, vapor-deposited mixture samples can be made and the reversing heat capacity of the glasses can be measured with *in situ* nanocalorimetry. Through a comparison of the onset temperatures, the data can answer whether a kinetically stable glass was formed in as little as two temperature scans. The possibility of preparing four identical samples within one deposition allows for a check on reproducibility and also for

the experimental parameters to be perfected without depositing fresh samples. These features make *in situ* nanocalorimetry a good technique for quickly surveying various mixtures for stable glass forming ability. For example, one day a stable glass mixture can be attempted of two glassformers with differing fragilities and the next day a mixture of molecules of two different sizes can be attempted. In this way, the characteristics that are important to enabling the formation of stable glasses of mixtures can be quickly narrowed down.

One interesting mixture to attempt is that of glycerol and decahydroisoquinoline (DHiQ). The glassformers have similar glass transition temperatures but fragilities at opposite extremes of the spectrum. Fragility is a method of characterizing glassformers based on the temperature dependence of the structural relaxation time of the material as it is cooled towards  $T_g$ . Strong glassformers, such as glycerol, exhibit Arrhenius behavior and have small fragilities, while for fragile glassformers, such as DHiQ, the structural relaxation time of the liquid changes more rapidly with temperature as  $T_g$  is approached. The glass transition temperatures of glycerol and DHiQ are 189 K and 181 K, respectively, but the fragilities are 51 and 128.<sup>134</sup> Given that the “sweet spot” for vapor-depositing stable glasses is  $\sim 0.85 T_g$  and such a substrate temperature is similar for the two materials, this could aid in the preparation of a stable glass of this mixture, despite the differing fragilities. In this context, it should be noted that vapor-deposited glycerol is reported to not form stable glasses when deposited near  $0.85 T_g$ .<sup>130</sup> However, pure *trans*-decalin also did not form a stable glass when vapor-deposited, but a mixture that was 25/75 *cis/trans*-decalin did

show stable glass behavior. Stable glass formation of a glycerol/DHiQ mixture could also fail if the components are not miscible. Since a time commitment of only one day is necessary to check stable glass forming ability with *in situ* nanocalorimetry, the penalty for attempting new mixtures is minor.

Other characteristics that would be interesting to investigate are how strengths of intermolecular attractions and molecular size play a role in the ability to form stable glasses of mixtures. It seems that molecules with strong hydrogen bonding networks such as glycerol and water do not form stable glasses when vapor-deposited.<sup>130-132</sup> In the mixture described above, glycerol and DHiQ could hydrogen bond. In this light, it would also be interesting to attempt a mixture of ethylene glycol ( $T_g = 151$  K)<sup>96</sup> and *cis*-decalin ( $T_g = 141$  K) as well. In order to test if molecular size is a limiting factor, toluene ( $T_g = 117$  K) and propylbenzene ( $T_g = 122$  K) could be co-deposited. With trial experiments that only require one day, many mixture combinations could be attempted within a month.

All of the mixtures suggested above have relatively similar glass transition temperatures. *cis*-Decalin and toluene would be a reasonable pair of glasses with differing glass transition temperatures to investigate first because the two systems have already been characterized individually as a function of substrate temperature.<sup>90-91</sup> Since four different deposition temperatures can be achieved in one deposition, substrate temperatures that permit stable glass mixture formation can be quickly assessed. In this high throughput manner, mixtures of glasses with differing  $T_g$ 's can be rapidly analyzed.

Perhaps after stable glass mixtures are better understood, more technologically relevant systems such as drug-excipient mixtures could be investigated.

## References

1. Wuttig, M.; Yamada, N., Phase-Change Materials for Rewriteable Data Storage. *Nat. Mater.* **2007**, *6*, 824-832.
2. Shirota, Y., Photo- and Electroactive Amorphous Molecular Materials - Molecular Design, Syntheses, Reactions, Properties, and Applications. *J Mater Chem* **2005**, *15*, 75-93.
3. Forrest, S. R.; Thompson, M. E., Introduction: Organic Electronics and Optoelectronics. *Chem Rev* **2007**, *107*, 923-925.
4. Soutis, C., Carbon Fiber Reinforced Plastics in Aircraft Construction. *Mat Sci Eng a-Struct* **2005**, *412*, 171-176.
5. Angell, C. A., Formation of Glasses from Liquids and Biopolymers. *Science* **1995**, *267*, 1924-1935.
6. Fredrickson, G. H., Recent Developments in Dynamical Theories of the Liquid-Glass Transition. *Annu. Rev. Phys. Chem.* **1988**, *39*, 149-180.
7. Stillinger, F. H., A Topographic View of Supercooled Liquids and Glass-Formation. *Science* **1995**, *267*, 1935-1939.
8. Kearns, K. L.; Swallen, S. F.; Ediger, M. D.; Wu, T.; Yu, L., Influence of Substrate Temperature on the Stability of Glasses Prepared by Vapor Deposition. *J. Chem. Phys.* **2007**, *127*, 154702.
9. Swallen, S. F.; Kearns, K. L.; Mapes, M. K.; Kim, Y. S.; McMahon, R. J.; Ediger, M. D.; Wu, T.; Yu, L.; Satija, S., Organic Glasses with Exceptional Thermodynamic and Kinetic Stability. *Science* **2007**, *315*, 353-356.
10. Kearns, K. L.; Swallen, S. F.; Ediger, M. D.; Wu, T.; Sun, Y.; Yu, L., Hiking Down the Energy Landscape: Progress toward the Kauzmann Temperature Via Vapor Deposition. *J. Phys. Chem. B* **2008**, *112*, 4934-4942.
11. Ishii, K.; Nakayama, H.; Moriyama, R.; Yokoyama, Y., Behavior of Glass and Supercooled Liquid Alkylbenzenes Vapor-Deposited on Cold Substrates: Toward the Understanding of the Curious Light Scattering Observed in Some Supercooled Liquid States. *Bull. Chem. Soc. Jpn.* **2009**, *82*, 1240-1247.
12. Leon-Gutierrez, E.; Sepulveda, A.; Garcia, G.; Clavaguera-Mora, M. T.; Rodriguez-Viejo, J., Stability of Thin Film Glasses of Toluene and Ethylbenzene Formed by Vapor Deposition: An in Situ Nanocalorimetric Study. *Phys. Chem. Chem. Phys.* **2010**, *12*, 14693-14698.

13. Efremov, M. Y.; Olson, E. A.; Zhang, M.; Zhang, Z.; Allen, L. H., Glass Transition in Ultrathin Polymer Films: Calorimetric Study. *Phys. Rev. Lett.* **2003**, *91*, 085703.
14. Huth, H.; Minakov, A. A.; Schick, C., Differential Ac-Chip Calorimeter for Glass Transition Measurements in Ultrathin Films. *J. Polym. Sci., Part B: Polym. Phys.* **2006**, *44*, 2996-3005.
15. Queen, D. R.; Hellman, F., Thin Film Nanocalorimeter for Heat Capacity Measurements of 30 Nm Films. *Rev. Sci. Instrum.* **2009**, *80*, 063901.
16. Inoue, A., Stabilization of Metallic Supercooled Liquid and Bulk Amorphous Alloys. *Acta Mater* **2000**, *48*, 279-306.
17. Wang, W. H.; Dong, C.; Shek, C. H., Bulk Metallic Glasses. *Materials Science & Engineering R-Reports* **2004**, *44*, 45-89.
18. Ediger, M. D.; Angell, C. A.; Nagel, S. R., Supercooled Liquids and Glasses. *J. Phys. Chem.* **1996**, *100*, 13200-13212.
19. Roy, R., Classification of Non-Crystalline Solids. *J Non-Cryst Solids* **1970**, *3*, 33-40.
20. Elliott, S. R., *Physics of Amorphous Materials*. Longman: London; New York, 1984.
21. Mishima, O.; Calvert, L. D.; Whalley, E., Melting Ice-I at 77-K and 10-Kbar - a New Method of Making Amorphous Solids. *Nature* **1984**, *310*, 393-395.
22. Mishima, O.; Calvert, L. D.; Whalley, E., An Apparently First-Order Transition between Two Amorphous Phases of Ice Induced by Pressure. *Nature* **1985**, *314*, 76-78.
23. Dislich, H., New Routes to Multicomponent Oxide Glasses. *Angew Chem Int Edit* **1971**, *10*, 363-&.
24. Dislich, H., Glassy and Crystalline Systems from Gels - Chemical Basis and Technical Application. *J Non-Cryst Solids* **1983**, *57*, 371-388.
25. Strawbridge, I.; Phalippou, J.; James, P. F., Characterization of Alkali Aluminoborosilicate Glass-Films Prepared by the Sol-Gel Process on Window Glass Substrates. *Phys Chem Glasses* **1984**, *25*, 134-141.
26. Onodera, N.; Suga, H.; Seki, S., Glass Transition in Amorphous Precipitates. *J Non-Cryst Solids* **1969**, *1*, 331-334.
27. Feltz, A., *Amorphous Inorganic Materials and Glasses*. VCH: Weinheim, 1993; p 446.
28. Suga, H., Thermodynamic Aspects of Glassy States. *J Mol Liq* **1999**, *81*, 25-36.

29. Mattox, D. M. Handbook of Physical Vapor Deposition (Pvd) Processing. <http://www.sciencedirect.com/science/book/9780815520375>.
30. Martin, P. M. Handbook of Deposition Technologies for Films and Coatings Science, Applications and Technology. <http://www.knovel.com/knovel2/Toc.jsp?BookID=3265>.
31. Tamulevicius, S., Stress and Strain in the Vacuum Deposited Thin Films. *Vacuum* **1998**, *51*, 127-139.
32. Leplan, H.; Robic, J. Y.; Pauleau, Y., Kinetics of Residual Stress Evolution in Evaporated Silicon Dioxide Films Exposed to Room Air. *J Appl Phys* **1996**, *79*, 6926-6931.
33. Watson, E. S.; O'Neill, M. J.; Justin, J.; Brenner, N., A Differential Scanning Calorimeter for Quantitative Differential Thermal Analysis. *Anal Chem* **1964**, *36*, 1233-1238.
34. Gill, P. S.; Sauerbrunn, S. R.; Reading, M., Modulated Differential Scanning Calorimetry. *J Therm Anal* **1993**, *40*, 931-939.
35. van Herwaarden, A. W., Overview of Calorimeter Chips for Various Applications. *Thermochim. Acta* **2005**, *432*, 192-201.
36. Mathot, V.; Pyda, M.; Pijpers, T.; Vanden Poel, G.; van de Kerkhof, E.; van Herwaardeng, S.; van Herwaardeng, F.; Leenaers, A., The Flash Dsc 1, a Power Compensation Twin-Type, Chip-Based Fast Scanning Calorimeter (Fsc): First Findings on Polymers. *Thermochim. Acta* **2011**, *522*, 36-45.
37. Hemminger, W. H. G., *Calorimetry : Fundamentals and Practice*. Verlag Chemie: Weinheim; Deerfield Beach, Fla., 1984.
38. Tool, A. Q., Relation between Inelastic Deformability and Thermal Expansion of Glass in Its Annealing Range. *J. Am. Ceram. Soc.* **1946**, *29*, 240-253.
39. Simon, S. L., Temperature-Modulated Differential Scanning Calorimetry: Theory and Application. *Thermochim. Acta* **2001**, *374*, 55-71.
40. Wunderlich, B.; Jin, Y. M.; Boller, A., Mathematical-Description of Differential Scanning Calorimetry Based on Periodic Temperature Modulation. *Thermochim. Acta* **1994**, *238*, 277-293.
41. Okazaki, I.; Wunderlich, B., Reversible Melting in Polymer Crystals Detected by Temperature-Modulated Differential Scanning Calorimetry. *Macromolecules* **1997**, *30*, 1758-1764.



42. Toda, A.; Oda, T.; Hikosaka, M.; Saruyama, Y., A New Method of Analysing Transformation Kinetics with Temperature Modulated Differential Scanning Calorimetry: Application to Polymer Crystal Growth. *Polymer* **1997**, *38*, 231-233.
43. Denlinger, D. W.; Abarra, E. N.; Allen, K.; Rooney, P. W.; Messer, M. T.; Watson, S. K.; Hellman, F., Thin-Film Microcalorimeter for Heat-Capacity Measurements from 1.5-K to 800-K. *Rev. Sci. Instrum.* **1994**, *65*, 946-958.
44. Efremov, M. Y.; Olson, E. A.; Zhang, M.; Schiettekatte, F.; Zhang, Z. S.; Allen, L. H., Ultrasensitive, Fast, Thin-Film Differential Scanning Calorimeter. *Rev. Sci. Inst.* **2004**, *75*, 179-191.
45. Minakov, A. A.; Roy, S. B.; Bugoslavsky, Y. V.; Cohen, L. F., Thin-Film Alternating Current Nanocalorimeter for Low Temperatures and High Magnetic Fields. *Rev. Sci. Instrum.* **2005**, *76*, 043906.
46. Lopeandia, A. E.; Valenzuela, J.; Rodriguez-Viejo, J., Power Compensated Thin Film Calorimetry at Fast Heating Rates. *Sensor Actuat a-Phys* **2008**, *143*, 256-264.
47. Minakov, A. A.; Adamovsky, S. A.; Schick, C., Non-Adiabatic Thin-Film (Chip) Nanocalorimetry. *Thermochim. Acta* **2005**, *432*, 177-185.
48. Zhuravlev, E.; Schick, C., Fast Scanning Power Compensated Differential Scanning Nano-Calorimeter: 1. The Device. *Thermochim. Acta* **2010**, *50*, 1-13.
49. Greer, A. L., Metallic Glasses. *Science* **1995**, *267*, 1947-1953.
50. Turnbull, D., Metastable Structures in Metallurgy. *Metall. Mater. Trans. A* **1981**, *12*, 695-708.
51. Oguni, M.; Hikawa, H.; Suga, H., Enthalpy Relaxation in Vapor-Deposited Butyronitrile. *Thermochim. Acta* **1990**, *158*, 143-156.
52. Takeda, K.; Yamamuro, O.; Oguni, M.; Suga, H., Thermodynamic Characterization of Vapor-Deposited Amorphous Solid. *Thermochim. Acta* **1995**, *253*, 201-211.
53. Takeda, K.; Yamamuro, O.; Suga, H., Calorimetric Study on Structural Relaxation of 1-Pentene in Vapor-Deposited and Liquid-Quenched Glassy States. *J. Phys. Chem.* **1995**, *99*, 1602-1607.
54. Hikawa, H.; Oguni, M.; Suga, H., Construction of an Adiabatic Calorimeter for a Vapor-Deposited Sample and Thermal Characterization of Amorphous Butyronitrile. *J. Non-Cryst. Solids* **1988**, *101*, 90-100.

55. Movchan, B. A.; Demchish.AV, Study of Structure and Properties of Thick Vacuum Condensates of Nickel, Titanium, Tungsten, Aluminium Oxide and Zirconium Dioxide. *Phys Metals Metallog* **1969**, *28*, 83-&.
56. Thornton, J. A., High-Rate Thick-Film Growth. *Annu Rev Mater Sci* **1977**, *7*, 239-260.
57. Zhu, L.; Yu, L. A., Generality of Forming Stable Organic Glasses by Vapor Deposition. *Chem. Phys. Lett.* **2010**, *499*, 62-65.
58. Sugisaki, M.; Suga, H.; Seki, S., Calorimetric Study of Glassy State .3. Novel Type Calorimeter for Study of Glassy State and Heat Capacity of Glassy Methanol. *B Chem Soc Jpn* **1968**, *41*, 2586-&.
59. Suga, H.; Seki, S., Thermodynamic Investigation on Glassy States of Pure Simple Compounds. *J Non-Cryst Solids* **1974**, *16*, 171-194.
60. Sugisaki, M.; Suga, H.; Seki, S., Calorimetric Study of Glassy State .4. Heat Capacities of Glassy Water and Cubic Ice. *B Chem Soc Jpn* **1968**, *41*, 2591-&.
61. Ishii, K.; Nakayama, H.; Okamura, T.; Yamamoto, M.; Hosokawa, T., Excess Volume of Vapor-Deposited Molecular Glass and Its Change Due to Structural Relaxation: Studies of Light Interference in Film Samples. *J. Phys. Chem. B* **2003**, *107*, 876-881.
62. Ishii, K.; Yoshida, M.; Suzuki, K.; Sakurai, H.; Shimayama, T.; Nakayama, H., Density Inhomogeneity in Amorphous Chlorobenzene Vapor-Deposited on Cold Substrates. *B Chem Soc Jpn* **2001**, *74*, 435-440.
63. Nakayama, H.; Ohta, S. I.; Onozuka, I.; Nakahara, Y.; Ishii, K., Direct Crystallization of Amorphous Molecular Systems Prepared by Vacuum Deposition: X-Ray Studies of Phenyl Halides. *B Chem Soc Jpn* **2004**, *77*, 1117-1124.
64. Yamamuro, O.; Tsukushi, I.; Matsuo, T.; Takeda, K.; Kanaya, T.; Kaji, K., Inelastic Neutron Scattering Study of Low-Energy Excitations in Vapor-Deposited Glassy Propylene. *J. Chem. Phys.* **1997**, *106*, 2997-3002.
65. Swallen, S. F.; Kearns, K. L.; Satija, S.; Traynor, K.; McMahon, R. J.; Ediger, M. D., Molecular View of the Isothermal Transformation of a Stable Glass to a Liquid. *J. Chem. Phys.* **2008**, *128*, 214514.
66. Zhu, L.; Brian, C. W.; Swallen, S. F.; Straus, P. T.; Ediger, M. D.; Yu, L., Surface Self-Diffusion of an Organic Glass. *Phys. Rev. Lett.* **2011**, *106*, 256103.
67. Keddie, J. L.; Jones, R. A. L.; Cory, R. A., Size-Dependent Depression of the Glass-Transition Temperature in Polymer-Films. *Europhysics Letters* **1994**, *27*, 59-64.

68. Keddie, J. L.; Jones, R. A. L.; Cory, R. A., Interface and Surface Effects on the Glass-Transition Temperature in Thin Polymer-Films. *Faraday Discussions* **1994**, *98*, 219-230.
69. Fakhraai, Z.; Forrest, J. A., Measuring the Surface Dynamics of Glassy Polymers. *Science* **2008**, *319*, 600-604.
70. Bell, R. C.; Wang, H. F.; Iedema, M. J.; Cowin, J. P., Nanometer-Resolved Interfacial Fluidity. *J. Am. Chem. Soc.* **2003**, *125*, 5176-5185.
71. Dawson, K.; Zhu, L.; Kopff, L. A.; McMahon, R. J.; Yu, L.; Ediger, M. D., Highly Stable Vapor-Deposited Glasses of Four Tris-Naphthylbenzene Isomers. *J. Phys. Chem. Lett.* **2011**, *2*, 2683-2687.
72. Kearns, K. L.; Still, T.; Fytas, G.; Ediger, M. D., High-Modulus Organic Glasses Prepared by Physical Vapor Deposition. *Adv. Mater.* **2010**, *22*, 39-42.
73. Fakhraai, Z.; Still, T.; Fytas, G.; Ediger, M. D., Structural Variations of an Organic Glassformer Vapor-Deposited onto a Temperature Gradient Stage. *J. Phys. Chem. Lett.* **2011**, *2*, 423-427.
74. Dawson, K. J.; Kearns, K. L.; Ediger, M. D.; Sacchetti, M. J.; Zografi, G. D., Highly Stable Indomethacin Glasses Resist Uptake of Water Vapor. *J. Phys. Chem. B* **2009**, *113*, 2422-2427.
75. Dawson, K. J.; Zhu, L.; Yu, L. A.; Ediger, M. D., Anisotropic Structure and Transformation Kinetics of Vapor-Deposited Indomethacin Glasses. *J. Phys. Chem. B* **2011**, *115*, 455-463.
76. Swallen, S. F.; Traynor, K.; McMahon, R. J.; Ediger, M. D.; Mates, T. E., Stable Glass Transformation to Supercooled Liquid Via Surface-Initiated Growth Front. *Phys. Rev. Lett.* **2009**, *102*, 065503.
77. Leon-Gutierrez, E.; Garcia, G.; Lopeandia, A. F.; Clavaguera-Mora, M. T.; Rodriguez-Viejo, J., Size Effects and Extraordinary Stability of Ultrathin Vapor Deposited Glassy Films of Toluene. *J. Phys. Chem. Lett.* **2010**, *1*, 341-345.
78. Kearns, K. L.; Ediger, M. D.; Huth, H.; Schick, C., One Micrometer Length Scale Controls Kinetic Stability of Low-Energy Glasses. *J. Phys. Chem. Lett.* **2010**, *1*, 388-392.
79. Guo, Y. L.; Morozov, A.; Schneider, D.; Chung, J.; Zhang, C.; Waldmann, M.; Yao, N.; Fytas, G.; Arnold, C. B.; Priestley, R. D., Ultrastable Nanostructured Polymer Glasses. *Nat. Mater.* **2012**, *11*, 337-343.
80. Singh, S.; de Pablo, J. J., A Molecular View of Vapor Deposited Glasses. *J. Chem. Phys.* **2011**, *134*, 194903.

81. Singh, S.; Ediger, M. D.; de Pablo, J. J., Ultrastable Glasses from *in Silico* Vapour Deposition. *Nat. Mater.* **2013**, *12*, 139-144.
82. Leonard, S.; Harrowell, P., Macroscopic Facilitation of Glassy Relaxation Kinetics: Ultrastable Glass Films with Frontlike Thermal Response. *J. Chem. Phys.* **2010**, *133*, 244502.
83. Shi, Z.; Debenedetti, P. G.; Stillinger, F. H., Properties of Model Atomic Free-Standing Thin Films. *J. Chem. Phys.* **2011**, *134*, 114524.
84. Sepulveda, A.; Swallen, S. F.; Ediger, M. D., Manipulating the Properties of Stable Organic Glasses Using Kinetic Facilitation. *J. Chem. Phys.* **2013**, *138*.
85. Sepulveda, A.; Swallen, S. F.; Kopff, L. A.; McMahon, R. J.; Ediger, M. D., Stable Glasses of Indomethacin and Alpha,Alpha,Beta-Tris-Naphthylbenzene Transform into Ordinary Supercooled Liquids. *J. Chem. Phys.* **2012**, *137*, 204508.
86. Kearns, K. L.; Swallen, S. F.; Ediger, M. D.; Sun, Y.; Yu, L., Calorimetric Evidence for Two Distinct Molecular Packing Arrangements in Stable Glasses of Indomethacin. *J. Phys. Chem. B* **2009**, *113*, 1579-1586.
87. Kearns, K. L.; Whitaker, K. R.; Ediger, M. D.; Huth, H.; Schick, C., Observation of Low Heat Capacities for Vapor-Deposited Glasses of Indomethacin as Determined by Ac Nanocalorimetry. *J. Chem. Phys.* **2010**, *133*, 014702.
88. Whitaker, K. R.; Ahrenberg, M.; Schick, C.; Ediger, M. D., Vapor-Deposited Alpha,Alpha,Beta-Tris-Naphthylbenzene Glasses with Low Heat Capacity and High Kinetic Stability. *J. Chem. Phys.* **2012**, *137*, 154502.
89. Ahrenberg, M.; Shoifet, E.; Whitaker, K. R.; Huth, H.; Ediger, M. D.; Schick, C., Differential Alternating Current Chip Calorimeter for in Situ Investigation of Vapor-Deposited Thin Films. *Rev. Sci. Instrum.* **2012**, *83*, 033902.
90. Ahrenberg, M.; Chua, Y. Z.; Whitaker, K. R.; Huth, H.; Ediger, M. D.; Schick, C., In Situ Investigation of Vapor-Deposited Glasses of Toluene and Ethylbenzene Via Alternating Current Chip-Nanocalorimetry. *J. Chem. Phys.* **2013**, *138*, 024501.
91. Whitaker, K. R.; Scifo, D. J.; Ediger, M. D.; Ahrenberg, M.; Schick, C., Highly Stable Glasses of Cis-Decalin and Cis/Trans-Decalin Mixtures. *The Journal of Physical Chemistry B* **2013**.
92. Leon-Gutierrez, E.; Garcia, G.; Lopeandia, A. F.; Fraxedas, J.; Clavaguera-Mora, M. T.; Rodriguez-Viejo, J., In Situ Nanocalorimetry of Thin Glassy Organic Films. *J. Chem. Phys.* **2008**, *129*.

93. Leon-Gutierrez, E.; Garcia, G.; Clavaguera-Mora, M. T.; Rodriguez-Viejo, J., Glass Transition in Vapor Deposited Thin Films of Toluene. *Thermochim. Acta* **2009**, *492*, 51-54.
94. Sepulveda, A.; Leon-Gutierrez, E.; Gonzalez-Silveira, M.; Clavaguera-Mora, M. T.; Rodriguez-Viejo, J., Anomalous Transformation of Vapor-Deposited Highly Stable Glasses of Toluene into Mixed Glassy States by Annealing above T-G. *J. Phys. Chem. Lett.* **2012**, *3*, 919-923.
95. Richert, R.; Angell, C. A., Dynamics of Glass-Forming Liquids. V. On the Link between Molecular Dynamics and Configurational Entropy. *J. Chem. Phys.* **1998**, *108*, 9016-9026.
96. Wang, L. M.; Angell, C. A.; Richert, R., Fragility and Thermodynamics in Nonpolymeric Glass-Forming Liquids. *J. Chem. Phys.* **2006**, *125*, 074505.
97. Angell, C. A.; Ngai, K. L.; McKenna, G. B.; McMillan, P. F.; Martin, S. W., Relaxation in Glassforming Liquids and Amorphous Solids. *J. Appl. Phys.* **2000**, *88*, 3113-3157.
98. Stevenson, K. P.; Kimmel, G. A.; Dohnalek, Z.; Smith, R. S.; Kay, B. D., Controlling the Morphology of Amorphous Solid Water. *Science* **1999**, *283*, 1505-1507.
99. Ishii, K.; Nakayama, H.; Hirabayashi, S.; Moriyama, R., Anomalous High-Density Glass of Ethylbenzene Prepared by Vapor Deposition at Temperatures Close to the Glass-Transition Temperature. *Chem. Phys. Lett.* **2008**, *459*, 109-112.
100. Ramos, S.; Oguni, M.; Ishii, K.; Nakayama, H., Character of Devitrification, Viewed from Enthalpic Paths, of the Vapor-Deposited Ethylbenzene Glasses. *J. Phys. Chem. B* **2011**, *115*, 14327-14332.
101. Dalal, S. S.; Sepulveda, A.; Pribil, G. K.; Fakhraai, Z.; Ediger, M. D., Density and Birefringence of a Highly Stable Alpha,Alpha,Beta-Trisnaphthylbenzene Glass. *J. Chem. Phys.* **2012**, *136*, 204501.
102. Dawson, K.; Kopff, L. A.; Zhu, L.; McMahon, R. J.; Yu, L.; Richert, R.; Ediger, M. D., Molecular Packing in Highly Stable Glasses of Vapor-Deposited Tris-Naphthylbenzene Isomers. *J. Chem. Phys.* **2012**, *136*, 094505.
103. Zhou, D.; Huth, H.; Gao, Y.; Xue, G.; Schick, C., Calorimetric Glass Transition of Poly(2,6-Dimethyl-1,5-Phenylene Oxide) Thin Films. *Macromolecules* **2008**, *41*, 7662-7666.
104. Lai, S. L.; Carlsson, J. R. A.; Allen, L. H., Melting Point Depression of Al Clusters Generated During the Early Stages of Film Growth: Nanocalorimetry Measurements. *Appl. Phys. Lett.* **1998**, *72*, 1098-1100.
105. Mahon, J. K.; Zhou, T.; Forrest, S. R.; Schwambera, M.; Meyer, N., Organic Vpd Shows Promise for Oled Volume Production. *Solid State Technol* **2002**, *45*, 131-+.

106. Yokoyama, D., Molecular Orientation in Small-Molecule Organic Light-Emitting Diodes. *J. Mater. Chem.* **2011**, *21*, 19187-19202.

107. Whitaker, C. M.; McMahon, R. J., Synthesis and Characterization of Organic Materials with Conveniently Accessible Supercooled Liquid and Glassy Phases: Isomeric 1,3,5-Tris(Naphthyl)Benzenes. *J. Phys. Chem.* **1996**, *100*, 1081-1090.

108. Magill, J. H., Physical Properties of Aromatic Hydrocarbons .3. A Test of Adam-Gibbs Relaxation Model for Glass Formers Based on Heat-Capacity Data of 1,3,5-Tri-Alpha-Naphthylbenzene. *J. Chem. Phys.* **1967**, *47*, 2802-&.

109. Schick, C.; Jonsson, U.; Vassilev, T.; Minakov, A. A.; Schawe, J. E. K.; Scherrenberg, R.; Lorinczy, D., Applicability of 8ocb for Temperature Calibration of Temperature Modulated Calorimeters. *Thermochim. Acta* **2000**, *347*, 53-61.

110. Boehm, L.; Ingram, M. D.; Angell, C. A., Test of a Year-Annealed Glass for the Cohen-Grest Percolation Transition. *J Non-Cryst Solids* **1981**, *44*, 305-313.

111. Richert, R.; Duvvuri, K.; Duong, L. T., Dynamics of Glass-Forming Liquids. Vii. Dielectric Relaxation of Supercooled Tris-Naphthylbenzene, Squalane, and Decahydroisoquinoline. *J. Chem. Phys.* **2003**, *118*, 1828-1836.

112. Chang, S. S.; Horman, J. A.; Bestul, A. B., Heat Capacities and Related Thermal Data for Diethyl Phthalate Crystal Glass and Liquid to 360 Degrees K. *J. Res. Natl. Bur. Stand. Sec. A* **1967**, *A 71*, 293-305.

113. Chang, S. S.; Bestul, A. B., Heat Capacities of Cis-1,4-Polyisoprene from 2 to 360 K. *J. Res. Natl. Bur. Stand. Sec. A* **1971**, *A 75*, 113-120.

114. Chang, S. S.; Bestul, A. B., Heat-Capacity and Thermodynamic Properties of Ortho-Terphenyl Crystal, Glass, and Liquid. *J. Chem. Phys.* **1972**, *56*, 503-516.

115. Chang, S. S.; Bestul, A. B., Heat-Capacities of Selenium Crystal (Trigonal), Glass, and Liquid from 5 to 360 K. *J. Chem. Thermodyn.* **1974**, *6*, 325-344.

116. Goldstein, M., Viscous-Liquids and Glass-Transition .5. Sources of Excess Specific-Heat of Liquid. *J. Chem. Phys.* **1976**, *64*, 4767-4774.

117. Wojnarowska, Z.; Adrjanowicz, K.; Wlodarczyk, P.; Kaminska, E.; Kaminski, K.; Grzybowska, K.; Wrzalik, R.; Paluch, M.; Ngai, K. L., Broadband Dielectric Relaxation Study at Ambient and Elevated Pressure of Molecular Dynamics of Pharmaceutical: Indomethacin. *J. Phys. Chem. B* **2009**, *113*, 12536-12545.

118. Wolynes, P. G., Spatiotemporal Structures in Aging and Rejuvenating Glasses. *Proc. Natl. Acad. Sci. U. S. A.* **2009**, *106*, 1353-1358.

119. Kovacs, A. J., La Contraction Isotherme Du Volume Des Polymères Amorphes. *Journal of Polymer Science* **1958**, *30*, 131-147.
120. Ediger, M. D.; Harrowell, P., Perspective: Supercooled Liquids and Glasses. *J. Chem. Phys.* **2012**, *137*, 080901.
121. Simon, S. L.; Sobieski, J. W.; Plazek, D. J., Volume and Enthalpy Recovery of Polystyrene. *Polymer* **2001**, *42*, 2555-2567.
122. McCaig, M. S.; Paul, D. R., Effect of Film Thickness on the Changes in Gas Permeability of a Glassy Polyarylate Due to Physical Aging Part I. Experimental Observations. *Polymer* **2000**, *41*, 629-637.
123. Stevenson, J. D.; Wolynes, P. G., On the Surface of Glasses. *J. Chem. Phys.* **2008**, *129*, 234514.
124. Sokolov, A. P.; Rossler, E.; Kisliuk, A.; Quitmann, D., Dynamics of Strong and Fragile Glass Formers - Differences and Correlation with Low-Temperature Properties. *Phys. Rev. Lett.* **1993**, *71*, 2062-2065.
125. Sastry, S., The Relationship between Fragility, Configurational Entropy and the Potential Energy Landscape of Glass-Forming Liquids. *Nature* **2001**, *409*, 164-167.
126. Speedy, R. J., Relations between a Liquid and Its Glasses. *J. Phys. Chem. B* **1999**, *103*, 4060-4065.
127. Martinez, L. M.; Angell, C. A., A Thermodynamic Connection to the Fragility of Glass-Forming Liquids. *Nature* **2001**, *410*, 663-667.
128. Huang, D. H.; McKenna, G. B., New Insights into the Fragility Dilemma in Liquids. *J. Chem. Phys.* **2001**, *114*, 5621-5630.
129. Lubchenko, V.; Wolynes, P. G., Theory of Structural Glasses and Supercooled Liquids. *Annu. Rev. Phys. Chem.* **2007**, *58*, 235-266.
130. Capponi, S.; Napolitano, S.; Wubbenhorst, M., Supercooled Liquids with Enhanced Orientational Order. *Nat. Commun.* **2012**, *3*, 1233.
131. Bhattacharya, D.; Payne, C. N.; Sadtchenko, V., Bulk and Interfacial Glass Transitions of Water. *J. Phys. Chem. A* **2011**, *115*, 5965-5972.
132. Sepulveda, A.; Leon-Gutierrez, E.; Gonzalez-Silveira, M.; Rodriguez-Tinoco, C.; Clavaguera-Mora, M. T.; Rodriguez-Viejo, J., Glass Transition in Ultrathin Films of Amorphous Solid Water. *J. Chem. Phys.* **2012**, *137*.

133. Duvvuri, K.; Richert, R., Dynamics of Glass-Forming Liquids. Vi. Dielectric Relaxation Study of Neat Decahydro-Naphthalene. *J. Chem. Phys.* **2002**, *117*, 4414-4418.
134. Wang, L. M.; Velikov, V.; Angell, C. A., Direct Determination of Kinetic Fragility Indices of Glassforming Liquids by Differential Scanning Calorimetry: Kinetic Versus Thermodynamic Fragilities. *J. Chem. Phys.* **2002**, *117*, 10184-10192.
135. Kaafarani, B. R.; Kondo, T.; Yu, J.; Zhang, Q.; Dattilo, D.; Risko, C.; Jones, S. C.; Barlow, S.; Domercq, B.; Amy, F., et al., High Charge-Carrier Mobility in an Amorphous Hexaazatrinaphthylene Derivative. *J. Am. Chem. Soc.* **2005**, *127*, 16358-16359.
136. Yu, L., Amorphous Pharmaceutical Solids: Preparation, Characterization and Stabilization. *Adv. Drug Delivery Rev.* **2001**, *48*, 27-42.
137. Kakumanu, V. K.; Bansal, A. K., Enthalpy Relaxation Studies of Celecoxib Amorphous Mixtures. *Pharm. Res.* **2002**, *19*, 1873-1878.
138. Huth, H.; Minakov, A. A.; Serghei, A.; Kremer, F.; Schick, C., Differential Ac-Chip Calorimeter for Glass Transition Measurements in Ultra Thin Polymeric Films. *Eur. Phys. J. - Special Topics* **2007**, *141*, 153-160.
139. Dixon, G. S.; Black, S. G.; Butler, C. T.; Jain, A. K., A Differential Ac Calorimeter for Biophysical Studies. *Anal. Biochem.* **1982**, *121*, 55-61.
140. Jakobi, R.; Gmelin, E.; Ripka, K., High-Precision Adiabatic Calorimetry and the Specific-Heat of Cyclopentane at Low-Temperature. *J. Therm. Anal.* **1993**, *40*, 871-876.
141. Hatase, M.; Hanaya, M.; Hikima, T.; Oguni, M., Discovery of Homogeneous-Nucleation-Based Crystallization in Simple Glass-Forming Liquid of Toluene Below Its Glass-Transition Temperature. *J. Non-Cryst. Solids* **2002**, *307-310*, 257-263.
142. Mossa, S.; La Nave, E.; Stanley, H. E.; Donati, C.; Sciortino, F.; Tartaglia, P., Dynamics and Configurational Entropy in the Lewis-Wahnstrom Model for Supercooled Orthoterphenyl. *Phys. Rev. E* **2002**, *65*.
143. Angell, C. A.; Yue, Y. Z.; Wang, L. M.; Copley, J. R. D.; Borick, S.; Mossa, S., Potential Energy, Relaxation, Vibrational Dynamics and the Boson Peak, of Hyperquenched Glasses. *J. Phys.: Condens. Matter* **2003**, *15*, S1051-S1068.
144. Chen, Z.; Richert, R., Dynamics of Glass-Forming Liquids. Xv. Dynamical Features of Molecular Liquids That Form Ultra-Stable Glasses by Vapor Deposition. *J. Chem. Phys.* **2011**, *135*, 124515.
145. Yamamuro, O.; Tsukushi, I.; Lindqvist, A.; Takahara, S.; Ishikawa, M.; Matsuo, T., Calorimetric Study of Glassy and Liquid Toluene and Ethylbenzene: Thermodynamic



Approach to Spatial Heterogeneity in Glass-Forming Molecular Liquids. *J. Phys. Chem. B* **1998**, *102*, 1605-1609.

146. Dawson, K. J.; Kearns, K. L.; Yu, L.; Steffen, W.; Ediger, M. D., Physical Vapor Deposition as a Route to Hidden Amorphous States. *Proc. Natl. Acad. Sci. U. S. A.* **2009**, *106*, 15165-15170.

147. Gallis, H. E.; van Miltenburg, J. C.; Oonk, H. A. J., Polymorphism of Mixtures of Enantiomers: A Thermodynamic Study of Mixtures of D- and L-Limonene. *Phys. Chem. Chem. Phys.* **2000**, *2*, 5619-5623.

148. Murthy, S. S. N.; Kumar, D., Glass-Formation in Organic Binary Liquids Studied Using Differential Scanning Calorimetry. *J. Chem. Soc., Faraday Trans.* **1993**, *89*, 2423-2427.

149. Cicerone, M. T.; Blackburn, F. R.; Ediger, M. D., How Do Molecules Move near  $T_g$ ? Molecular Rotation of 6 Probes in O-Terphenyl across 14 Decades in Time. *J. Chem. Phys.* **1995**, *102*, 471-479.

150. Hansen, C.; Stickel, F.; Berger, T.; Richert, R.; Fischer, E. W., Dynamics of Glass-Forming Liquids .3. Comparing the Dielectric Alpha- and Beta-Relaxation of 1-Propanol and O-Terphenyl. *J. Chem. Phys.* **1997**, *107*, 1086-1093.

151. Jackson, C. L.; McKenna, G. B., The Glass-Transition of Organic Liquids Confined to Small Pores. *J Non-Cryst Solids* **1991**, *131*, 221-224.

152. Petry, W.; Bartsch, E.; Fujara, F.; Kiebel, M.; Sillescu, H.; Farago, B., Dynamic Anomaly in the Glass-Transition Region of Orthoterphenyl - a Neutron-Scattering Study. *Zeitschrift Fur Physik B-Condensed Matter* **1991**, *83*, 175-184.

153. Greet, R. J.; Turnbull, D., Glass Transition in O-Terphenyl. *J. Chem. Phys.* **1967**, *46*, 1243-1251.

154. Mapes, M. K.; Swallen, S. F.; Kearns, K. L.; Ediger, M. D., Isothermal Desorption Measurements of Self-Diffusion in Supercooled O-Terphenyl. *J. Chem. Phys.* **2006**, *124*, 054710.

155. Adam, G.; Gibbs, J. H., On the Temperature Dependence of Cooperative Relaxation Properties in Glass-Forming Liquids. *J. Chem. Phys.* **1965**, *43*, 139.

156. Guttman, C. M., Low-Temperature Heat-Capacity Differences between Glasses and Their Crystals. *J. Chem. Phys.* **1972**, *56*, 627-&.

157. Wagner, H.; Richert, R., Equilibrium and Non-Equilibrium Type B-Relaxations: D-Sorbitol Versus O-Terphenyl. *The Journal of Physical Chemistry B* **1999**, *103*, 4071-4077.

158. Leyser, H.; Schulte, A.; Doster, W.; Petry, W., High-Pressure Specific-Heat Spectroscopy at the Glass Transition in O-Terphenyl. *Phys. Rev. E* **1995**, *51*, 5899-5904.
159. Plazanet, M.; Schober, H., Anharmonicity in a Fragile Glass-Former Probed by Inelastic Neutron Scattering. *Phys. Chem. Chem. Phys.* **2008**, *10*, 5723-5729.
160. Shamblin, S. L.; Tang, X. L.; Chang, L. Q.; Hancock, B. C.; Pikal, M. J., Characterization of the Time Scales of Molecular Motion in Pharmaceutically Important Glasses. *J. Phys. Chem. B* **1999**, *103*, 4113-4121.
161. Xi, H.; Sun, Y.; Yu, L., Diffusion-Controlled and Diffusionless Crystal Growth in Liquid O-Terphenyl near Its Glass Transition Temperature. *J. Chem. Phys.* **2009**, *130*, 094508-094509.
162. Ishii, K.; Kobayashi, Y.; Sakai, K.; Nakayama, H., Structural Relaxation in Amorphous 1,2-Dichloroethane Studied by Transformation between Conformation Isomers. *J. Phys. Chem. B* **2006**, *110*, 24827-24833.
163. Yamamuro, O.; Matsuo, T.; Onoda-Yamamuro, N.; Takeda, K.; Munemura, H.; Tanaka, S.; Misawa, M., Neutron Diffraction and Thermal Studies of Amorphous Cs<sub>2</sub> Realised by Low-Temperature Vapour Deposition. *EPL (Europhysics Letters)* **2003**, *63*, 368.
164. Tatsumi, S.; Aso, S.; Yamamuro, O., Thermodynamic Study of Simple Molecular Glasses: Universal Features in Their Heat Capacity and the Size of the Cooperatively Rearranging Regions. *Phys. Rev. Lett.* **2012**, *109*, 045701.
165. Wyart, M.; Nagel, S. R.; Witten, T. A., Geometric Origin of Excess Low-Frequency Vibrational Modes in Weakly Connected Amorphous Solids. *EPL (Europhysics Letters)* **2005**, *72*, 486.
166. Silbert, L. E.; Liu, A. J.; Nagel, S. R., Vibrations and Diverging Length Scales near the Unjamming Transition. *Phys. Rev. Lett.* **2005**, *95*, 098301.
167. Kimmel, G. A.; Stevenson, K. P.; Dohnalek, Z.; Smith, R. S.; Kay, B. D., Control of Amorphous Solid Water Morphology Using Molecular Beams. I. Experimental Results. *J. Chem. Phys.* **2001**, *114*, 5284-5294.
168. Dohnalek, Z.; Kimmel, G. A.; Ayotte, P.; Smith, R. S.; Kay, B. D., The Deposition Angle-Dependent Density of Amorphous Solid Water Films. *J. Chem. Phys.* **2003**, *118*, 364-372.
169. White, W. P., Silicate Specific Heats; Second Series. *Am J Sci* **1919**, *47*, 1-43.
170. Parks, G. S.; Thomas, S. B.; Light, D. W., Studies on Glass Xii. Some New Heat Capacity Data for Organic Glasses. The Entropy and Free Energy of DL-Lactic Acid. *J. Chem. Phys.* **1936**, *4*, 64-69.

171. Westrum, E. F.; Grenier, G., The Heat Capacities and Thermodynamic Properties of Crystalline and Vitreous Anhydrous Sodium Tetraborate from 6 to 350 °K. *Journal of the American Chemical Society* **1957**, *79*, 1799-1802.

172. Roháč, V.; Růžička, K.; Růžička, V.; Zaitsau, D. H.; Kabo, G. J.; Diky, V.; Aim, K., Vapour Pressure of Diethyl Phthalate. *The Journal of Chemical Thermodynamics* **2004**, *36*, 929-937.

173. Dalal, S. S.; Ediger, M. D., Molecular Orientation in Stable Glasses of Indomethacin. *J. Phys. Chem. Lett.* **2012**, *3*, 1229-1233.